

Modeling and Analysis of Production of Propylene
Glycol over Copper Chromite

A Thesis

Presented to the

Graduate Faculty of the

University of Louisiana at Lafayette

In Partial Fulfillment of the

Requirements for the Degree

Master of Science

Swarom R. Kanitkar

Fall 2014

UMI Number: 1585860

All rights reserved

INFORMATION TO ALL USERS

The quality of this reproduction is dependent upon the quality of the copy submitted.

In the unlikely event that the author did not send a complete manuscript and there are missing pages, these will be noted. Also, if material had to be removed, a note will indicate the deletion.



UMI 1585860

Published by ProQuest LLC (2015). Copyright in the Dissertation held by the Author.

Microform Edition © ProQuest LLC.

All rights reserved. This work is protected against unauthorized copying under Title 17, United States Code



ProQuest LLC.
789 East Eisenhower Parkway
P.O. Box 1346
Ann Arbor, MI 48106 - 1346

©Swarom R. Kanitkar

2014

All Rights Reserved

Modeling and Analysis of Production of Propylene Glycol over Copper Chromite

Swarom R. Kanitkar

APPROVED:

Stephen Dufreche, Chair
Assistant Professor of Chemical
Engineering

Rakesh Bajpai
Professor of Chemical Engineering

Ramalingam Subramaniam
Assistant Professor of Chemical
Engineering

Rafael Hernandez
Head and Professor of Chemical
Engineering

Mary Farmer-Kaiser
Interim Dean of the Graduate School

Acknowledgements

First of all, I would like to thank my parents Dr. Ravindra Kanitkar and Mrs. Dhanashree Kanitkar for their constant love, support, and encouragement throughout my academic career. I would also like to thank other members of family Ms. Gouravee Kanitkar and Mr. Amit Athavale for their immense support and encouragement. I would like to thank the Chair of my committee, Dr. Stephen Dufreche, for his continual support, guidance, and efforts throughout my research work and draft processes. To my committee members Dr. Rafael Hernandez, Dr. Ramalingam Subramaniam, and Dr. Rakesh Bajpai for their support, guidance, and valuable help. I would like to thank Terra Bio-Chem for the research opportunity and collaboration. Also, I would like to thank Clean Power Energy Research Consortium (CPERC) for financial support for the project. Finally, I would like to thank undergrad research assistants Claire Maraist, Joshua Robinson, Michael Foulcard, Jatin Patel, and Melissa Sandoval for their help with my research.

Table of Contents

Acknowledgements	iv
Table of Contents	v
List of Tables	viii
List of Figures	ix
List of Abbreviations	xii
Chapter 1: Introduction	1
Chapter 2: Literature Review	10
2.1 Hydrogenolysis of Glycerol.....	10
2.2 Catalyst Types	12
2.2.1 Heterogeneous Catalysts.....	12
2.3 Kinetics of Hydrogenolysis of Glycerol.....	14
2.3.1 Dehydration of Glycerol	18
2.3.2 Propylene glycol formation	19
2.4 Glycerol Hydrogenolysis over Copper Chromite	19
2.4.1 Effect of catalyst activation on hydrogenolysis of glycerol.....	21
2.4.2 Effect of catalyst activation time on hydrogenolysis of glycerol	22
2.4.3 Effect of catalyst activation temperature on hydrogenolysis of glycerol.....	22
2.4.4 Effect of reaction temperature on hydrogenolysis of glycerol.....	23
2.4.5 Effect of hydrogen pressure on hydrogenolysis of glycerol	25
2.4.6 Effect of addition of promoters to the catalyst on hydrogenolysis of glycerol.....	26
2.4.7 Effect of catalyst weight on hydrogenolysis of glycerol	27
2.4.8 Effect of initial glycerol content on hydrogenolysis of glycerol	28
2.4.9 Effect of agitation on hydrogenolysis of glycerol	29
2.4.10 Effect of Cu to Cr ratio in the catalyst over hydrogenolysis of glycerol.....	30
2.5 Kinetic study of hydrogenolysis of glycerol over copper chromite	34
Chapter 3: Theory	36
3.1 Catalyst Preparation.....	36
3.1.1 Sol-gel route	36
3.1.2 Co-precipitation.....	36
3.1.3 Impregnation method	37
3.2 Heterogeneous Catalytic Reaction.....	38
3.2.1 Steps involved in a heterogeneous catalytic reaction.....	38
3.3 Mass Transfer Limited vs. Reaction Limited	40

3.4 Rate expressions for heterogeneous catalytic reactions	41
3.5 Methods for calculation of reaction orders	43
3.5.1 Integral method	43
3.5.2 Differential Method	45
3.5.3 Nonlinear Regression	47
Chapter 4: Materials and Methods	48
4.1 Materials	48
4.2 Reactor Configuration	48
4.3 Catalyst Activation and Reactor Preparation	52
4.3.1 Catalyst Properties	52
4.3.2 Catalyst Activation	53
4.3.3 Feed Solution Preparation	54
4.3.4 Reactor Start-Up	56
4.3.5 Product Sampling	59
4.3.6 Reactor Shutdown	60
4.4 Analytical Methods	62
4.4.1 GC Analysis of Liquid Samples	62
4.4.2 GC Analysis of Gas Samples	65
4.4.3 Surface Area Analysis	66
4.5 Liquid-liquid extraction of the Mono Propylene Glycol (MPG)	68
4.5.1 Recoverability of the TXIB	68
4.5.2 Removal of impurities from the best extractable MPG stream	69
Chapter 5: Results and Discussion	71
5.1 Identification of the impurities	71
5.1.1 Types of impurities	73
5.1.2 Removal of impurities using liquid-liquid extraction	75
5.1.3 Partition coefficient	78
5.2 Surface Area Analysis of Catalyst	79
5.3 Kinetic Study	82
5.3.1 Mass Transfer Effects	82
5.3.2 Absence of Stirring	87
5.3.3 Heat Transfer Effects	89
5.3.4 Concentration of hydrogen in the liquid phase	90
5.3.5 Effect of various reaction parameters	91
5.3.6 Mass Balance	103
5.4 Kinetic Model	104
5.4.1 Preliminary order determination by Integral Method	104
5.4.2 Rate Equations	108
5.4.3 Nonlinear Regression Analysis for the First Approach	112
5.4.4 Nonlinear regression analysis for the second approach	114
Chapter 6: Engineering Significance	117

Chapter 7: Conclusions	120
Chapter 8: Future Work	122
Bibliography	123
Abstract	131
Biographical Sketch	132

List of Tables

Table 2.1: Performance of non-copper catalysts in hydrogenolysis of glycerol.....	13
Table 2.2: Performance of the copper based catalysts in hydrogenolysis of glycerol.....	14
Table 4.1: List of chemicals.....	48
Table 4.2: List of reaction parameters studied and their variation range.....	59
Table 4.3: GC-FID method (Oven Details)	65
Table 4.4: GC-TCD method (Oven Details).....	65
Table 5.1: Summary of results from surface area analysis	80
Table 5.2: Results from the Aspen Simulation for the solubility of hydrogen.....	91
Table 5.3: Mass balance for hydrogenolysis of glycerol at 230 °C and 400 psig.....	103
Table 5.4: Results from the nonlinear regression analysis (1 st Approach)	113
Table 5.5: Nonlinear regression results for the second approach	114
Table 5.6: Kinetic parameter values from acetol reaction	116
Table 6.1: Bulk costs of MPG and Glycerol.....	117

List of Figures

Figure 1-1: Energy scenario in the United States ⁴	2
Figure 1-2: Energy production in the United States ⁴	3
Figure 1-3: Typical biodiesel production reaction ⁷	4
Figure 1-4: Biodiesel and Glycerol production in the United States ⁸	5
Figure 1-5: Comparison of mixture of reaction products and mixture of pure products	8
Figure 2-1: Reactions occurring during hydrogenolysis of glycerol	10
Figure 2-2: Reaction mechanism proposed by Montassier et al. ⁴³	15
Figure 2-3: Reaction mechanism proposed by Dasari et al. ¹⁸	15
Figure 2-4: Reaction mechanism proposed by Wang et al. ²⁸	16
Figure 2-5: Reaction mechanism for liquid phase products by Torres et al. ²¹	16
Figure 2-6: Reaction mechanism proposed by Vasiliadou et al. ⁴⁴	17
Figure 2-7: Reaction mechanism suggested by Xiao et al. ²²	35
Figure 3-1: Steps involved in a heterogeneous catalytic reaction ⁵⁷ (porous catalyst)	38
Figure 3-2: Steps involved in Liquid phase hydrogenolysis of glycerol over non-porous copper chromite catalyst	39
Figure 4-1: Reaction System Schematic	49
Figure 4-2: Reactor Setup (Actual)	51
Figure 4-3: Schematic for the inside of the reactor	52
Figure 4-4: Star shaped pattern for tightening bolts	57
Figure 4-5: Calibration curves for GC-FID analysis	63
Figure 4-6: Micromeritics FlowSorb III Surface Area Analyzer	66
Figure 5-1: Chromatogram of calibration sample	71
Figure 5-2: Chromatogram for a reaction sample	72

Figure 5-3: Classification of impurities on chromatogram of reaction sample	73
Figure 5-4: Percentage distribution of product and impurities	77
Figure 5-5: Variation of glycerol concentration with time at different RPM (T = 230 °C, P = 400 psig, Glycerol content = 90 wt% and Catalyst Weight = 3 g).....	84
Figure 5-6: Variation of acetol concentration with time at different RPM (T = 230 °C, P = 400 psig, Glycerol content = 90 wt%, Catalyst weight = 3 g)	85
Figure 5-7: Variation of MPG concentration with time at different RPM (T = 230 °C, P = 400 psig, Glycerol content = 90 wt%, Catalyst weight = 3 g)	86
Figure 5-8: Concentration profiles under without stirring (T = 230 °C, P = 400 psig, Agitation = 500 RPM, Glycerol content = 90 wt%, Catalyst wt. = 3 g).....	88
Figure 5-9: Concentration profiles at different temperatures [P = 500 psig, Agitation = 1000 RPM, Glycerol content = 90 wt%, Catalyst weight = 3 g].....	92
Figure 5-10: Concentration profiles at different temperatures [P = 400 psig, Agitation = 1000 RPM, Glycerol content = 90 wt%, Catalyst weight = 3 g].....	93
Figure 5-11: Concentration profiles at different pressures [T = 200 °C, Agitation = 1000 RPM, Glycerol content = 90 wt%, Catalyst weight = 3 g]	95
Figure 5-12: Concentration profiles at different pressures [T = 230 °C, Agitation = 1000 RPM, Glycerol content = 90 wt%, Catalyst weight = 3 g]	96
Figure 5-13: Effect of pressure on light impurities [T = 230 °C, Agitation = 1000 RPM, Glycerol content = 90 wt%, Catalyst weight = 3 g].....	98
Figure 5-14: Effect of pressure on heavy impurities [T = 230 °C, Agitation = 1000 RPM, Glycerol content = 90 wt%, Catalyst weight = 3 g].....	99
Figure 5-15: Concentration profiles at different initial glycerol content [T = 230 °C, P = 500 psig, Agitation = 500 RPM, Weight of catalyst = 3 g].....	101
Figure 5-16: Concentration profiles at different initial glycerol contents [T = 200 °C, P = 500 psig, Agitation = 1000 RPM, Catalyst weight = 3 g]	102
Figure 5-17: Order analysis for the reaction data at [T = 230 °C, P = 400 psig, Agitation = 1000 RPM, Glycerol content = 90 wt%, Catalyst weight = 3 g].....	106
Figure 5-18: Order analysis for the reaction data at [T = 230 °C, P = 500 psig, Agitation = 1000 RPM, Glycerol content = 90 wt%, Catalyst weight = 3 g].....	107

Figure 5-19: Order analysis for the reaction data at [T = 230 °C, P = 400 psig, Agitation = 1200 RPM, Glycerol content = 90 wt%, Catalyst weight = 3 g].....	108
Figure 5-20: Proposed hydrogenolysis reaction model	109
Figure 5-21: Final kinetic model for calculations.....	116
Figure 6-1: Effect of residence time on conversion of glycerol and on selectivity towards products	119

List of Abbreviations

MEG	Mono Ethylene Glycol
MPG	Mono Propylene Glycol
1,2 PDO	1,2-Propanediol
1,3 PDO	1,3-Propanediol
GC	Gas Chromatograph
GC-FID	Gas Chromatograph-Flame Ionization Detector
GC-TCD	Gas Chromatograph-Thermal Conductivity Detector
TPD	Temperature Programmed Desorption
XRD	X-Ray Diffraction
XPS	X-Ray Photoelectron Spectroscopy
INS	Inelastic Neutron Scattering
EDX	Energy Dispersive X-ray Spectroscopy
TPR	Temperature Programmed Reduction
SEM	Scanning Electron Microscopy
TEM	Transmission Electron Microscopy
STEM	Scanning Transmission Electron Microscopy

Chapter 1: Introduction

Energy is needed to drive any process. This need drove the human race in search of energy sources. Homo erectus first started using wood as a fuel nearly 2 million years ago.¹ Animal fat and wood were the only sources of fuel available at that time. This use of biodegradable and renewable resources has continued until recent times. Starting in 6000 BCE, charcoal was used as a source of fuel for melting metals. Around 1000 BCE the use of coal started in China, which continues to date. After the invention of steam engine power in 1769, coal has become a common power source throughout the world.² This dependence of the chemical industry on coal and renewable resources, which are basically biomass-based, and hence, are biofuels, continued until the discovery of petroleum at the beginning of the twentieth century. After the discovery of petroleum, chemical products which were mostly produced from biomass started to get produced from chemical syntheses dependent on petroleum.³

The first reorientation process was triggered by an oil crisis which first surfaced in 1970s after it was discovered that petroleum resources were exhaustible and too valuable to be burned in low efficiency operations like power plants or combustion engines. This discovery caused people to start thinking about the efficiency of processes and other alternatives for petroleum products. This reorientation started a shift from processes which were conventionally derived from chemical or petroleum derivatives to production from renewable resources.³

The current energy situation in the United States as of 2013 is as shown in Figure 1-1.⁴ It clearly indicates that consumption is greater than production in the U.S., resulting in a net import of energy. Even though production is rising annually it is still 15-20 Quadrillion Btus short of annual consumption.

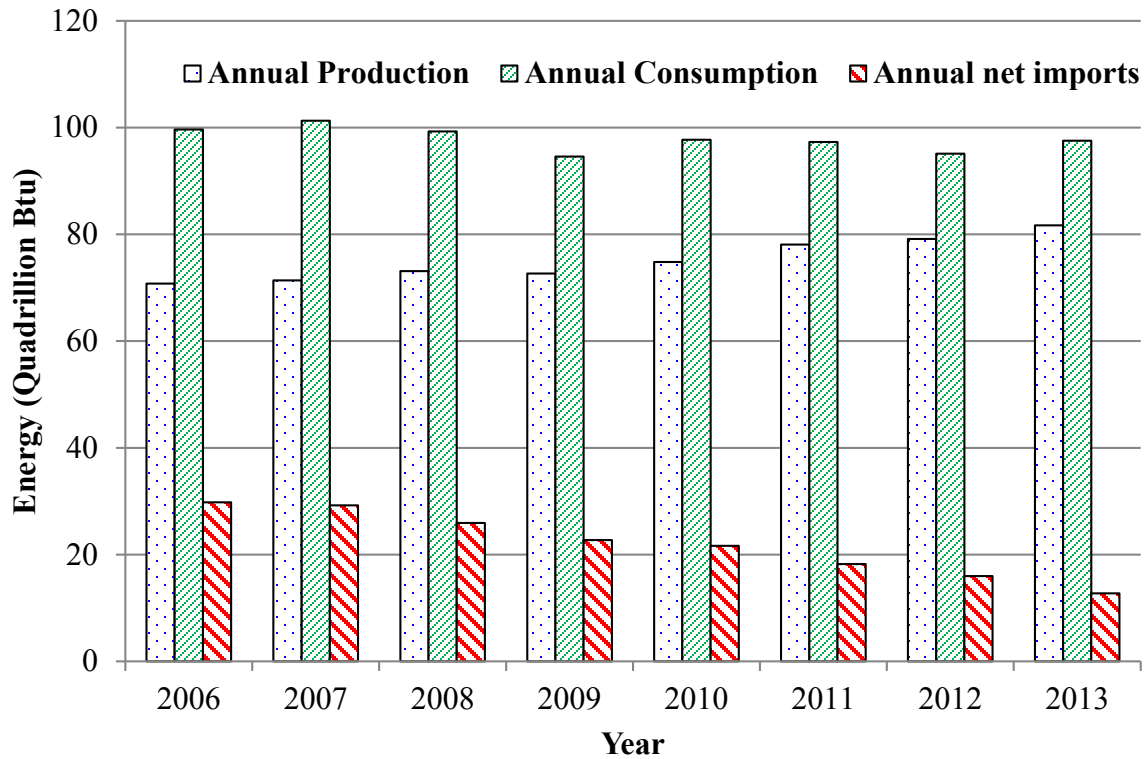


Figure 1-1: Energy scenario in the United States⁴

Although energy provided by renewable sources is increasing annually, it is still a long way from fully substituting Petroleum and Crude Oil. Out of the renewable energy sources currently in use, 21 % comes from biofuels, making it third significant type after hydroelectric power and wood. Increases in energy from biofuels in total production and a steady decrease of net imports are shown in Figure 1-2, and can be seen as a positive sign of renewables use.⁴ However, according to recent energy outlook suggested that by 2040, 13 % of total US energy use will come from renewables including biofuels.⁴

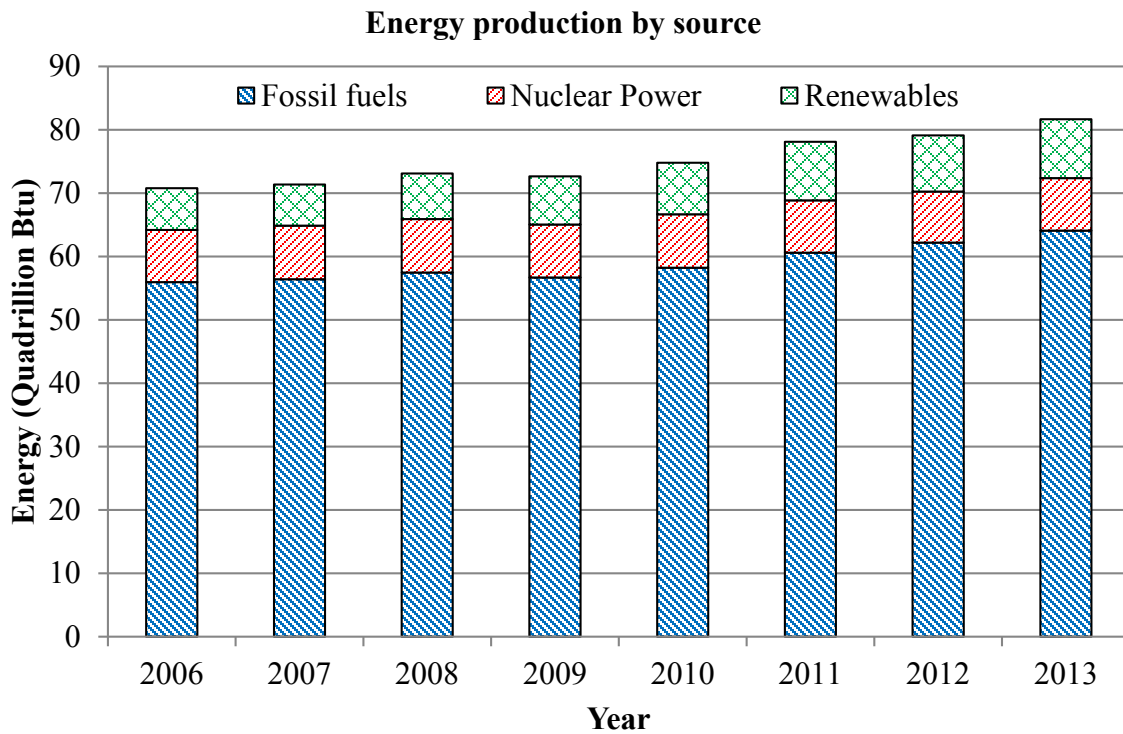


Figure 1-2: Energy production in the United States⁴

Energy demand, which is rising day by day, is posing questions on current limited resources whether they are adequate enough to meet the growth requirements.⁵ Also, population growth, which is cause of higher energy demand, is also a cause of increase in pollution. Emission standards are getting stringent and stringent and these norms demand highly efficient processes generating less by-products or less hazardous products, which would have several applications or would be biodegradable. These three: energy demand⁵, population growth, growing environmental pollution⁵ are the important problems that need to be solved for a better future. So there is a need for alternative resources that will be able to meet energy demands and would be renewable. This need caused the emergence of biofuels that are renewable and biodegradable as well.⁵ Other reasons involved in the re-emergence of

biofuels are reduced hazards for environment, foreign exchange policies and socio-economic issues of rural sectors.⁵

A renewable energy source produced from natural materials that can be used as a substitute for petroleum fuels is known as biofuel. Most common biofuels are ethanol and biodiesel. Ethanol can be produced from many resources like corn, sugar beet, or wheat, whereas biodiesel is produced from vegetable oils or animal fats. Both of these biofuels are derived from classic food crops that require high quality agricultural land for growth. But bioethanol, which finds application as petrol additive, can be produced from plentiful, cellulosic biomass resources such as herbaceous and woody plants or agricultural and forestry residues. Annual production of ethanol from all the sources in the U.S. was approximately 13 billion US gallons for the year of 2012.⁶

Other important biofuel is Biodiesel. Biodiesel is a fatty acid alkyl ester obtained from acylglycerides, which are derived from renewable resources like palm, rapeseed, or soy. There are many methods of production of biodiesel but the popular choice is biodiesel produced from transesterification reaction in which oil undergoes transesterification directly with alcohol resulting in a biodiesel molecule.⁷ Typical reaction for biodiesel production through transesterification is shown in Figure 1-3:

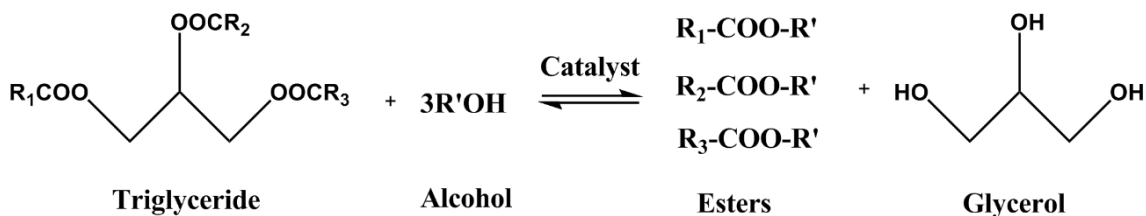


Figure 1-3: Typical biodiesel production reaction⁷

Current biodiesel production in US is shown in Figure 1-4. It is increasing very rapidly every year and recently crossed 1.0 billion gallons of annual production in 2013.⁸

Glycerol or glycerin is the main by-product of this biodiesel production process.

Approximately 1 Kg of glycerol is produced for every 10 Kg of biodiesel.^{9,10} Using this proportion, we can say approximately that production of glycerol as a byproduct from biodiesel plants comes to around 455 kilotons annually as per 2013 statistics, which is quite significant.⁸ On a volumetric basis it comes to about 100 million gallons annually as shown in Figure 1-4.⁸

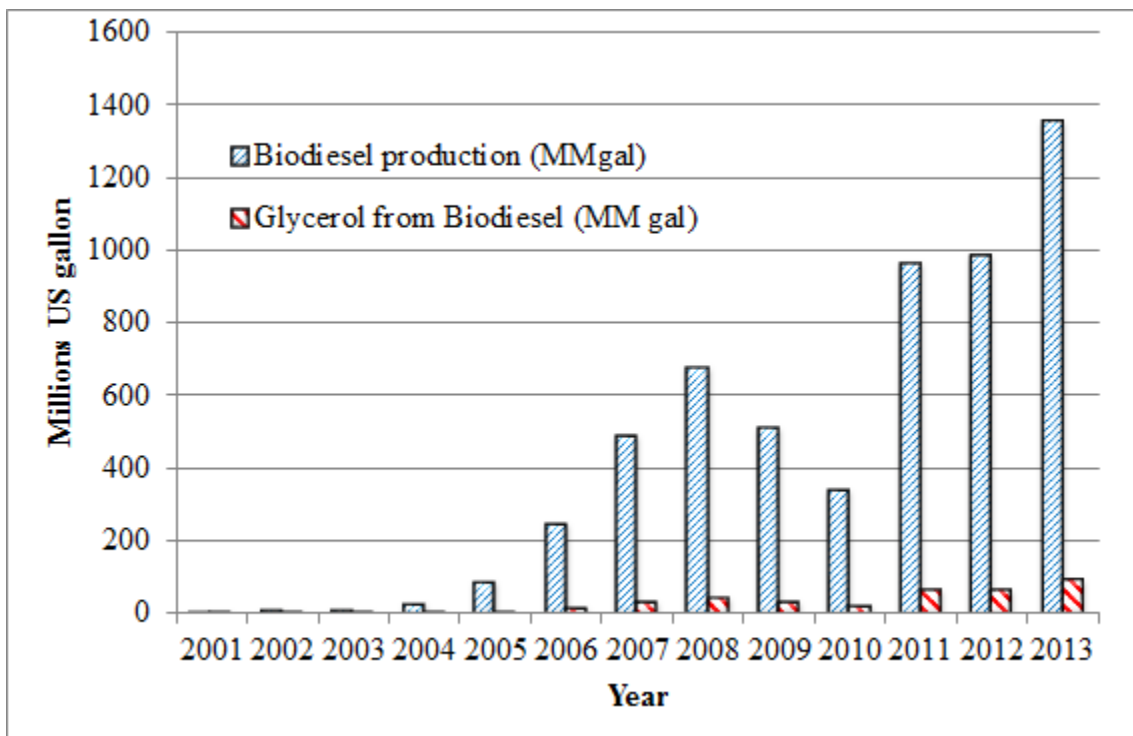


Figure 1-4: Biodiesel and Glycerol production in the United States⁸

1,2,3-propanetriol or glycerol or more commonly called as glycerin is a trihydric alcohol, which is a colorless, odorless, sweet-tasting, low toxicity, syrupy liquid. It belongs to the

class of polyols having 3 hydroxyl groups.¹¹ It is present in the form of glycerides in all animal and vegetable fats and oils. Pure glycerol has many applications in pharmaceutical, cosmetics and food industries. The US Department of Energy in 2004 identified glycerol as one of the twelve building blocks for future production of value added chemicals.¹²

Glycerol obtained from biodiesel production is often classified as a crude glycerol with a purity less than 80%. Refining this crude glycerol to the industrial standard Technical Grade (99.5% purity) is often not economical and hence, has been under constant attention by researchers in search for its direct applications or for its conversion to useful value added derivatives. This research has the potential of making biodiesel production more economical and competitive with gasoline or conventional diesel fuels.⁹

Glycerol can be used to produce many derivatives that have a wide range of applications. Typical examples of glycerol derivatives include glycerol esters, glycerol ethers, glycerol acetals, propanediols, epoxides, glycerol oxidation and dehydration products, and synthesis gas. Out of these, Propanediols such as 1,2-propanediol (1,2-PDO) and 1,3-propanediol (1,3-PDO) are useful as a raw material for production of different kinds of polymers and they themselves can be used as a finished product.¹⁰

Out of these two propanediols, one crucial derivative is 1,2-propanediol or Mono Propylene Glycol (MPG), which is a commodity chemical that can be used in several applications such as antifreeze liquids, coolants, heat transfer fluids, cosmetics, pharmaceuticals, polyurethanes, as a solvent for colorings and flavors, lubricants etc.

Conventionally 1,2-propanediol is manufactured from hydrolysis of propylene oxide with water at temperatures between 125 °C and 200 °C at a pressure of 14 bar.¹³ But a more novel

and eco-friendly way of production is by the hydrogenolysis of glycerol under different reaction conditions around 200 °C, 2 - 5 MPa and a catalyst.^{10,13} Technical grade MPG sells at \$ 0.89/lb¹⁴, more than twice the cost of technical grade glycerol (\$ 0.42/lb)¹⁵, which makes this reaction pathway one of the most attractive. If the crude glycerol (\$ 0.08/lb)¹⁵ obtained from biodiesel could yield high conversions, the process would be even more economical. Chiu et al.¹⁶ proposed that propylene glycol production from glycerol could reduce cost of biodiesel by \$ 0.40/Kg.

Copper chromite is an excellent catalyst for the production of MPG using technical grade glycerol and shows superior performance in obtaining higher yields of 1,2-propanediol. Even though hydrogenolysis of glycerol over copper chromite is already commercialized, there are a few issues that limit the profitability from improving any further. Hydrogenolysis being a complex reaction, a variety of interactions between the reaction components take place and some of them auto catalyze at the reaction temperature to form variety of other byproducts or impurities through side reactions.¹⁴ It is commonly observed that the presence of these byproducts in the smallest of amounts (< 0.5 % v/v), has a significant color and odor effect on the final product solution. These byproducts might have been forming out of polymerization of acetol or conjugation of polymerized acetol products. Color comparison for a mixture of technical grade components and for a final product solution from the hydrogenolysis reaction is shown in the Figure 1-5 below.

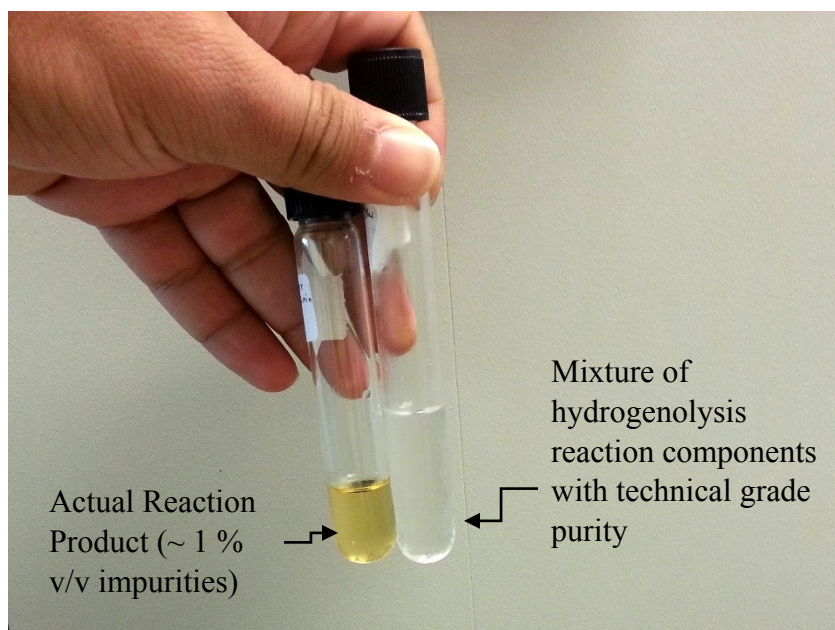


Figure 1-5: Comparison of mixture of reaction products and mixture of pure products

Presence of the color and odor causes a considerable drop in the selling price of MPG.

Removal of the color and odor is possible with the use of distillation but increases cost.

It therefore becomes important to know more about these byproducts by identifying them. It is also important to know how they are formed and what reaction conditions favor their formations. Furthermore, it becomes essential to identify alternative ways by which we can separate or remove them from final product. A study of all these factors will contribute in developing a better understanding of the product formation.

To address these issues, certain objectives were defined for the current work which are summarized below:

Objective 1 Identification of the various impurities formed during the hydrogenolysis reaction.

Identification of the byproducts or impurities is essential and could be done using Mass Spectrometer (MS) in conjunction with Gas Chromatography (GC) technique. The known identity of byproducts will lead us to the possible reaction pathway. This can further guide us to the ways to remove them. As an alternative to the conventional distillation, liquid-liquid extraction could be studied as a possible way to remove impurities.

Objective 2 Kinetic study of the liquid phase glycerol hydrogenolysis reaction over copper chromite

Kinetic study involves study of the speed or rate of the reaction and also involves study of the effect of various parameters on the reaction rate. An understanding of the reaction network will enable us to choose a proper catalyst that would be economical and will have high selectivity for the desired product Mono Propylene Glycol (MPG), and which will give minimal fraction of byproducts. The study can also help in developing future catalysts. It will also provide us with valuable inputs for future research in hydrogenolysis of glycerol and will tell us about optimized conditions or environments in which one can get desirable results.

All these efforts could eventually lead to improved profitability of the hydrogenolysis of glycerol over copper chromite, which is already a commercialized process.

Chapter 2: Literature Review

2.1 Hydrogenolysis of Glycerol

Hydrogenolysis is a reaction that is catalytically carried out in presence of hydrogen and in which C-C bond or C-X bond is cleaved where X could be any heterogeneous element like N, S, O. Since glycerol is a trihydric alcohol having three hydroxyl groups, C-C bond or C-O bond cleavage due to hydrogen is called hydrogenolysis in this context. C-O bond cleavage is thought to be occurring via dehydration whereas, C-C bond cleavage is thought to be occurring due to retro-aldol mechanism.¹⁷ Commonly, hydrogenolysis of glycerol reaction could be presented as shown in Figure 2-1.

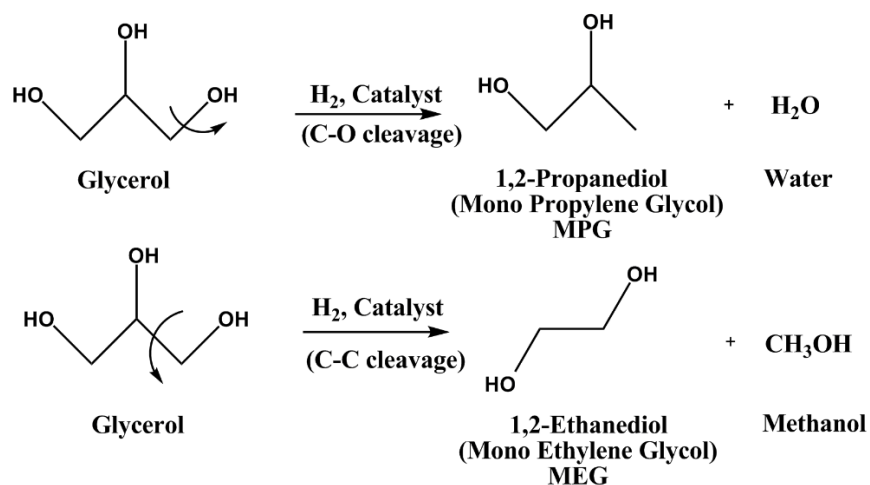


Figure 2-1: Reactions occurring during hydrogenolysis of glycerol

C-C and C-O bond cleavages are competitive reactions and occur simultaneously during the hydrogenolysis of glycerol.¹⁸ However, C-O bond scission is more preferred while preventing C-C scission. It is because, Mono Propylene Glycol (MPG), which is commonly formed via C-O bond scission has more value and applications, than products formed out of C-C scission. That's also one of the reasons why, products formed out of C-C scission are considered as byproducts in the hydrogenolysis reaction.¹⁹

Although, hydrogenolysis of glycerol as shown in Figure 2-1, appears simple, it is not so. In real situation, it is a much more complex process that occurs through multiple intermediates as many consecutive and parallel reactions take place.^{17,20}

Hydrogenolysis reaction is usually carried out in a liquid phase with main reactant being liquid glycerol. Hydrogen, which also takes part in the reaction, is supplied in the gas phase that gets dissolved in the liquid solution and becomes available for the reaction. Catalyst that is usually solid, is either in the suspended form or it is well dispersed within the liquid solution itself. Glycerol from the liquid phase and dissolved hydrogen in the solution get diffused at the interface and subsequently adsorbed on the catalyst surface, and it is at the surface of the catalyst where the hydrogenolysis reaction takes place. Details of the reaction system are discussed in Chapter 3.

Type of catalyst used has significant effect on the type of products formed as some catalysts favor C-O scission over C-C scission and some others favor C-C scission over C-O scission. Hence, it is important to understand what type of catalysts are used and how they perform in the hydrogenolysis reaction.

Before we move to the types of catalyst; it is important to define conversion, selectivity, and the yield, that are used as performance parameters for a catalyst. Dasari et al.¹⁸ defined selectivity as a ratio of the number of moles of desired product produced to the number of moles of reactant consumed. Authors¹⁸ further defined conversion as the ratio of the number of moles of reactant consumed to the number of moles of reactant initially present and Yield was defined as the ratio of number of moles of the desired product formed to the theoretical number of moles of product.¹⁸ Similar definitions were also seen in other literature

reports^{21,22} that are based on carbon balance. Values based on these definitions are presented throughout this thesis.

2.2 Catalyst Types

Three types of catalysts that can be used for hydrogenolysis of glycerol are: homogeneous, heterogeneous, and biocatalysts. For hydrogenolysis, homogeneous catalysts particularly used are Pt-group, either in complexes of iodocarbonyl compounds²³ or in phosphorus, arsenic, and antimony ligands²⁴ as reported by Behr et al¹⁰. But selectivity for 1,2-PDO is generally below 25 % that makes it economically less viable. Processes involving use of biocatalysts are still under development and nothing could be said right now, about its selectivity, conversion achievable, etc.¹⁰

Heterogeneous catalysts typically involve metallic ones or bimetallic ones involving Cu, Pt, Pd, Ni, Ru with a support like C or precursors etc. Out of these three types of catalysts, heterogeneous type provides maximum glycerol conversion and selectivity towards 1,2 PDO and hence, these type of catalysts are mostly researched for hydrogenolysis to make process economically viable.

2.2.1 Heterogeneous Catalysts

Various heterogeneous catalysts (especially metallic) have been studied for this reaction and their activity could be ordered in $\text{Pd} \approx \text{Cu} \approx \text{Ni} > \text{Pt} > \text{Ru}$ as suggested by Chheda et al.²⁵ Recent studies are focusing on bimetallic catalysts like Ru-Re^{20,21}, Pt-Ru²⁶, Au-Ru²⁶, Ru-Cu²⁷, Raney[®]Cu¹⁹, Raney[®]Cu-Cr²⁸, etc. Some studies are done using oxides of these metals and their combinations like Cu-ZnO^{29,30}, Cu-Al₂O₃³¹, Cu-ZnO-Al₂O₃²⁹, CoO³². Some studies

indicated use of promoters like Ba, Al, Zn, etc.³³ More recent studies show incorporation of nano-particles in catalysts to improve selectivity. However, mostly studied catalysts are Cu based as they show superior performances.³⁰ Summary of the performance of copper based catalysts is presented in the next section, Section 2.2.1.1. Selectivity towards MPG and conversion of glycerol results reported in various literatures for non-copper catalysts are summarized in Table 2.1.

Table 2.1: Performance of non-copper catalysts in hydrogenolysis of glycerol

Type of Catalyst	Catalyst	Max. Glycerol Conversion	1,2-PDO selectivity	Temperature (K)	Pressure (bar)
Ru based Catalysts	Ru-TiO ₂ ³⁴	93.0 %	45.0 %	463 K	100 bar
	1% Ru-1% Re/C ²¹	57.7 %	36.6 %	493 K	69 bar
	1 % Ru-C ²¹	52.1 %	18.9 %	493 K	69 bar
Co based Catalysts	Co nanoparticles ³²	70.6 %	57.8 %	473 K	20 bar
	CoO ³²	67.7 %	50.5 %	473 K	20 bar
Ni based Catalysts	Raney Ni ³⁵	80.0 %	54 %	503 K	40 bar
Pt based catalysts	Pt/C (base catalyzed) ³⁶	92.0 %	46 %	473 K	40 bar

2.2.2.1 Cu based catalysts

Cu based catalysts show very good results for the production of MPG. This is because Cu helps in hydrogenolysis i.e. selectively breaking C-O bond, instead of the undesired C-C bond thereby giving maximum selectivity and less byproducts. Also, they are cheap when compared to noble metals like Ru, Pt, Ni, Re.³⁷ Results for performance of all commonly used copper based catalyst is summarized in Table 2.2. It also summarizes performance of copper chromite catalysts that show superior performance than other Cu based catalysts.

Table 2.2: Performance of the copper based catalysts in hydrogenolysis of glycerol

Type of Catalyst	Catalyst	Max. Glycerol Conversion	1,2-PDO selectivity	Temperature (K)	Pressure (bar)
Cu Based Catalysts	Cu-ZnO (50:50) ³⁰	37.0 %	92.0 %	473 K	20 bar
	Cu-ZnO-Al ₂ O ₃ ²⁹	81.5 %	93.4 %	493 K	40 bar
	Raney Cu ¹⁹	100.0 %	94.0 %	473 K	14.8 bar
	Cu-ZnO ²⁸	7.8 %	51.3 %	473 K	14 bar
	CuO ²⁸	4.0 %	76.8 %	473 K	14 bar
	Cu-Al ₂ O ₃ ³¹	55.4 %	61.1 %	573 K	30 bar
Copper Chromite Catalysts	Cu-Cr (Ba promoter) ³³	65.0 %	91.0 %	493 K	30 bar
	Cu-Cr (1:3) ³⁷	80.0 %	83.9 %	493 K	80 bar
	Cu-Cr(4) ²²	85.9 %	98.5 %	483 K	41 bar
	Cu-Cr (Pd promoter) ³⁸	83.4 %	92.9 %	493 K	40 bar
	CuCr ₂ O ₄ ¹⁸	54.8 %	85.0 %	473 K	13.8 bar
	CuCr ₂ O ₄ ³⁹	76.9 %	90.7 %	483 K	30 bar

2.3 Kinetics of Hydrogenolysis of Glycerol

Very few studies have been done on kinetics of hydrogenolysis of glycerol. Some efforts have been taken to analyze kinetics of the reaction based on byproducts formed. It is known that a series of reactions occur during hydrogenolysis leading to gas and liquid phase products like 1,2- PDO, 1,3- PDO, ethylene glycol, methanol, ethanol, and propanol.²¹

Usually type of intermediates and type of products formed, depends on the type of catalyst being used. In fact, type of catalyst used greatly influences hydrogenolysis.^{22,40} Also, pH of a solution has significant influence on hydrogenolysis of alcohol.^{22,40} Formation of 1,2-PDO via glyceraldehyde is favored under alkaline conditions.⁴¹ But, under acidic conditions 1,2-PDO is formed by direct dehydration and subsequent hydrogenation via acetol.⁴² Hence, different researchers report different mechanisms as discussed below.

Montassier et al.⁴³ was the first one to suggest the mechanism: through Glyceraldehyde intermediate as shown in Figure 2-2. They proposed that glycerol is converted first to glyceraldehyde through its enolic tautomers. Glyceraldehyde undergoes further hydrogenation to MPG.⁴³

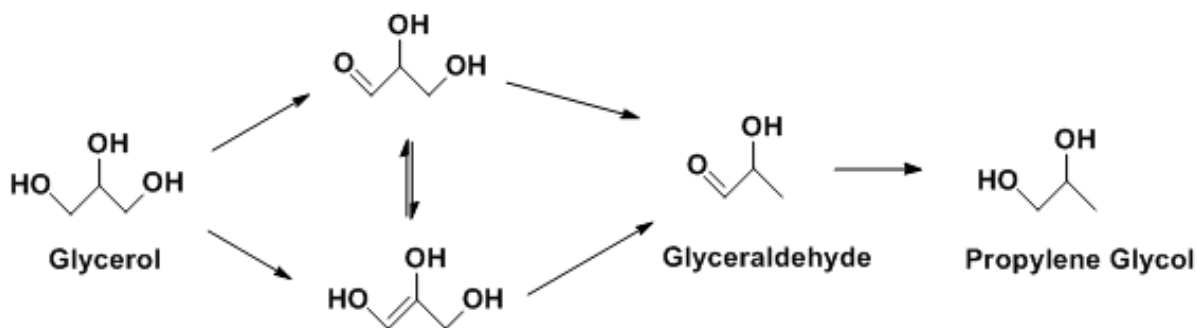


Figure 2-2: Reaction mechanism proposed by Montassier et al.⁴³

Dasari et al.¹⁸ suggested mechanism through acetol intermediate as shown in Figure 2-3.

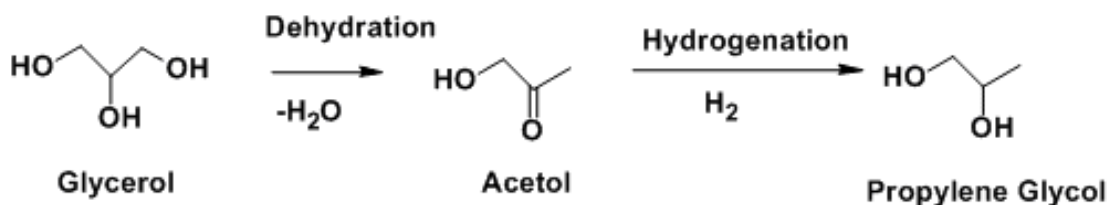


Figure 2-3: Reaction mechanism proposed by Dasari et al.¹⁸

Their reaction study by isolating intermediates showed that acetol was being formed and hence, they proposed a two-step reaction mechanism as shown above in Figure 2-3. Dasari et al.¹⁸ studied this reaction at 200 °C and mild pressure of 200 psi.

Wang et al.²⁸ suggested mechanism through either acetol intermediate or glycidol intermediate as shown below in Figure 2-4. They used Cu-ZnO catalyst around temperature range of 200-220 °C at a pressure of 4.2 MPa with 20 wt% initial glycerol content. They

proposed that dehydration occurs at acid sites resulting in either acetol or glycidol, which undergoes hydrogenation on Cu surface.²⁸

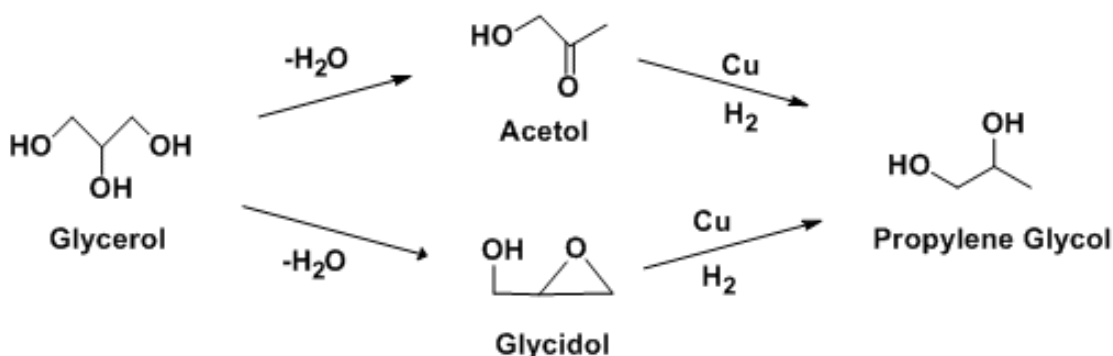


Figure 2-4: Reaction mechanism proposed by Wang et al.²⁸

Torres et al.²¹ suggested following mechanism as shown in Figure 2-5 through glyceraldehyde intermediate as a possibility over Ru/Re catalyst. Their results suggested EG, propanol, and lactic acid as liquid phase byproducts.²¹

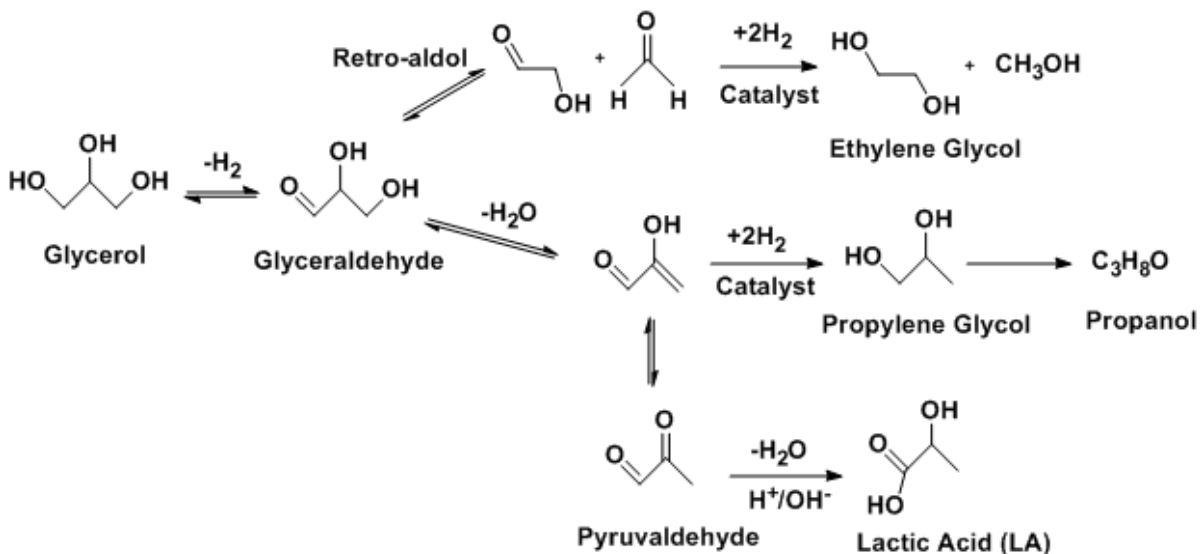


Figure 2-5: Reaction mechanism for liquid phase products by Torres et al.²¹

They kinetically modeled hydrogenolysis network over Ru/Re catalyst using a batch slurry reactor to perform several experiments, in which gas and liquid distributions were measured.

Experiments were performed at different glycerol concentrations and catalyst loading, in presence and absence of H₂ over a temperature range of 453-493 K. They found Re to have a promoter effect for the selectivity to 1,2-PDO as well as liquid-phase products, such as EG, propanol, and ethanol, but had no effect on the activity of glycerol. They reported activation energy for glycerol conversion to 1,2-propanediol over Ru-Re to be 54.19 kJ/mol.²¹

In a most recent study by Vasiliadou et al.⁴⁴, kinetic modeling of liquid-phase glycerol hydrogenolysis over Cu/SiO₂ catalyst was done. Their results also confirmed one of the commonly proposed mechanisms that glycerol hydrogenolysis reaction proceeds via two-step mechanism of dehydration-hydrogenation with different intermediates (acetol for 1,2-propanediol formation and 3-hydroxypropionaldehyde for 1,3-propanediol formation). They also found that glycerol consumption and 1,2-propanediol formation rate was highly influenced by reaction temperature, hydrogen pressures, and dilution. They proposed reaction mechanism and rate equations as follows in Figure 2-6.⁴⁴

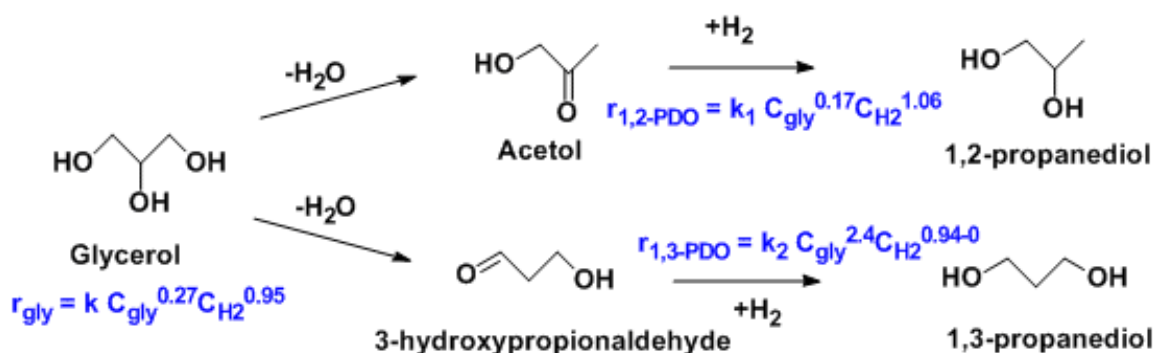


Figure 2-6: Reaction mechanism proposed by Vasiliadou et al.⁴⁴

Their study found activation energy to be around 96.8 kJ/mol for glycerol consumption and around 94.3 kJ/mol for 1,2-propanediol formation.

Reaction to intermediate Acetol has been confirmed by many researchers throughout time over Cu catalyst in which hydrogenolysis is a two-step process.^{18,19,22,22,28,30,37,45} The first step is formation of acetol by dehydration of glycerol and the second step will be hydrogenation of acetol to propylene glycol.

2.3.1 Dehydration of Glycerol

Glycerol is converted to acetol either directly through dehydration, or via glyceraldehyde (dehydrogenation, dehydration) route.²² Dehydration step, which is confirmed by many researchers, is found to be promoted on acidic supports.^{18,37,46} These acidic supports effectuate the dehydration step to yield acetol from glycerol.^{47,48} This could be due to elimination reaction being favored by acid catalysts, as dehydration occurs selectively on lewis acid sites^{45,46} and carbonylation reaction getting promoted by transition metal catalyst. That is why popular catalysts used in this production are metal supported acid catalysts.^{45,46}

Acetol or 1-hydroxyacetone that is highly reactive, has both hydroxyl and carbonyl groups present in its structure. It is hygroscopic, and miscible with other liquids like ethanol, ethyl ether, etc. Acetol finds extensive uses in food industry, organic synthesis, tanning industry, textile industry, etc. Presence of catalyst, influences production of acetol from glycerol. Propylene glycol produced from acetol has a low production cost.⁴⁶ Acetol made from petroleum costs \$ 12.5/Kg whereas acetol produced from biomass sources could cut production cost to \$ 1.25/Kg.⁴⁹

Xiao et al.²² observed that the selectivity towards acetol increased with increase in temperature and decreased with increasing pressure. Authors²² explained this using the

observations made by Huang et al.⁵⁰ who observed acetol formation to be thermodynamically favorable and acetol hydrogenation getting limited by thermodynamic equilibrium.

A previous report¹⁷ suggests that glycerol has higher affinity for adsorption at active catalyst sites than 1,2-PDO. Catalysts had sufficient reaction sites for glycerol and 1,2-PDO conversion at low glycerol concentrations.¹⁷ Xiao et al.²² observed that as the concentration of glycerol increased, reaction sites for 1,2-PDO converting to 1-Propanol (1-PO) were occupied by glycerol that resulted in the increase of 1,2-PDO selectivity. Their results indicated that the copper species are mainly responsible for the glycerol conversion.²²

2.3.2 Propylene glycol formation

The second step of hydrogenolysis that is hydrogenation, occurs on metal site, usually on Cu for Cu based catalysts.⁴⁵ This hydrogenation step is a faster step as compared to dehydration as it is favored at low reaction temperature and high hydrogen partial pressure from chemical equilibrium viewpoint.⁵⁰ Further, hydrogenation step can become the predominant step upon increase of hydrogen pressure forming negligible acetol.^{31,45,47}

Zhou et al.²⁹ observed that high conversion of glycerol is favored by high temperature and pressure and high selectivity of propylene glycol is favored by low temperature and pressure.

Balance between these two steps is necessary for better yields of propylene glycol.

2.4 Glycerol Hydrogenolysis over Copper Chromite

Starting from 2005 publication of Dasari et al.¹⁸ research got focused onto hydrogenolysis of glycerol over copper chromite and then many research groups have studied various aspects of

hydrogenolysis reaction over copper chromite. Table 2.2 above has already summarized the work done by various authors on Cu-Cr catalyst.

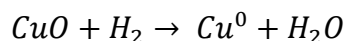
Before Dasari et al.¹⁸ studied glycerol hydrogenolysis over copper chromite, conditions used by researchers were very harsh and had to carry out hydrogenolysis at pretty high temperatures and extremely high pressures that had limited this reaction to lab scale only. Dasari et al.¹⁸ studied this reaction at mild temperatures and pressures and obtained pretty good results by getting a conversion of almost 55 % with MPG selectivity of 85 %. This result prompted major thrust in this research area and this process was commercialized in the following few years.

Various parameters like temperature, pressure, catalyst weight, agitation, etc. and their influence on the hydrogenolysis reaction over copper chromite catalysts, have been studied by different researchers over time. These studies have been summarized in the sections that follow.

Before we discuss effect of various parameters, it is important to understand the copper chromite catalyst. Copper chromite is a tetragonally distorted normal spinel, in which copper ions are distorted towards square than a tetrahedron and chromium ions at some distance from their ideal positions.⁵¹ Cu-O-Cu bond angle is around 103° instead of 109° for a regular tetrahedron.⁵¹ Properties and preparation methods of copper chromite have been discussed in subsequent chapters.

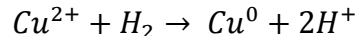
The structure and mechanical features of copper chromite catalyst before activation by reduction and after reduction have also been studied by Khasin et al.⁵² Authors observed the presence of metallic copper phase when the catalyst was treated with a hydrogen flow at

different temperatures of 250, 320 and 450 °C. Also they observed only 0.5 % weight loss due to copper reduction in the reduction temperature range of 180-450 °C. Copper oxide (CuO) traditionally reacts with hydrogen as shown below, eliminating water.⁵²



This traditional mechanism contributes only 7% weight loss, which they attributed due to copper cations.⁵² But their further study using XRD results showed 42-55% reduction of Cu²⁺.

Volumetric kinetic study reaffirmed this reduction in which amount of hydrogen consumed in the reaction was much higher than the amount of water formed. Hence, they proposed following route to be the main reduction route for Cu²⁺



in which they observed absorption of protons up to 0.9 hydrogen atoms per one copper chromite formula unit in the oxide structure. These protons are known to display excellent activity in hydrogenation reactions.⁵² This process of reducing Cu²⁺ to Cu⁰ is known as the reduction and Cu⁰ is the site where the reactions take place. Hence, in order to activate catalyst, reduction of catalyst under H₂ environment at a preset temperature is necessary for superior performance.

2.4.1 Effect of catalyst activation on hydrogenolysis of glycerol

A study done by Wolosiak-Hnat et al.³¹ showed that selectivity of MPG was highly influenced by the activation of the catalyst through reduction process due to the formation of

metallic copper phase. Results obtained by Wolosiak-Hnat et al.³¹ further showed that co-precipitated copper chromite catalysts manufactured in the lab had more crystallinity and displayed 200 % increase in the MPG selectivity upon activation as compared to 58 % increase upon activation in commercial copper chromite catalyst. Homogeneity and presence of spherical agglomerates in the co-precipitated catalysts was attributed as a reason for the improved MPG selectivity.³¹ A crystalline homogeneous structure might be necessary for better incorporation of hydrogen in the structure. Further, activation of the catalyst under a stream of hydrogen is an important aspect from the commercial point of view.

2.4.2 Effect of catalyst activation time on hydrogenolysis of glycerol

A study done by Wolosiak-Hnat et al.³¹ showed that longer the catalyst activation time, higher was the acetol selectivity. Authors had further observed considerable variance in the conversion of glycerol and the selectivity towards MPG as the catalyst activation time was changed. The best result in terms of glycerol conversion and MPG selectivity was obtained for an activation time of 8 hrs. Beyond this activation time, sintering of copper particles due to epitaxial bond breaking was observed by the authors³¹ that dropped down the glycerol conversion by 5% from 8 hrs of activation time to 24 hours of activation time, while MPG selectivity increased by 4 % from around 66 % to 70 %. Authors³¹ finally concluded that 8 hrs of activation time was the best from the overall performance point of view.

2.4.3 Effect of catalyst activation temperature on hydrogenolysis of glycerol

A study done by Dasari et al.¹⁸ on the effect of catalyst activation temperature showed that selectivity towards MPG increased steadily from 40 % at 150 °C to 85% at 300 °C after which a 25 % drop was observed till 400 °C. A similar catalyst activation temperature was

recommended by Wolosiak-Hnat et al.³¹ who had also observed best glycerol conversion and MPG selectivity results at this activation temperature. Interestingly, catalysts used in both the cases were different. Dasari et al.¹⁸ tested commercial copper chromite by Sud Chemie whereas Wolosiak-Hnat et al.³¹ had tested lab prepared copper chromite, but both reported similar results. This similarity might be due to the reduction mechanism that copper chromite undergoes during activation, which seems to be unaffected by the composition of the catalyst. These results further tell that the activation temperature of the catalyst can also be a critical aspect for a better catalyst performance.

2.4.4 Effect of reaction temperature on hydrogenolysis of glycerol

It was commonly observed in the literature that when the reaction temperature was increased glycerol conversion increased irrespective of the type of copper chromite used. Extents of increase in the glycerol conversions were however different in each case. Dasari et al.¹⁸ reported 47 % increase in the glycerol conversion when temperature was raised by 50 °C from 150 °C to 200 °C. Wolosiak-Hnat et al.³⁹ at 2 MPa pressure however, observed around 25 % increase when the temperature was raised from 180 °C to 230 °C. Wolosiak-Hnat et al.³⁹ at 3 MPa pressure reported different trend in the glycerol conversion. Authors³⁹ observed that glycerol conversion rose by 30 % when temperature was raised by 30 °C from 180 °C to 210 °C and further increase till 230 °C did not make any significant difference (~1.5 %) to the glycerol conversion values that stayed around 60 %. Authors³⁹ attributed this difference to the drop in the degradation of glycerol and MPG, to lower alcohols at higher hydrogen pressures. (3 MPa as compared to 2 MPa)

Dasari et al.¹⁸ at 1.5 MPa observed that selectivity of MPG increased by around 55 % when the reaction temperature was changed from 150 °C to 200 °C and decreased by 80 % afterwards till 260 °C. Dasari et al.¹⁸ observed highest MPG selectivity of 85 % at 200 °C. Wolosiak-Hnat et al.³⁹ at 2 MPa observed similar trend in that selectivity towards MPG rose 20 % when temperature was raised by 20 °C from 180 °C to 200 °C. Beyond 200 °C, MPG selectivity dropped by 20-25 % to 230 °C. Interestingly, same authors at 3 MPa observed that selectivity towards MPG increased by 10 % from 180 °C to 190 °C. After 190 °C, further changes in the reaction temperature produced only 1 % rise per 10 °C rise in the reaction temperature.

In contrast to the results above, Rode et al.⁵³ at 5.2 MPa observed a minimal decrease of 2-3 % in MPG selectivity when the reaction temperature was raised from 180 °C to 220 °C and a marginal decrease of around 5 - 7 % in the MPG selectivity, when the reaction temperature was raised from 220 °C to 240 °C. Xiao et al.²² at 4.1 MPa, similarly, observed significant decrease of almost 50 % in the MPG selectivity upon rise in the reaction temperature from 180 °C to 230 °C. These authors further observed increase in the byproduct selectivity at higher temperatures, out of either excessive hydrogenolysis^{18,53} or C-C bond breaking⁵³ at higher temperatures that led to the drop in MPG selectivity. Wolosiak-Hnat et al.³⁹ however attributed catalyst deactivation as the reason for the drop in MPG selectivity.

Although results observed by the authors were contrasting, they might be due to studying the effect of reaction temperature at different pressures of H₂. It seems like, if the hydrogen pressure is towards low side around 1 – 2.5 MPa, effect of temperature will show a rise till a certain maximum in MPG selectivity is reached after which, a drop in the MPG selectivity will be observed. At higher pressures, 3.5 – 5.2 MPa, MPG selectivity will drop down

drastically with the rise in the reaction temperature. This might be due to relative effects of the temperature and pressure on the hydrogenolysis reaction. At relatively higher pressures, pressure might be playing an accountable role in addition to the reaction temperature.

Furthermore, all these results indicate that an optimum reaction temperature is required for better MPG selectivity, less byproducts, and better catalyst lifetime. This optimum temperature would come around 200-210 °C, but depending on the exact composition of the catalyst, these values may differ as well.

2.4.5 Effect of hydrogen pressure on hydrogenolysis of glycerol

In the lower pressure range, from 0.35 MPa to 1.8 MPa, Dasari et al.¹⁸ had observed an increase in the glycerol conversion and an increase in the selectivity towards acetol.

Effect of hydrogen pressure on hydrogenolysis of glycerol has shown contrasting results in the literature. Rode et al.⁵³ in the batch mode, observed a marginal drop in the conversion of glycerol from 34 % to 27 %, when hydrogen pressure was increased from 3.5 MPa to 6.7 MPa. Wolosiak-Hnat et al.³⁹ and Xiao et al.²² however, had observed an increase in the conversion of glycerol from 30 % to 48 % and 32 % to 58 % respectively, when the hydrogen pressure was increased around the same pressure range.

In the case of selectivity towards MPG, Rode et al.⁵³ and Xiao et al.²² observed a drop from 84 % to 77% and from 84 % to 44 %, respectively, when the hydrogen pressure was increased to 5 MPa. Wolosiak-Hnat et al.³⁹ however, had observed an increase in the selectivity towards MPG when the pressure was increased in the same range from 3.5 MPa to 5.5 MPa.

Wolosiak-Hnat et al.³⁹ and Xiao et al.²² have reported drop in the selectivity of acetol when the hydrogen pressure was increased.

All these contrasting results in the same pressure range might have been due to different initial glycerol content that was (20 wt% in the case of Rode et al.⁵³, 60 wt% in the case of Xiao et al.²², and 80 wt% in the case of Wolosiak-Hnat et al.³⁹), or due to the difference in the catalyst weights (~1 wt% in the case of Rode et al.⁵³, 5 wt% in the case of Xiao et al.²², and 6 wt% in the case of Wolosiak-Hnat et al.³⁹), or due to different temperatures (200 °C, 210 °C and 220 °C). Another difference in their conditions was the dilution solvent, which was 2-propanol in the case of Rode et al.⁵³ whereas water was used in the case of Wolosiak-Hnat et al.³⁹ and Xiao et al.²² Presence of 2-propanol might have an effect on 2-PO production reaction equilibrium but not on the acetol hydrogenation. Out of all these different parameters, temperature seems to be the more prominent parameter for the differences in results.

2.4.6 Effect of addition of promoters to the catalyst on hydrogenolysis of glycerol

Mane et al.³³ studied effect of addition of small amounts of Ba, Al, and Zn to the copper chromite catalyst and further its effect on hydrogenolysis of glycerol. These small additions act as promoters that enhance the catalyst activity to a certain extent. Authors³³ observed that Ba promoted catalyst gave highest glycerol conversion and highest selectivity towards MPG because of the stability of Cu⁰ phase, strong acid characteristics, and the inhibition of agglomerate formation of catalyst particles with the addition of Ba.

Best performance of Ba promoted copper chromite was obtained when Ba content was 30 wt% beyond which, a loss in the hydrogenation activity originating from the inhibition of Cu migration from bulk to the surface, was observed.³³

Kim et al.³⁸ studied the effect of the addition of Pd to the catalyst and on the conversion of glycerol and the selectivity towards MPG. Pd was found to be highly dispersed and indistinguishable, which underlined its role in the reduction process.³⁸ Kim et al.³⁸ further observed a decrease in the strength and amount of the acid sites, upon addition of small amounts of Pd. But, a drastic rise in Bronsted acid characteristics was observed that indicated significant activity in the dehydration reaction.³⁸

Pd with 0.5 wt% in copper chromite was found to be a stable and very effective catalyst for the bio-renewables industry; that showed highest yield of 77.4 % with glycerol conversion of 83.4 % and 92.9 % of MPG selectivity in 12 hours.³⁸

2.4.7 Effect of catalyst weight on hydrogenolysis of glycerol

A study performed by Dasari et al.¹⁸ of the effect of catalyst weight on the hydrogenolysis reaction showed that glycerol conversion increased as the amount of catalyst increased due to more surface area availability. But MPG selectivity increased by 22 % from 63 % at 1 wt% of catalyst (glycerol basis) till 85 % at 5 wt% of catalyst and further increase in the catalyst weight to 8 wt% lowered the MPG selectivity by 23 %, which was thought to be due to the formation of lower alcohols through excessive hydrogenolysis.¹⁸ Similar effects on the glycerol conversion and MPG selectivity were observed by Rode et al.⁵³ and Wolosiak-Hnat et al.³⁹ irrespective of the temperature and pressure differences in all the three studies.

Rode et al.⁵³ had also suggested that higher catalyst amount leads to higher acetol hydrogenation rate, thus lowering the acetol selectivity. Further it was observed by the authors⁵³ that selectivity towards byproduct MEG was, however, unaffected. Wolosiak-Hnat et al.³⁹ however, observed mixed response for the selectivity towards acetol and other byproducts and found 8 wt% to be the optimum catalyst weight for best results.

2.4.8 Effect of initial glycerol content on hydrogenolysis of glycerol

Dasari et al.¹⁸ and Wolosiak-Hnat et al.³⁹ observed an increase in the glycerol conversion and MPG selectivity, when the initial glycerol content was increased from 20 wt% to 80 wt%.

Both of these studies were done in aqueous glycerol solutions.^{18,39} Dasari et al.¹⁷ had observed degradation of the reaction product due to polymerization, when the initial glycerol content was decreased. Dasari et al.¹⁸ had further recommended use of around 80-90 wt% of initial glycerol for a better balance between MPG selectivity and the reactor volume.

Wolosiak-Hnat et al.³⁹ also got best results in terms of glycerol conversion and MPG selectivity at initial glycerol content of 80-90 wt%. Xiao et al.²² observed increase in the glycerol conversion and MPG selectivity throughout, when the initial glycerol content was changed from 20 wt% to 100 wt%. All these researchers have suggested shifting of the equilibrium of dehydration reaction from forward direction to the backward in presence of water, to be the main cause of low conversion at low glycerol contents.^{18,22,39}

In contrast to all these results, Rode et al.⁵³ in the batch mode, observed drastic decrease in the conversion of glycerol with the increase in the initial glycerol content. It was attributed to the lack of sufficient catalytic sites due to a fixed catalyst weight as compared to available glycerol molecules that were increased.⁵³ MPG selectivity was however, marginally

decreased and MEG selectivity almost doubled with increase in glycerol loading.⁵³ One interesting thing to be noted was that Rode et al.⁵³ had used 2-propanol as dilution solvent rather than water. Considering the reaction equilibrium for the hydrogenation of MPG that forms 2-propanol, presence of 2-propanol as a dilution solvent should shift the reaction in the backward direction, which explains the drop in the 2-propanol selectivity as observed by Rode et al.⁵³ It was also worth noting that if the solvent was 2-propanol itself, how could its selectivity be measured (as it will be in excess) by GC analysis?

2.4.9 Effect of agitation on hydrogenolysis of glycerol

Since no study on the effect of agitation on glycerol conversion and MPG selectivity was studied earlier, Wolosiak-Hnat et al.³⁹ studied that influence. They found that as the stirring speed or agitation was increased from 100 RPM to 1250 RPM, glycerol conversion showed a substantial increase in conversion from 76.9 % to 85 % till around 500 RPM after which, it increased only marginally from 85 % to 90.8 %. This indicated that at higher stirring speeds, more glycerol conversion was obtained, which would be due to more rapid transport of mass onto the catalyst surface and more contact time. MPG selectivity however, showed a reverse response as compared to the conversion. MPG selectivity decreased sharply from 90.7 % at 100 RPM to 62 % at 500 RPM after which, it steadily decreased to 54.3 % till 1250 RPM. They concluded that vigorous stirring might be causing C-C bonds to break and selectivity towards byproducts to increase.³⁹

In contrast, a study done by Xiao et al.²² of the effect of RPM on glycerol conversion and MPG selectivity showed that increase in the rotation speed from 300 RPM to 900 RPM increased glycerol conversion from 73.4 % to 85.9 % and MPG selectivity from 84.6 % to

98.5 %. Also, they observed that below 300 RPM speed, at 150 RPM, glycerol conversion was very less almost 49.2 % with MPG selectivity of 59.7 %, which they attributed to diffusion retardation of the reaction and mass transfer limitations.²² Their results are also indicative of higher mass transfer at high speeds causing rise in conversion and selectivity.²²

Based on concentration-time profiles at different RPM, Xiao et al.²² concluded that faster stirring gave faster hydrogenation rate. However, Wolosiak-Hnat et al.³⁹ concluded that stirring speed did not significantly influence rate of acetol hydrogenation. This difference in the hydrogenation rate might have arisen from the differences in other parameters. Xiao et al.²² studied effect of RPM at 210 °C, 4.1 MPa, and 5 wt% catalyst (based on glycerol); Wolosiak-Hnat et al.³⁹ had studied at 210 °C, 3.0 MPa, and 8 wt% catalyst (based on glycerol).

Furthermore, catalyst composition in the case of Xiao et al.²² consisted of Cu to Cr molar ratio of 4 whereas in the case of Wolosiak-Hnat et al.³⁹, it was close to 1. It has already been seen that Cu⁰ is the main component that facilitates hydrogenation, so more copper content and higher hydrogen pressure might have been the reasons of higher hydrogenation rate in the case of results of Xiao et al.²² as compared to the results of Wolosiak-Hnat et al.³⁹

2.4.10 Effect of Cu to Cr ratio in the catalyst over hydrogenolysis of glycerol

Kim et al.³⁷ studied promotion effect of Cr on Cu catalyst in hydrogenolysis of glycerol reaction. They prepared copper chromite catalysts by mixing Cr to Cu in different ratios, starting from 0 % chromium till 100 %, which is complete chromium. They analyzed these catalysts using X-ray Diffraction (XRD), X-ray Photoelectron Spectroscopy (XPS) techniques, and for reducibility measurements, Temperature Programmed Reduction (TPR)

technique was used. For acidity measurements, Temperature Programmed Desorption of Ammonia (NH₃-TPD) technique was used. Their study indicated that the formation of the Copper Chromite (CuCr₂O₄) spinel phase was favorable in copper and chromium mixtures only. Out of the various catalyst ratios studied, catalyst that showed highest acidity was the one having Copper to Chromium ratio of 0.33. It showed the largest amount and highest temperature of desorbed ammonia.³⁷ In general, first step of hydrogenolysis reaction that is the dehydration of glycerol, is favored by acidic conditions³⁰ and hence, it was expected from the catalyst having Copper to Chromium ratio of 1:3 to show good catalytic activity in the dehydration reaction and their results confirmed it. It was also confirmed from their results that reduced copper chromite catalysts have high activity in hydrogenation reactions that was previously observed by various researchers.³⁷ Largest amount of hydrogen was desorbed in copper chromite catalyst with Cu:Cr ratio of 1:3, which also contained highest amount of copper chromite spinel structures, imparting this catalyst very high catalytic activity for hydrogenation reactions. Further analysis of their reduced catalyst samples with different copper to chromium ratios indicated that chromium was not an active site for Cu/Cr catalysts in hydrogenolysis reaction. Their results showed a conversion of 80.3 % with 83.9 % MPG selectivity and a total yield of 67.4 % for a 24 hr reaction on Copper Chromite catalyst with a Cu:Cr ratio of 1:3.³⁷

A study done by Xiao et al.²² on the effect of Cu:Cr molar ratio on the surface area showed strong influence. Their results also showed that high copper loading produced samples with less surface areas and they attributed it to the aggregation of copper at high temperature. As chromium content was increased, the surface area of the sample started increasing. Sample with 1:5 molar ratio of Cu:Cr gave 88 m²/g of surface area whereas, sample with Cu:Cr

molar ratio of 1:2 gave a surface area of 33 m²/g. They concluded that Cu-Cr molar ratio can control the surface area.²²

Kim et al.³⁷ studied the effect of preparation method on the structure and the catalytic activity of Cu-Cr catalyst. Authors prepared catalysts having different Cu:Cr molar ratios using two different techniques: impregnation and precipitation. Structural analysis and characterization was done using XRD technique. Reducibility of the prepared catalysts was examined using Temperature Programmed Reduction (TPR) technique. Binding energies were calculated using X-ray Photoelectron Spectroscopy (XPS) and the catalytic activities of the prepared catalysts were evaluated by studying conversion and selectivity in hydrogenolysis of glycerol.³⁷

XRD results indicated independence of copper species from chromium species in impregnated catalysts whereas, in the case of precipitated catalysts, authors³⁷ observed formation of solid solution by elemental copper with chromium. Analysis by the H₂-TPR showed presence of variety of copper species in the catalyst, including bulk state copper and copper species interacting with chromium support. However, in the case of precipitated catalysts, H₂-TPR showed the formation of a single phase structure that affirmed their XRD results.³⁷ Changes in the diffraction pattern prompted them that CuO species are converted to Cu⁰ species during reduction and the transformation of phase from the tetragonal spinel phase to the cubic spinel phase was affirmed as reported by Makarova et al.⁵⁴ Precipitated catalyst however, had low reducibility suggesting difficulty in changing a solid solution spinel structure. Precipitated catalyst also required higher temperatures for reduction, affirming their XRD results. XPS analysis of reduced catalyst samples showed that impregnated catalysts mostly contained Cu⁰ as the surface copper species and in the case of

precipitated catalysts, Cu^{2+} species were large in number post reduction, showing a binding energy of 934.0 eV. Cu^0 surface species corresponded to a binding energy of 932.4 eV.³⁷ Hydrogenolysis of glycerol over these prepared catalysts showed that the catalyst sample prepared by precipitation method was catalytically more active than the catalyst prepared by impregnation. Study over this reaction also showed that more the copper, more is the activity affirming requirement of high copper content for better yields. Cr_2O_3 , the oxide form of chromium was found to be acting as a support for the copper particles and no significant promotion effect was observed due to it. Their catalyst activity study of the impregnated sample with chromium and without chromium, however, showed that a polymerized compound was getting formed as a byproduct under the presence of chromium and so they conferred that chromium support was causing cracking of products and production of polymerized byproducts. This was not observed by them in the case of precipitated catalysts that showed very small fraction of byproducts getting formed. They attributed this high catalytic activity of the precipitated ones to the formation of a uniform spinel structure that was found to maintain its intactness even after reduction.³⁷

XRD analysis done by Xiao et al.²² on the copper chromite catalyst, showed higher degree of crystallinity and crystal growth at higher copper loading in the catalyst. Furthermore, XRD and HRTEM results showed the formation of CuO and CuCr_2O_4 phases that was thought to be thermodynamically favorable in mixtures of Cu and Cr. Other analyses like Energy Dispersive X-ray Spectroscopy (EDX) and STEM showed a uniform dispersion of copper and chromium species in the catalyst structure.²² They concluded that copper to chromium molar ratio had a significant impact on the phase composition of the catalyst.²²

Analysis of the hydrogenolysis reaction and its products done by Xiao et al.²² showed an increase in the conversion of glycerol from 32 % to 49 % and an increase in the MPG selectivity from 55 % to 68 % upon increase in the copper content of the catalyst initially. But after Cu/Cr molar ratio above 4 was reached, it made no subsequent difference to the conversion of glycerol and to the MPG selectivity, which they attributed to the increase in the particle size. They observed a maximum glycerol conversion of 85.9 % with the MPG selectivity of 98.5 % in 10 hours with 5 wt% Cu-Cr (molar ratio 4) catalyst at 210 °C and 4.1 MPa hydrogen pressure.²²

2.5 Kinetic study of hydrogenolysis of glycerol over copper chromite

Most of the previous research was focused on evaluation of the effect of various parameters like pressure, temperature, glycerol concentration, catalyst weight, RPM, etc. on the hydrogenolysis of glycerol. Some studies focused on comparing commercially available catalysts and the prepared ones, others studied effect of Cu:Cr ratio on glycerol hydrogenolysis by preparing different catalyst samples with different preparation methods in their research labs. Many researchers did propose possible routes for this reaction but very few focused on the insights of the reaction. Xiao et al.²² shed some light on the reaction mechanism.²² Xiao et al.²² proposed that hydrogenolysis of glycerol to 1,2-PDO could occur via either D-H route (Dehydration, Hydrogenation), most commonly conferred route, or DDH (Dehydrogenation, Dehydration, Hydrogenation) route. Xiao et al.²² observed formation of a small amount of glyceraldehyde when hydrogenolysis of solvent free glycerol was carried out. Formation of glyceraldehyde was observed by other researchers too and hence, proposed DDH mechanism^{22,45} Based on the observations, Xiao et al.²² proposed the following mechanism as shown in Figure 2-7.

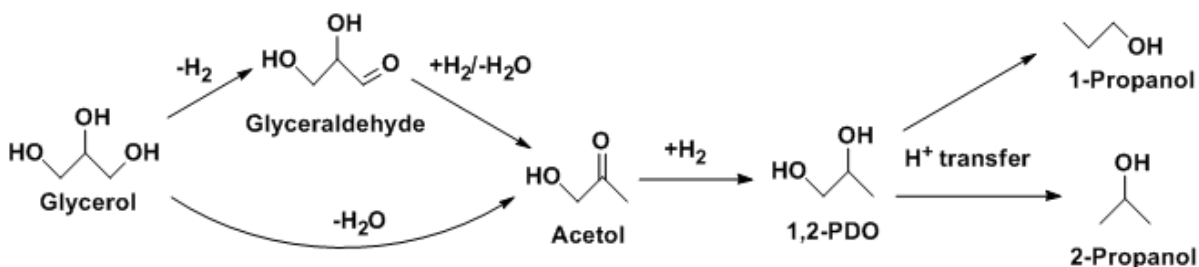


Figure 2-7: Reaction mechanism suggested by Xiao et al.²²

Catalyst reuse study performed by this research group indicated that after three recycles a small decrease in the glycerol conversion was observed while selectivity of MPG was around the same.²²

Kim et al.³⁸ performed a kinetic study on Pd promoted copper chromite. They studied the effect of hydrogen pressure and the glycerol concentration on the reaction rate. Increase in the hydrogen pressure showed a power increase in the reaction rate and thus a log vs. log plot was used to obtain a rate expression. So, a linear relationship with a slope of +1.09 was observed when $\ln(\text{rate})$ was plotted against $\ln(\text{H}_2 \text{ pressure})$. Similar trend was observed when $\ln(\text{rate})$ was plotted against $\ln(\text{glycerol concentration})$ giving a straight line of slope +2.28. Thus they found rate of formation of MPG (r') to be given by the following expression:

$$r' = k \times C_{\text{glycerol}}^{2.28} \times C_{\text{H}_2}^{1.09}$$

Further analysis done by the authors³⁸ over Pd promoted copper chromite showed a 70 percent increase in the rate constant as compared to pure copper chromite.

Chapter 3: Theory

3.1 Catalyst Preparation

Literature reports different preparation techniques used for the preparation of Copper Chromite catalyst. More commonly found techniques are the Sol-gel route, Co-precipitation, and Impregnation. A good summary of the other various techniques can be found in a review done by Prasad and Singh⁵⁵.

3.1.1 Sol-gel route

In this technique, as described by Xiao et al.²² catalysts are prepared typically by dissolving 2.9 g of $\text{Cu}(\text{NO}_3)_2 \cdot 3\text{H}_2\text{O}$ and 9.8 g $\text{Cr}(\text{NO}_3)_3 \cdot 9\text{H}_2\text{O}$ at a desired molar ratio (Cu/Cr) into 47 mL of ethanol at 60 °C to give a dark blue solution. To this, 18 mL of 1,2-propylene oxide is added to get a dark green transparent gel. After this, wet gel is aged under air and subsequently dried at 75 °C for 15 hr, and the resulting xerogel is further calcined at 500 °C for 2 hours. The prepared oxides need to be reduced under H_2 stream for few hours for activation, before they can be used in the hydrogenolysis reaction.²²

3.1.2 Co-precipitation

Kim et al.³⁷ described the co-precipitation procedure as discussed next. First, a known amount of copper nitrate ($\text{Cu}(\text{NO}_3)_2 \cdot 2.5\text{H}_2\text{O}$) is dissolved in water. Then, a known amount of chromium nitrate ($\text{Cr}(\text{NO}_3)_3 \cdot 9\text{H}_2\text{O}$) is added and mixed vigorously. Sodium hydroxide (NaOH) is then added until the pH of the solution becomes 12. Precipitate obtained is then filtered and dried around 12 hours. Dry precipitate then undergoes grinding and subsequent calcining at 550 °C in air. Final catalyst obtained after calcining, usually undergoes activation by reduction in H_2 stream before actual use in the reaction. Amounts of these nitrates alter the desired molar ratio between Cu and Cr, and hence the composition of the catalyst.

Wolosiak-Hnat et al.³⁹ prepared catalysts by co-precipitation based on the method described by Kim et al.⁵⁶. First, 0.35 M of aqueous solutions of $\text{Cu}(\text{NO}_3)_2 \cdot 3\text{H}_2\text{O}$ and $\text{Cr}(\text{NO}_3)_3 \cdot 9\text{H}_2\text{O}$ are mixed vigorously.³⁹ Aqueous solution of 0.5 M NaOH is then added to the mixture. A precipitate of the mixture is formed during this process. This precipitate is then aged for 12 hrs and then filtered off. The filtered precipitate obtained is then washed with deionized water. After this, it is dried at 90 °C for 6 hrs and calcined subsequently at 300 °C for 6 hrs. The oxides obtained are then reduced with H_2 at 300 °C for 8 hrs.³⁹

Rode et al.⁵³ reported slightly different procedure in which, $\text{Cu}(\text{NO}_3)_2 \cdot 3\text{H}_2\text{O}$ and nitrates of activity promoters like Ba, Al, and Zn are first dissolved in deionized water. Aq. solution of ammonium chromate $(\text{NH}_4)_2\text{Cr}_2\text{O}_7$ is then added to the solution. (This aqueous solution of ammonium chromate was prepared by the drop by drop addition of 30 % aqueous ammonia to an aqueous solution of ammonium dichromate.) Brown precipitate obtained with the addition of aq. ammonium chromate, is filtered, separated, and washed with deionized water. Precipitate is further dried in a static air oven at 373 K for 8 hrs and subsequently calcined at 673 K for 4 hrs.⁵³

3.1.3 Impregnation method

Kim et al.⁵⁶ prepared catalysts with different Cu:Cr molar ratio using the impregnation method as described next. Firstly, an aqueous copper nitrate solution ($\text{Cu}(\text{NO}_3)_2 \cdot 2.5\text{H}_2\text{O}$) is impregnated onto the chromium oxide support (Cr_2O_3) by the incipient wetness impregnation method. Samples are usually dried overnight after impregnation, and the dried samples are further calcined in air atmosphere at 550 °C for 6 hrs.⁵⁶

3.2 Heterogeneous Catalytic Reaction

Heterogeneous catalytic reactions typically involve different phases of reactants, products, and catalysts. Usually the catalyst will be a solid, and reactants and products will be either liquid or gas. This reaction occurs at or very near the fluid-solid interface. Gas-liquid or gas-liquid-solid are the other types of heterogeneous catalytic systems.⁵⁷

3.2.1 Steps involved in a heterogeneous catalytic reaction

Heterogeneous catalytic reaction involves multiple steps of diffusion, adsorption, desorption, and reaction.⁵⁷ In general, for porous catalysts they can be presented as shown below in Figure 3-1.

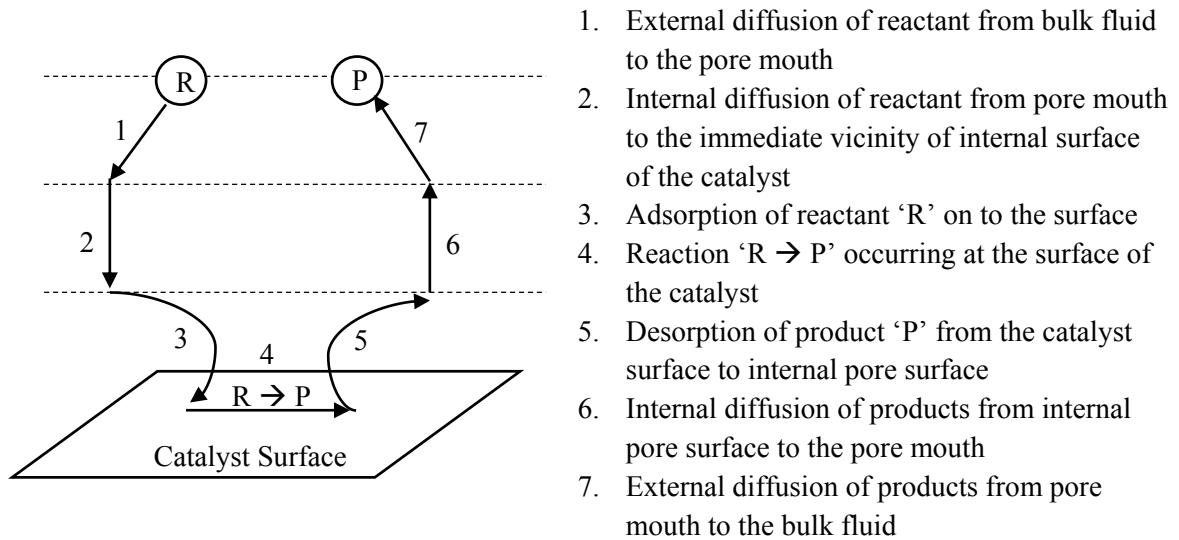


Figure 3-1: Steps involved in a heterogeneous catalytic reaction⁵⁷ (porous catalyst)

In terms of the non-porous catalyst, steps involving internal diffusion won't play a role as external diffusion will bring reactant directly from the fluid to the interface and adsorption will bring the reactant to the catalyst surface. At the catalyst surface, reactions will take place and the product formed will desorb to the interface. From the interface, it will externally

diffuse back to the bulk phase. So, in the non-porous system, steps 2 and 6 from Figure 3-1 will be absent.

For a typical 2-step liquid phase glycerol hydrogenolysis on a solid catalyst, a model reaction system could be presented as shown below in Figure 3-2. Liquid phase hydrogenolysis of glycerol over a solid non-porous catalyst is a very complex reaction with many steps involved in the production of MPG.

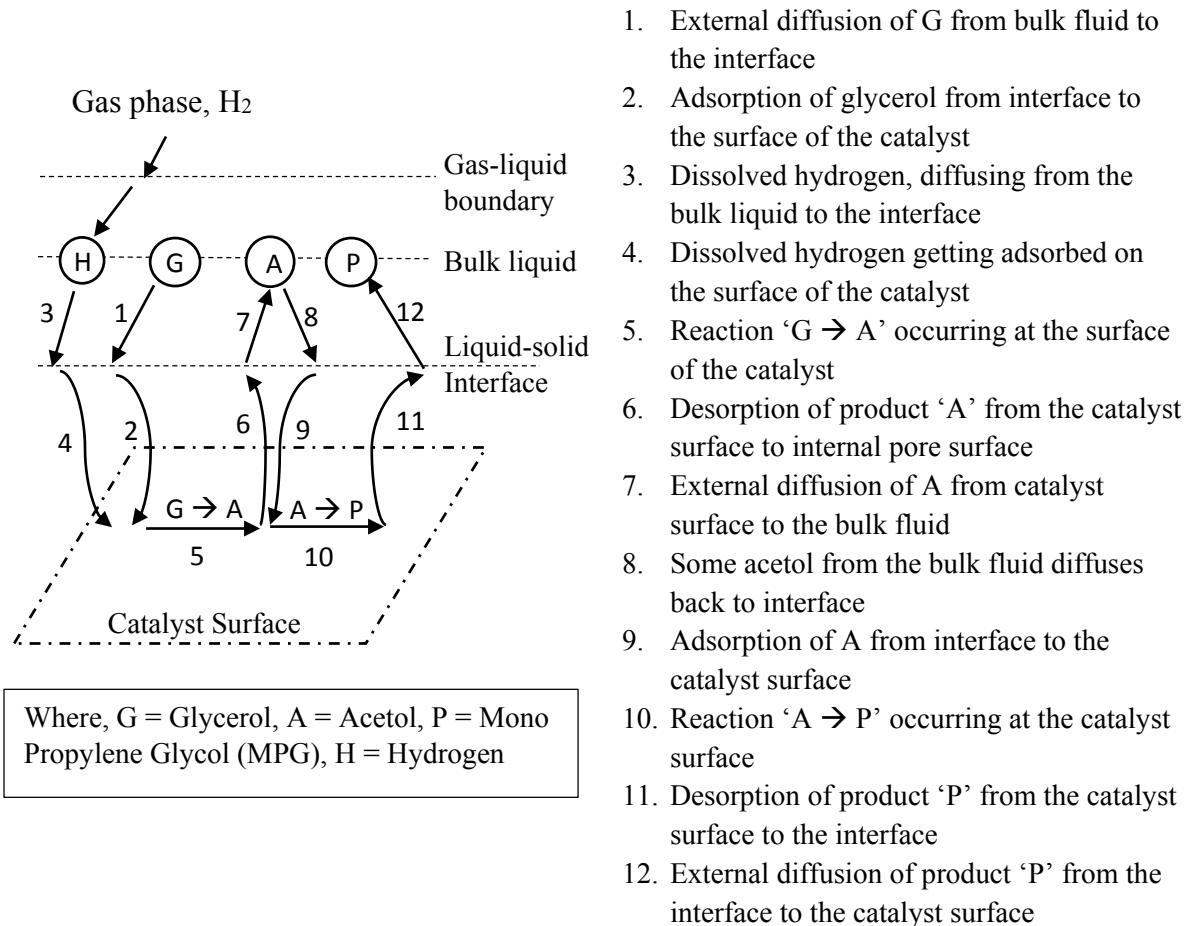


Figure 3-2: Steps involved in Liquid phase hydrogenolysis of glycerol over non-porous copper chromite catalyst

Some of the steps that are not shown, but may exist, are external diffusion of MPG from the bulk liquid to the interface and subsequent adsorption on the catalyst surface to undergo hydrogenation reaction at the catalyst surface. Hydrogenation products from MPG that are

usually lower alcohols will further get desorbed from the catalyst surface and will subsequently get diffused to the bulk liquid. Also, desorption of H₂ from the catalyst surface to the solid-liquid interphase and the external diffusion of H₂ from the solid-liquid interphase to the bulk are other steps that will be involved in this reaction.

A competition between glycerol, acetol, MPG, and hydrogen exists for getting adsorbed onto the catalyst surface. This competition can become more significant when the reaction conditions favor a certain component. Zhou et al.²⁹ suggested the adsorption order in terms of likeliness to be Glycerol > Acetol > MPG. Glycerol has more affinity and chance of getting adsorbed on the catalyst surface than acetol and MPG would have the least chance of getting adsorbed.²⁹ Zhou et al.²⁹ also had proposed their model based on the two different active sites mechanism. On one type of active sites, they proposed that molecular hydrogen dissociates whereas, on the second type of active sites, reaction of glycerol to acetol, and acetol to MPG occurs.²⁹

3.3 Mass Transfer Limited vs. Reaction Limited

Considering the various reaction steps in Figure 3-1 for porous catalysts, the slowest step could be any one of the seven steps described. This slowest step limits the overall reaction rate and causes it to go slow. For non-porous catalysts, the only steps involved will be the external diffusion, adsorption-desorption, and reaction. If the external diffusion for reactants/products occurs very slowly, then the concentration of the reactant in the bulk, near the interface, or near the catalyst active sites will not be uniform. Further any of the sorption step that is adsorption or desorption can be slower than the rest of the steps. Under conditions when external diffusion steps are slower, a reaction will be mass transfer limited (external

mass transfer) for non-porous catalysts. However, if external diffusion steps are made to proceed very fast by providing high agitation (in the case of batch reactors), or high flow rate for reactants (in the case of packed bed reactors), the limiting step will be one of the three steps: adsorption, surface reaction, or desorption from the catalyst surface. When the adsorption step is slow, the reaction system is known as adsorption limited and when the desorption is slow, it is known as desorption limited.

If the steps of external diffusion or adsorption-desorption for a non-porous catalyst are fast enough, so that they don't impact the overall rate of the reaction, then only the surface reaction step will determine the overall rate of the reaction. That is, if the reaction occurring at the catalyst surface is slow as compared to all the other mass transfer steps, then it will be the rate determining step and the reaction system will be referred to as a 'surface reaction limited' system.

Fogler⁵⁷ has stated that almost 75 % of all heterogeneous reactions are surface reaction limited under absence of diffusion limitations.

3.4 Rate expressions for heterogeneous catalytic reactions

Rate expression for homogeneous catalytic reactions are relatively straight forward equations. However, in the case of heterogeneous catalytic reactions, the equations are more complex involving adsorption terms, equilibrium constants, desorption terms, etc.

For a typical reaction $A + B \leftrightarrow C + D$ that occurs on different active sites through dual site mechanism, the reaction steps could be written as follows.





$$r_{(AD)a} = k_A(P_A * C_v - \frac{C_{A.S}}{K_A}) \quad (\text{Adsorption of A})$$

$$r_{(AD)b} = k_B(P_B * C_v - \frac{C_{B.S}}{K_B}) \quad (\text{Adsorption of B})$$

$$r_s = k_s(C_{A.S} * C_{B.S} - \frac{C_{C.S} * C_{D.S}}{K_S}) \quad (\text{Surface reaction})$$

$$r_{(D)c} = k_C(C_{C.S} - \frac{P_C * C_v}{K_{DC}}) \quad (\text{Desorption of C})$$

$$r_{(D)d} = k_D(C_{D.S} - \frac{P_D * C_v}{K_{DD}}) \quad (\text{Desorption of D})$$

If the reaction system is surface reaction limited, then upon solving all the equations stated above, it will give:

$$\text{rate of the reaction} = r_s = \frac{k * (P_A P_B - \frac{P_C P_D}{K_P})}{(1 + K_A P_A + K_B P_B + K_C P_C + K_D P_D)^2}$$

$$\text{where, } k = k_s * K_A * K_B * C_t^2$$

P_A, P_B, P_C, P_D are partial pressures of A, B, C and D

K_P = Gas-phase equilibrium constant

K_A, K_B, K_C, K_D are adsorption equilibrium constants for A, B, C and D

C_t = Total molar concentration of active sites (mol/gcat)

k_s = rate constant for a surface reaction

3.5 Methods for calculation of reaction orders

A procedure for calculating reaction order based on the data measured has been given very neatly by Fogler⁵⁷. It is stated as below:

First, the most probable rate law equation is guessed, which usually involves writing power law model based equations for homogeneous reaction systems, or writing Langmuir-Hinshelwood model based equations for heterogeneous reaction systems. Once the probable rate equations are written, corresponding mole balance equations are equated to those rate equations. In the next step, an equation is rewritten in terms of the measured process variable, if needed. Next, using either of the three types of primary methods, a reaction order could be calculated. Those three primary methods for calculating reaction rate orders based on the reaction data are: differential method, integral method, and the nonlinear regression (least square analysis) method.

3.5.1 Integral method

Integral method is the one that takes less time to determine the reaction order from the reaction data as compared to other methods. It is based on a trial and error procedure. First, the reaction order needs to be guessed for a particular reactant. Consider a simple irreversible reaction, $R \rightarrow P$ and assume reaction order with respect to R as 'a'. For a batch reactor, in terms of mole balance, we can write the rate of consumption of reactant R as

$$-\frac{dC_R}{dt} = k * C_R^a$$

where, C_R = concentration of reactant 'R' and k = rate constant

We can then integrate this differential equation with respect to time. If order is zero i.e. $a = 0$, above differential equation upon integration will yield,

$$C_R = C_{R_0} - kt$$

where, C_{R_0} = Initial concentration of reactant 'R'

If we plot the above equation in terms of concentration of R (C_R) vs. time (t), it will yield a straight line with a slope of '-k', and an intercept of C_{R_0} . So, for a zeroth order reaction with respect to 'R', C_R vs. t should always yield a straight line with a slope = -k.

Similarly, if the reaction order with respect to 'R' is one i.e. $a = 1$, upon integration of Equation 1, it will yield

$$\ln\left(\frac{C_{R_0}}{C_R}\right) = kt$$

Thus, a plot of $\ln(C_{R_0}/C_R)$ vs. t should always yield a straight line with slope = k for a first order reaction.

Furthermore, if the reaction order with respect to 'R' is two, i.e. $a = 2$, upon integration of equation 1, it yields

$$\frac{1}{C_R} = \frac{1}{C_{R_0}} + kt$$

Hence, a plot of $1/C_R$ vs. time (t) should always yield a straight line if the reaction order is two.

In summary, if we plot actual reaction data, C_R vs t , $\ln(C_{R0}/C_R)$ vs. t , or $1/C_R$ vs. t and if it yields a straight line, it's a zero, first, or second order reaction respectively, with respect to reactant R.

Real data usually does not follow as closely as the theory predicts, hence we measure goodness of fit for the data using the regression coefficient 'R²'. R² varies between 0 and 1 where value of 0 indicates no fit to the data and value of 1 indicates an exact fit to the data.

3.5.2 Differential Method

For an irreversible reaction ($R \rightarrow P$) with a reaction order of b with respect to R, carried out in an isothermal constant volume batch reactor, rate law could be written as

$$-\frac{dC_R}{dt} = k * C_R^b$$

If we take natural logarithm of the above equation, we get

$$\ln\left(-\frac{dC_R}{dt}\right) = \ln(k) + b * \ln(C_R)$$

So if we plot $\ln(-dC_R/dt)$ vs. $\ln(C_R)$, it should yield a straight line with slope equal to 'b'.

Value of 'k' can be subsequently found out using the same equation once the value of 'b' is found out.

For calculating the values for the derivative term (dC_R/dt), there are again three methods available.

1. Graphical differentiation
2. Numerical differentiation
3. Differentiation of a polynomial fit to the data

3.5.2.1 Graphical differentiation

In this method, first $(-\Delta C_R/\Delta t)$ is plotted as a function of time, and equal area differentiation is then used to obtain $(-dC_R/dt)$

3.5.2.2 Numerical differentiation

If the data for independent variable is equally spaced such as $t_3 - t_2 = t_2 - t_1 = t_1 - t_0 = \Delta t$, numerical differentiation formulas can be used as described by Carnahan et al.⁵⁸ as cited by Fogler⁵⁷. For example:

Reaction data with values as given below:

Time (s)	t_0	t_1	t_2	t_3	t_4	t_5	t_6
Concentration (mol/L)	C_{R0}	C_{R1}	C_{R2}	C_{R3}	C_{R4}	C_{R5}	C_{R6}

Carnahan et al.⁵⁸ gave three point differentiation formulas as:

1. For the initial point, it could be calculated by

$$\left(\frac{dC_R}{dt}\right)_{t_0} = \frac{-3C_{R0} + 4C_{R1} - C_{R2}}{2\Delta t}$$

2. For the interior points, it could be calculated by

$$\left(\frac{dC_R}{dt}\right)_{t_i} = \frac{C_{R(i+1)} - C_{R(i-1)}}{2\Delta t}$$

3. For the last point, it could be calculated by

$$\left(\frac{dC_R}{dt}\right)_{t_6} = \frac{C_{R4} - 4C_{R5} + 3C_{R6}}{2\Delta t}$$

3.5.2.3 Polynomial fit

In the case of polynomial fit method, reaction data that is concentration vs. time, is first fit to a certain order of polynomial depending on goodness of fit. For ex. Reaction data for reactant R obtained can be written as

$$C_R = A + B * t + C * t^2 + D * t^3 + \dots + Z * t^n$$

Once, this concentration is obtained in terms of independent variable (t), values for (dC_R/dt) could be easily obtained just by taking derivative of the above equation. Thus,

$$\frac{dC_R}{dt} = B + 2C * t + 3D * t^2 + \dots + nZ * t^{n-1}$$

3.5.3 Nonlinear Regression

In nonlinear regression, the most probable rate law should be defined first. Once it is defined, unknown parameter values are proposed and tested within a range specified for a best fit for the given data. The parameter values are estimated that give the least sum of squares of difference between the measured value and the predicted value.

Fogler⁵⁷ has given the formula as:

$$\sigma^2 = \frac{s^2}{Z - K} = \sum_{i=1}^Z \frac{(C_{xm} - C_{xc})^2}{Z - K}$$

where,

$$s^2 = \sum_{i=1}^N (C_{xm} - C_{xc})^2$$

N = number of runs; K = number of parameters to be determined

C_{xm} = measured concentration rate for run x; C_{xc} = calculated concentration rate for run x

Chapter 4: Materials and Methods

4.1 Materials

All chemicals and gases used and their suppliers are listed below in Table 4.1.

Table 4.1: List of chemicals

Chemical Name	Catalog Number	Quantity	Supplier
Glycerol	15892-0025	2.5 L	Acros Organics
Mono-Propylene Glycol or 1,2-propanediol	220872500	250 mL	Acros Organics
Ethylene Glycol	E178-500	500 mL	Fischer Scientific
Acetol or Hydroxyacetone	160341000	100 gm	Acros Organics
n-Butanol	23208-0010	1 L	Acros Organics
Methanol	UN1230	4 L	Fischer Scientific
Copper Chromite Catalyst	G99B-0	100 gm	Süd Chemie
Nitrogen	Industrial grade	--	Airgas
Hydrogen	Industrial grade	--	Airgas
Air	Breathable grade	--	Airgas

4.2 Reactor Configuration

For kinetic studies, a modified Parr High Pressure/High Temperature (HP/HT) Reactor

4575A was used. The schematic for a Parr Reactor Model 4575A can be seen in Figure 4-1.

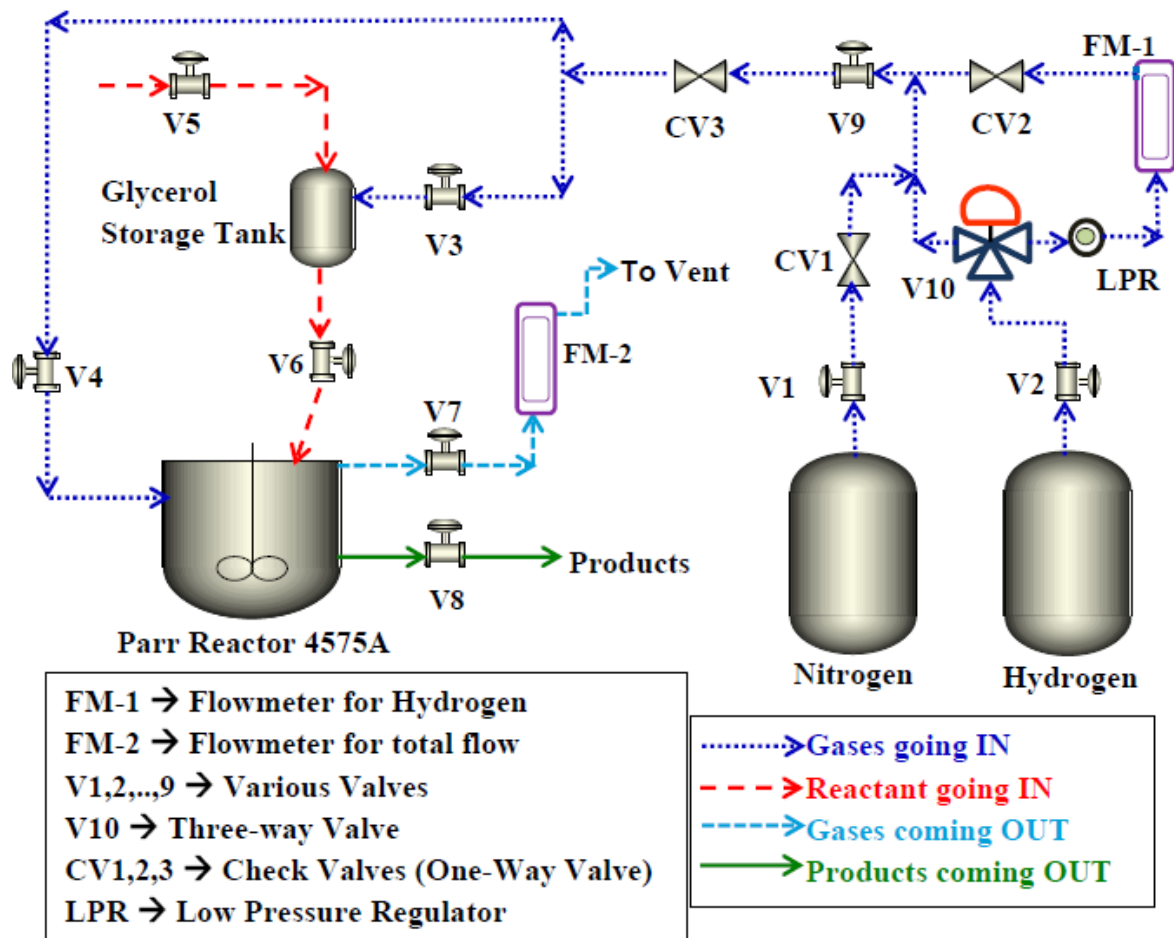


Figure 4-1: Reaction System Schematic

Several modifications were done to the reactor connections as needed. To ensure correct start time for the reaction by the addition of the entire reactant mass at once, it was modified by attaching a liquid storage tank with a capacity of 300 mL. Glycerol is not directly charged into the reactor from the start because of the requirement of the catalyst reduction before the start of the reaction to obtain better yields. An electrical heating tape wrapped in fiber glass insulation was attached to this top reactant storage tank to heat glycerol to the reaction temperature. Before this addition, a drop of almost 70 °C in the reactor temperature was observed upon charging of the unheated glycerol. A 1/16" O.D. SS tube for liquid product sampling was inserted by removing pre-installed cooling loop from the reactor. Two

flowmeters, FM-2 for controlling the total gas flow coming out from the reactor, and FM-1 for controlling the inlet hydrogen flow, were used. Both the flow-meters in fact were attached to a metal plate that was designed to be a small control panel involving electronic thermometer, both of the flow meters (FM-1 and FM-2) discussed above, a regular two way ball valve (V9), and one three way ball valve (V10) as shown in Figure 4-1. At the back of this control panel, a Low Pressure Regulator (LPR) was attached for regulating hydrogen pressure during the reduction. Three check valves (CV1, CV2 and CV3) were put in the various sections of this system shown in Figure 4-1, one in the nitrogen line (CV1) before going into the three-way valve (V10), one in the hydrogen line (CV2) before it meets with the nitrogen/high pressure hydrogen line, and the other one (CV3) was introduced before the line carrying mixed gases to the reactor inlet. All of these check valves were installed with the purpose of stopping the flow in the case of flow reversal due to backpressure. The three way valve (V10) shown in the Figure 4-1, was installed with the purpose of switching the flow of hydrogen from high pressure to low pressure hydrogen, and vice versa. The main advantage with this valve, was the elimination of the need of using high pressure regulator installed on the hydrogen tank itself, to control the lower side hydrogen pressure during the reduction process that was very difficult to control otherwise. A two-way ball valve (V9) was installed with the purpose of switching the gas flow to the reactor and the overhead tank, ON or OFF. Valves (V3, V5, V6, and V8) had similar purposes of switching the flows of either liquid or gas, depending on the location. Valves (V4) and (V7) however, were needle valves that could be opened partially and hence, they were used to regulate the gas flow going in and the gas flow coming out. All the connections in the system shown in Figure 4-1, were made from 1/8" O.D. S.S. tubing with the exception of a sampling line, which was 1/16"

O.D. S.S. and the line connecting the overhead storage tank to the reactor head, which was 1/4" O.D. S.S. tubing.

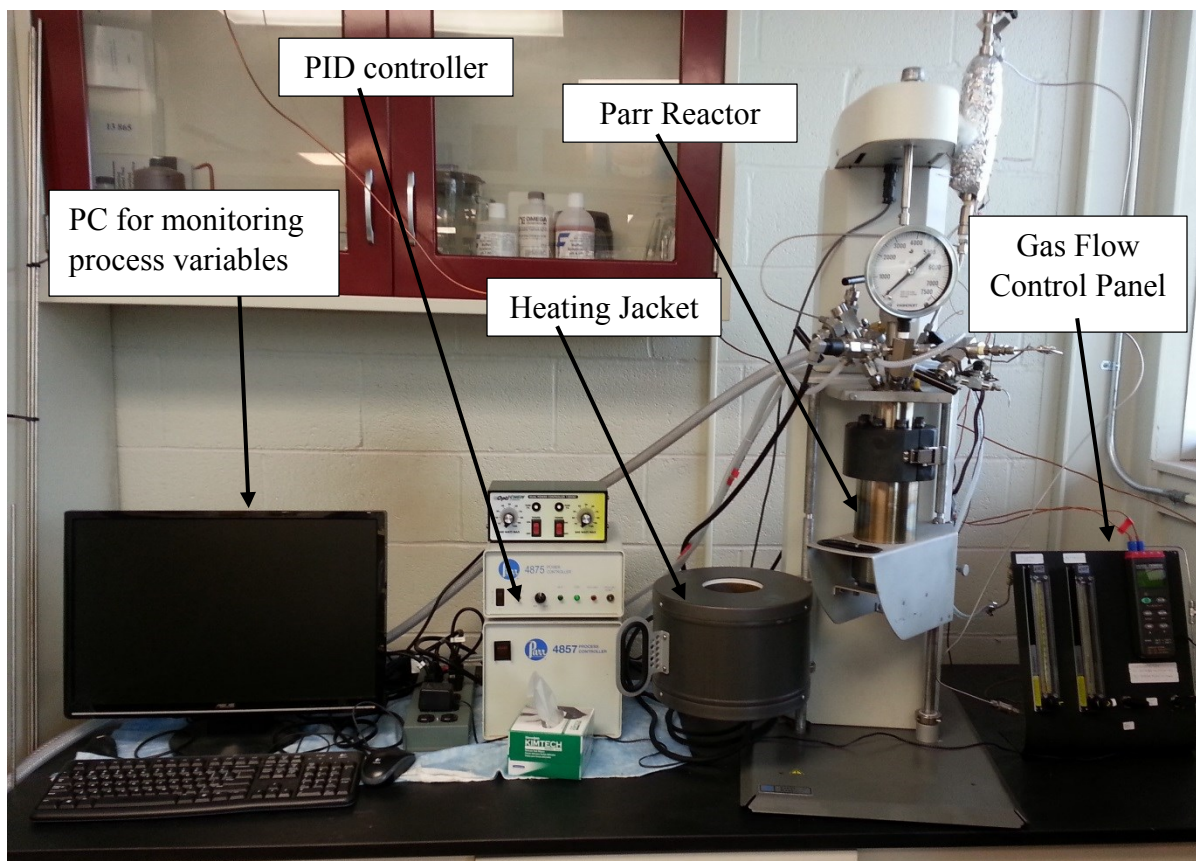


Figure 4-2: Reactor Setup (Actual)

Parr Reactor Model 4575A was a high pressure/high temperature reactor with the operating pressure limit of 5000 psi, and operating temperature limit of 350 °C. The reactor bomb had a capacity of 500 mL, but a liquid level of only up to 375 mL was recommended as a safety measure. Heating of the reactor was done through a ceramic electrical heating jacket that could surround the reactor bomb completely as can be seen in Figure 4-2. A 3-blade impeller with magnetic stirrer drive was used for proper mixing of the reaction components. A static catalyst basket with a volume of 40 mL was used to store the catalyst inside reactor during

the reaction. Basket was fitted with a 50 micron mesh sized cloth to prevent loss of the catalyst during use. Similar sized mesh was also fitted at the mouth of the sampling tube to prevent catalyst from blocking the tube. Schematic for the inside of the reactor is presented in Figure 4-3 as shown below.

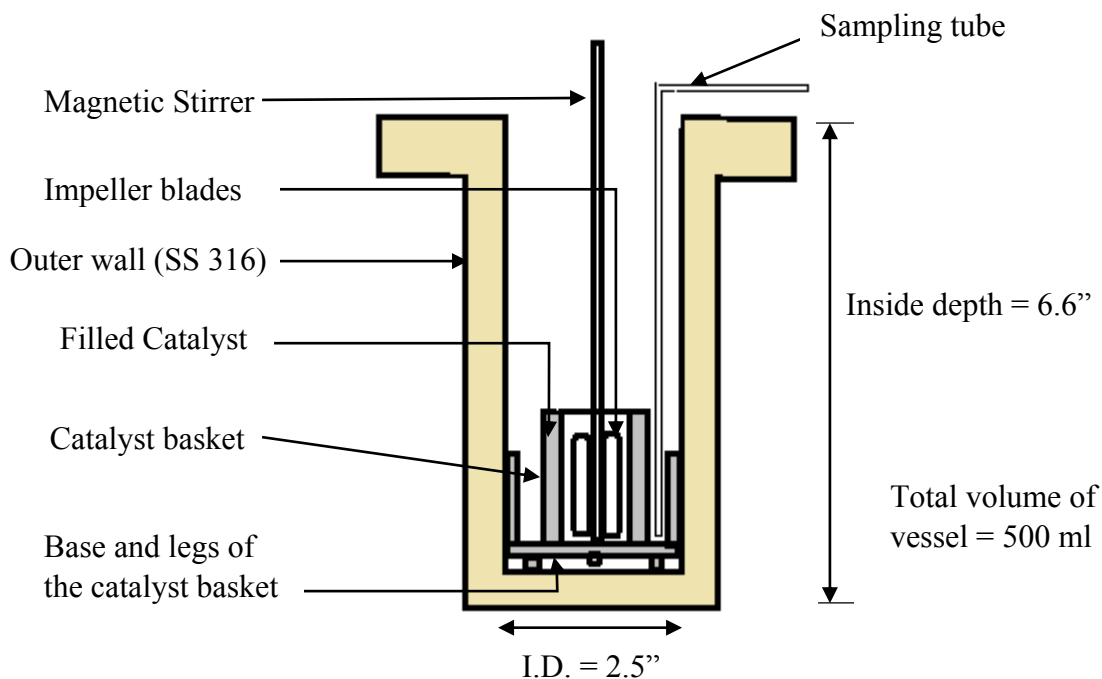


Figure 4-3: Schematic for the inside of the reactor

4.3 Catalyst Activation and Reactor Preparation

4.3.1 Catalyst Properties

The catalyst used in all these experiments was a Copper Chromite (G99B-0) obtained from Süd Chemie with a composition 47% CuO, 46% Cr₂O₃, 2% BaO, and 4% MnO₄. The active species in this catalyst are copper cations, and Chromium gives support against sintering of the catalyst.³⁷ Chromium oxide helps in enhancing the catalytic activity as it can offer both geological and electronic promotion effect.³⁷ Barium oxide is used as a promoter because Ba gives stability to the Cu⁰ state, which is responsible for the hydrogenolysis of glycerol. Ba

also inhibits agglomeration of crystallites and leads to prolonged catalyst activity.³³ Fresh catalyst has a surface area of $38.73 \pm 0.95 \text{ m}^2/\text{g}$ with a crystal size of about 79 \AA , and particle size from 0.710 to 0.300 mm .¹⁴ Copper chromite is a non-porous catalyst with a density of 3.925 g/cm^3 . Unreduced catalyst has a crystal structure containing $\text{CuO/Cr}_2\text{O}_3$, while a reduced catalyst contains $\text{Cu/Cr}_2\text{O}_3$.¹⁴

4.3.2 Catalyst Activation

Catalyst is usually provided in an oxidized form, and needs to be reduced for activation before it is used for the actual reaction. This is commonly performed by passing a hydrogen stream mixed with an inert gas like nitrogen over the catalyst at elevated temperatures.

Appropriate proportions of H_2/N_2 are required as this process is highly exothermic and can result in catalyst damage if not controlled. The catalyst activation procedure was developed by modifying a procedure given by Johnson Matthey Catalysts for reduction of PRICAT Copper and PRICATE Copper/Zinc catalyst. It is described as below.

The reactor was first purged with a stream of Nitrogen for 15 minutes in order to remove any oxygen present. It was done by opening valves in the sequence of V1, V9, V4 and V7 as shown in Figure 4-1. V7 was adjusted to control flow out. Reactor temperature was then raised to $140 \text{ }^\circ\text{C}$ ($270 \text{ }^\circ\text{F}$) that is, Set-Point 1 of Module 1 of process controller on computer, was set to $140 \text{ }^\circ\text{C}$ and once temperature reached $140 \text{ }^\circ\text{C}$, it was allowed to stabilize for 10 minutes. Once the temperature was stabilized around $140 \text{ }^\circ\text{C}$, H_2 was allowed to flow by opening Valve V2, and by directing the three-way valve V10 towards the low pressure side where the flow goes through Low Pressure Regulator (LPR) at an adjusted composition of 2

% v/v (2 % H₂ and 98 % N₂). This flow was regulated with Flowmeter 1 (FM-1) as shown in Figure 4-1. This mixed flow was then passed through the reactor for 30 minutes.

Set-Point 3 of Module 1 was set at the temperature of 230 °C (446 °F) to ensure safety. After it was ensured that temperatures were not going beyond 230 °C, Set-Point 1 of Module 1 was changed to 200 °C (392 °F) and reactor was allowed to stabilize at 200 °C. Once it stabilized at 200 °C for 10 minutes, the hydrogen concentration was increased to 20 % v/v (20 % H₂ and 80 % N₂) by adjusting flow via FM-1. This condition was held for 40 minutes to 1 hour, which helped ensure that the water formed during reduction is fully removed. Once this reduction process was done, steps were taken to ensure that the system remains anoxic to prevent deactivation of the catalyst. In cases where the reaction was run immediately post reduction, influent nitrogen was slowly turned off by closing V1 to give a pure H₂ influent, which was allowed to flow to pressurize the reactor for the desired reaction pressure. If an experiment was not to be run immediately post reduction, the outlet flow was closed and hydrogen and nitrogen were turned off in the following sequence of valves: V7 first, followed by V4 and V9, and finally V1 and V2 on the respective gas tanks.

4.3.3 Feed Solution Preparation

In most cases, the standard solution used was 90:10 (w/w) glycerol-water mixture. Since the overhead tank used had a capacity of 300 mL, maximum amount of charged feed was set at 275 mL.

First, 241 mL of glycerol was measured using several charges of a 100 mL volumetric flask. This measured glycerol was then added to a standard Pyrex 600 mL glass beaker. After that, 34 mL of Distilled Water was measured using the same 100 mL volumetric flask, and was

added to the beaker containing glycerol. These quantities of 241 mL of glycerol and 34 mL of water were determined by converting weight ratio of 90:10 into the volumetric ratio using standard densities of glycerol and water.

This 275 mL mixture containing 90:10 glycerol was then stirred with a glass rod to create a uniform mixture. After a uniform mixture of 90:10 weight percent was created, it was placed in a Fisher Scientific FS110D Ultrasonic Cleaner to remove any dissolved oxygen or gas since, oxygen hampers the selectivity of the catalyst by forming copper oxides on surfaces. The ultrasonic cleaner was first drained to remove any previous water or liquid solution by opening up the tap fully. Then, it was filled with clean tap water up to the level of 1 inch from top. Once it was filled with water, it was set on the 'degas' mode for 10 minutes to remove any gas or dissolved component from the water in order to remove obstruction for the sound waves, when the beaker containing the feed solution would be put on the sonicating mode.

After this, a beaker containing the uniform feed solution was fitted with a retaining O-ring above the level of feed solution and it was then put in the Ultrasonic Cleaner such that water level was higher than the level of feed solution in the beaker. Once set and properly installed in the adapter plate on Ultrasonic Cleaner, the unit was set on 'sonicate' mode for 15 minutes to remove dissolved oxygen or other gas from the feed solution.

After degassing the feed solution, it was heated to approximately 80 °C using a Thermo Scientific plate-heater and simultaneously stirred via a magnetic stir bar. This heating lowered the viscosity of the feed solution that eases injection of the feed in the overhead storage tank.

After it was heated to desired temperature (approximately 30 minutes with the normal heating procedure), it was put in the overhead feed tank using a 50 mL luer-lock injection syringe. Once the solution was charged, the overhead feed tank was purged for 15 minutes with Nitrogen by opening valve V1 on the nitrogen tank, then opening valve V9 on the control panel, and afterwards opening valves V3 and V5 on the overhead reactant storage tank to remove any air from the tank. These valves were then closed after purging, in the sequence of V5, V3, V9, and V1. This served to isolate air from entering the tank and kept the feed solution anoxic when it was dropped down from the tank to the reactor. The feed solution was now ready for the reaction.

In most of the cases, feed solution prepared had 90:10 (w/w) glycerol: water composition. But, when the effect of the initial feed ratio on the rate of the reaction was to be studied, solutions with different compositions of glycerol were produced. Other two compositions tested were 80:20 (w/w) glycerol: water, and 100 % glycerol. 80 wt% glycerol's clear solution was prepared by adding 209 mL of glycerol to 66 mL of water and by constantly stirring after mixing. In the case of 100 wt% glycerol solution, 275 mL of pure glycerol was directly taken. The rest of the procedure for preparing the feed solution involved the same procedure as discussed above by first removing air, then heating the mixture while constant stirring, and finally putting in the overhead tank.

4.3.4 Reactor Start-Up

The reactor bomb was first rinsed with methanol, and subsequently washed and cleaned by tap water and detergent. Other parts of the reactor were also ensured to be clean.

Approximately around three grams of copper chromite catalyst was measured and placed in

the catalyst basket having a volume of 40 cc, and the remaining space of the basket was filled with glass beads of size 70 microns. Then, the basket was attached to the magnetic stirrer shaft by tightening the retaining bolts. The bomb was then placed in its swing carrier attached to the system and brought to the head of the reactor. It was then attached to the reactor head using the supplied split ring clamp. The clamp was then seated by tightening the integrated bolts to 40 ft-lbs of torque. The bolts were always tightened in a star fashion as shown in the Figure 4.3 to ensure proper attachment and equal torque.

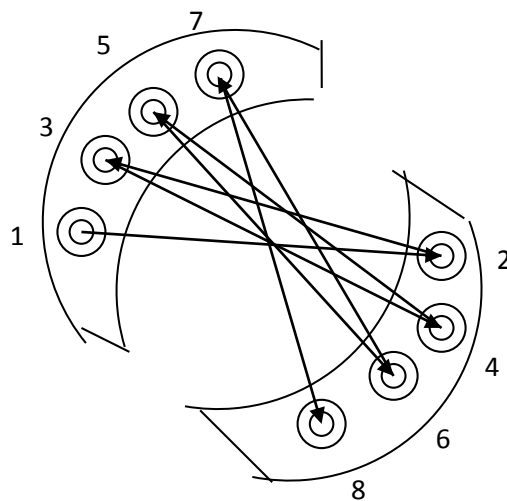


Figure 4-4: Star shaped pattern for tightening bolts

The heating jacket was then lifted and placed so that it would encircle the reactor bomb completely. All valves as shown in the Figure 4-1 were checked for proper closure and connections. Valve V1 on the nitrogen tank was opened followed by valve V9 on the control panel. Then gas inlet valve V4 and gas outlet valve V7 as shown in Figure 4-1 were opened, and N₂ was passed for purging the reactor. After 5 minutes of purging, gas inlet valve V4 and gas outlet valve V7 were closed. The jacket's power cord was then inserted into the unit and the process controller was turned on. Once the controller was ON, the CALogix program on

the attached PC was started for monitoring temperature, pressure, and stirring speed. At this point the external cooling water valve was opened since temperatures during reduction and normal operation go beyond 100 °C (212 °F) and can damage the magnetic drive.

Reduction of the catalyst was started as per the standard reduction procedure given in the Section 4.3.2. After reduction, H₂ gas was kept flowing in the pressurized reactor at the desired reaction pressure of 400 psi. Setpoint 1 within Module 2 of the CALogix program was set at 450 psi. This ensured that the System would have turned off heating to the unit, had the pressure gone above 450 psi.

Setpoint 1 of Module 1(temperature) was adjusted to 200 °C (392 °F) and the maximum power in Module 1 was set to 30 W for better control over temperature. Setpoint 3 of Module 1 was also set at 250 °C (482 °F) so that heater will automatically get deactivated during an alarm condition.

The computer was used to keep track of temperature and pressure variations as the PID controller tried to maintain desired setpoints. Valve V6 on top of the reactor head was then opened to drop off glycerol solution in to the reactor bomb. Once the solution was charged in the reactor bomb, valve V6 was closed. The mixture was then agitated using the magnetic stirrer at the desired RPM speed that was set using Module 3, Setpoint 1. After temperature (Module 1, SP 1) and pressure (Module 2, SP 1) had stabilized, liquid samples were taken every 5 minutes from the liquid sampling valve V8.

Samples were diluted as needed and 50 µL of 10 % v/v n-butanol was added as an internal standard and the solution was analyzed using GC-FID. After 6 hours, reactor bomb was started depressurizing and the heat was turned off. Magnetic stirrer was turned off by turning

off the switch on the controller. Depending on the shutdown time, appropriate procedures as described in Section 4.3.6 were followed.

Using the procedure as described above, various parameters were studied in different ranges.

All these parameter variation ranges are summarized in the Table 4.2 below.

Table 4.2: List of reaction parameters studied and their variation range

Parameter	Range
Temperature	200 – 230 °C
Pressure	400 – 500 psig
Speed of agitation	500 – 1200 RPM
Initial glycerol content	80 – 90 wt%
Catalyst weight	2 – 7.5 g

4.3.5 Product Sampling

4.3.5.1 Liquid Sampling

Sampling was performed by opening the outlet valve V8 on the reactor head. For each sampling point, approximately 1-2 mL of liquid was collected in a test tube. A small amount of liquid was first flushed into a waste beaker to clear the line from previous samples. For first 30 minutes of a run, samples were taken every 5 minutes. From 30 to 120 minutes, samples were taken every 15 minutes, followed by samples every 30 minutes for the remainder of the reaction. Samples were removed from the reactor and subsequently diluted as given in Section 4.4.1.2. All the samples including diluted ones were stored in the test tubes for future analysis.

4.3.5.2 Gaseous Sampling

Gas samples during the reaction were collected from the rubber septum at the back of the outlet of Flowmeter FM-2 as shown in Figure 4-2. These gaseous samples were collected using a 2.5 ml valve-fitted Hamilton GASTIGHT® syringe. Sample collection was done by inserting the needle of the syringe in the rubber septum and by opening the valve on the syringe and pulling up the plunger to the point of 2.5 ml and then closing the valve and pulling up the syringe from the septum. Each collected sample was then taken to Agilent 6890N Gas Chromatograph fitted to Thermal Conductivity Detector (TCD) for analysis.

Samples were collected every 30 minutes during the reaction run using the procedure described in the above paragraph. Before every sample was collected, a trial sample was collected and was immediately purged out, to remove any air that might have gotten in the system and to clean out the syringe of its previous contents.

4.3.6 Reactor Shutdown

4.3.6.1 Standard Shutdown

The heater was first turned off by changing the Set Point 1 of Module 1 on the CALogix software on computer to temperature of 15 °C. The heating jacket surrounding the reactor bomb was then removed. Reactor inlet valve V4 is then turned off along with valve V3 on overhead storage tank, valve V9 on the control panel, and valve V2 on the hydrogen tank in order to stop the flow of hydrogen from getting into the reactor. After this, gaseous contents from the reactor were allowed to flow through valve V7 to depressurize the reactor. It took about 30 minutes for the reactor to get completely depressurized. Once it was vented to 1-2

psig, valve V7 was closed. Split ring clamp was then opened by loosening the bolts using torque-wrench. After removing it, the reactor bomb was opened and the catalyst basket was taken out and the reactor contents were drained in a beaker. One extra sample of the final contents from the reactor was prepared with the dilution procedure given in the section 4.4.1.2 and rest of the beaker contents were tossed into a hazardous waste drum. The reactor bomb was then flushed with methanol, and was subsequently cleaned with soap water and brush. Once the reactor bomb was clean, it was allowed to air-dry overnight. Catalyst basket also was cleaned by washing it with a small stream of methanol. After catalyst basket stopped pouring viscous liquid, the methanol stream was stopped and the basket was allowed to air-dry overnight.

4.3.6.2 Emergency Shutdown

In case of an alarming condition, the heating cord was removed from the unit, stopping the temperature rise. In addition, the H₂ gas valve V2 on top of the gas tank and valves V9, V3, and V4 were turned off while outlet valve V7 was kept open to reduce pressure.

Rupture disc on the Parr reactor had an operating limit of 1500 psig, so when pressure was on the rise and was out of limits, valves were closed by following the procedure as given in the above paragraph. The gas line connected to valve V7 takes it to a condenser where any liquid formed was dropped and the flow rate of gas was measured using FM-2 before sending gases into the hood. Rest of the procedure was same as standard shutdown.

4.4 Analytical Methods

4.4.1 GC Analysis of Liquid Samples

Samples that were taken from the reaction, were analyzed by using Gas Chromatography. Liquid samples taken were mostly analyzed using Agilent 6890N GC-FID or Varian CP-3800 GC-FID instruments installed with Restek wax column with a length of 30 m, with a thickness of 0.53 mm, and with a film thickness of 1 μm . These instruments were used in conjunction with Agilent 7683 and Varian CP8200 autosamplers respectively.

4.4.1.1 Calibration Method

In this method of Gas Chromatography, five compounds or components namely MPG, MEG, Acetol, Glycerol, and N-Butanol that are involved in this reaction were calibrated. Highest calibration level (Calib 1) was decided based upon the preliminary results from GC analysis considering the level of concentration upto which voltage peaks (from GC-FID analysis) did not indicate overloading of components by slanting of the peaks. So, four calibration standards were chosen with each component concentration of 5 mg/mL, 2.5 mg/mL, 1.0 mg/mL, and 0.5 mg/mL. Highest level calibration sample (Calib 1) was made by first taking a weighed and tared test tube, which was then filled with 50 mg of each of the component and finally with 10 mL of pure methanol giving us 5 mg/mL as the concentration of each of the component. Other calibration levels were created using this standard solution of 5 mg/mL. 2.5 mg/mL calibration level (Calib 2) was created by mixing 5 mL of pure methanol into 5 mL of 'Calib 1' sample, whereas 1 mg/mL (Calib 3) and 0.5 mg/mL (Calib 4) levels were created by the successive dilution method. 'Calib 3' was prepared by mixing 8 mL of pure methanol into 2 mL of 'Calib 1' solution and 'Calib 4' was prepared by mixing 9 mL of

pure methanol into 1 mL of 'Calib 3' solution. Calibration curves for the reaction compounds based on the various calibration levels are presented in Figure 4-5 as shown below.

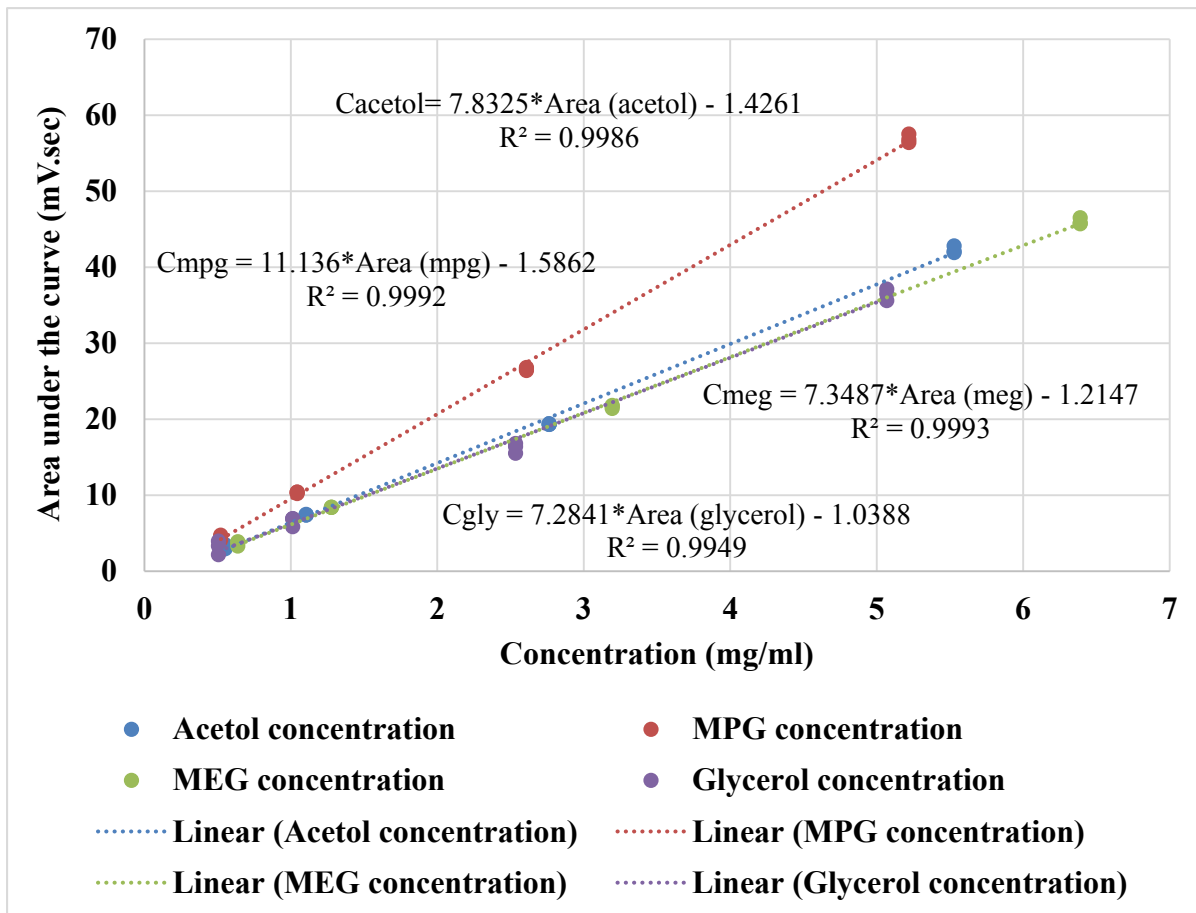


Figure 4-5: Calibration curves for GC-FID analysis

For injecting these different levels of calibration, 1.5 mL of each of the levels Calib 1, Calib 2, Calib 3, and Calib 4 were taken into the GC vial. In that, 50 μ L of 10 % v/v N-Butanol-Methanol mixture was added using Fisherbrand Eppendorf 2-20 μ L pipette. N-Butanol was used as an internal standard to correct errors occurring between repetitions for each of the sample. Each level sample (Calib 1 to 4) was injected thrice in GC-FID system to get most accurate reading for the calibration curve.

Results obtained from GC-FID analysis were used to plot the calibration curve. Curve was obtained on the PC itself using the Agilent Chemstation software or the Varian Workstation software.

4.4.1.2 Sample preparation for GC-FID injection

Samples that were taken from the reactor, needed dilution before they could be injected into the GC-FID sample. 0.1 mL of each of the sample was added to a tared 10 mL volumetric flask, and the weight of the 0.1 mL of the sample was recorded. 9.9 mL of pure methanol was then added to make 10 mL of total solution in order to achieve 1:100 dilution. This solution was then shaken well by shaking volumetric flask upside down (with cap on). 1.5 mL of this solution was then added to the GC vial. To this 50 μ L of 10 % (v/v) N-Butanol was also added as an internal standard.

Since calibration curve was already made in the software, it gave direct value for concentration of all/detected components, when the reaction samples were injected. Each reaction sample was injected thrice in the GC-FID and the values obtained were averaged to get accurate readings of the concentration.

4.4.1.3 GC method for analysis

A GC method is essentially comprised of temperature setpoints and increment ramps for a GC oven. It was designed with some predefined setpoints from company literature.

Following method as described in Table 4.3 was finalized for the analysis of the reaction samples on GC-FID.

Table 4.3: GC-FID method (Oven Details)

Oven Ramp	Temperature	Rate Increase	Holding Time	Run Time
Initial	70 °C	-----	1 min	1.00 min
Ramp 1	110 °C	6.00 °C/min	0 min	7.67 min
Ramp 2	170 °C	10.00 °C/min	0 min	13.67 min
Ramp 3	240 °C	15.00 °C/min	0 min	18.33 min

1 µL of each sample was injected in GC-FID from GC vials. Each sample vial was injected thrice using the Varian 8200 Autosampler. Methanol was used as a pre-wash solvent for the GC system.

4.4.2 GC Analysis of Gas Samples

Gaseous samples collected from the back of the Flowmeter FM-2 during the reaction, were analyzed using Gas Chromatography. They were analyzed using Agilent 6890N GC-TCD system installed with Restek PORAPAK-Q column with a length of 30 m, with a thickness of 0.53 mm, and with a film thickness of 1 µm. This instrument required manual injections that were done using a 2.5 ml valve-fitted Hamilton GASTIGHT® syringe. Average run time for each sample was 10 minutes and Argon (Ar) was used as a carrier gas. Summary of the oven temperature details for the method is presented in Table 4.4.

Table 4.4: GC-TCD method (Oven Details)

Oven Ramp	Temperature	Rate Increase	Holding Time	Run Time
Initial	70 °C	-----	2 min	1.00 min
Ramp 1	130 °C	10.00 °C/min	2 min	10.00 min

4.4.3 Surface Area Analysis

Surface area analysis for all of the catalyst samples was done using Micromeritics FlowSorb III Surface Area Analyzer as shown in Figure 4-6.



Figure 4-6: Micromeritics FlowSorb III Surface Area Analyzer

The specific composition (30 % N₂ and 70 % He) gas was used for running this instrument. To start the gas flow, valve on the gas tank was opened and then the instrument gas flow was turned on. Gas was then allowed to flow through the instrument for 15 minutes in both the short and the long path modes to clear out everything from the instrument. After flushing was done on both the path modes, power to the system was turned ON. The Dewar at the cold

trap was then filled with liquid nitrogen and then instrument was first calibrated by injecting 1 ml of pure nitrogen gas into the injection port using 1 ml valve-fitted Hamilton GASTIGHT® syringe. Gas was then allowed to pass through both the detectors and the detector reading on the instrument was allowed to stabilize (which first jumps and then drops back to 0.03 ± 0.01), at that point reading of the surface area was noted down in m^2 . For the pure nitrogen gas at the STP conditions, the surface area reading should come around 2.84 m^2 on the instrument, and it did come to 2.80, which was then adjusted to 2.84 using the coarse and fine calibration knobs on the instrument.

Once the instrument was calibrated, a small amount of the sample was added to the sampling glass U-tube so that the bottom surface of the U-tube was sufficiently covered with the catalyst surface. Sampling U-tube filled with catalyst sample was then attached at the degas port and the sample was then degassed at 150 °C for 15 minutes. While the sample was degassing, it was ensured that the other U-tubes were in the designated positions (sample position and the cold-trap position) to ensure no gas leakage. After degassing, sample was then allowed to cool to the room temperature, and Dewar at the sample position was filled with liquid nitrogen. Once the sample was cooled down to the room temperature, only the sampling tubes were swapped from the sample position and the degas position, during which a small amount of air may enter the system. Once the degassed sample tube was put in the test position, a Dewar containing liquid nitrogen was placed such that the bottom of the U-tube containing sample would be submerged in the liquid nitrogen. System was then allowed to run and stabilize (during which detector reading will rise initially and then will drop to about 0.03 ± 0.01). Surface area value was then read out by pressing the surface area button on the instrument and the value in m^2 was noted down. The value obtained was of adsorption

surface area. Once it was read out, surface area value was cleared by pressing the 'clear display' button and the Dewar at the sample port was removed. The sample containing U-tube was then allowed to equilibrate to the room temperature during which period, again the detector value rose and came down to about 0.03 and once the value was stabilized, surface area value was read by pressing the surface area button and was noted down. This value represented desorption surface area. To get better accuracy of the result, three to four repetitions of each of the samples were taken as described above by continuing the cycle of adsorption and desorption. After 3-4 repetitions of each of the samples were done, they were then weighed in a tared weighing pan. Finally, the specific surface areas (m^2/g) of all the samples were calculated by dividing surface area values in (m^2) by the weight of the sample in (grams). Once the measurements for all the samples were done, the instrument power was turned OFF and the gas was allowed to flow for 15 minutes and then gas flow was also turned OFF on both the instrument as well as the gas tank.

4.5 Liquid-liquid extraction of the Mono Propylene Glycol (MPG)

Liquid-liquid extraction method was used for purifying the reactor effluent obtained from the Terra Bio Chem LLC, TX with TXIB as extraction solvent.

4.5.1 Recoverability of the TXIB

Before any extractions from the reactor effluent were performed, it was verified that the TXIB solvent could be recovered in two washes from dirty or impure TXIB using equal volume of distilled water. For achieving that, first a GC analysis as described in Section 4.4.1.3 was performed on the 'Dirty' TXIB and the analysis data was recorded. After this, using full volume of the 'Dirty' TXIB was measured and weighed and then an equal volume

of distilled water was mixed thoroughly/vigorously for 5 minutes to achieve equilibrium. Mixture was then allowed to settle and separate in a Separatory funnel. Once mixture was settled into two phases, they were isolated and weighed. Finally, a GC and water (Karl Fisher) analysis on TXIB phase was ran and the data obtained was recorded.

For second wash, a similar procedure as described in the previous paragraph was repeated using the TXIB raffinate generated from the first wash and the data obtained from the GC analysis was recorded.

4.5.2 Removal of impurities from the best extractable MPG stream

In step 1, the 'Selected PG' material and the 'Clean' TXIB were mixed together and were agitated thoroughly/vigorously for 5 minutes for equilibrium to be achieved. The phases were then allowed to settle and separate in a Separatory funnel. Once the two phases were formed, they were isolated and weighed, and a GC analysis was ran on both the phases and the results for Wash number 1 were recorded. In the second step, raffinate of the 'Selected PG' generated in wash number 1 and an equal volume of the 'Clean' TXIB, were weighed and recorded.

After this, in the third step, the raffinate of the 'Selected PG' material generated in wash number 1 and 'Clean' TXIB were mixed together and were agitated thoroughly/vigorously for 5 minutes till they achieved equilibrium. Components were then allowed to settle and get separated in a Separatory funnel. Separated phases were then isolated and weighed and a GC analysis on both the phases was ran and the results obtained were recorded and the number of washes applied to the raffinate of the 'Selected PG' were also noted down. Similar steps of mixing the raffinate of the selected PG from the previous wash with 'Clean TXIB' and allowing them to settle and separate, was repeated upto 10 washes. Data was recorded from

the GC and water analysis ran on separated components obtained in all washes. Once the data was generated, it was analyzed and was used to determine if it was sufficient for achieving separation in the range of low impurity concentrations (i.e. - 0.1% to 0.5% total for impurities 1 - 5). Previously described procedure was repeated until sufficient equilibrium data in the range of low impurity concentrations was achieved.

Once, the equilibrium was achieved, weight and volume of the final raffinate phase of 'Selected PG' was recorded and a volume of ISOPAR M equal to 20% of the volume of final raffinate phase of 'Selected PG' was added to the 'Selected PG' raffinate.

The final raffinate of the 'Selected PG' material and the ISOPAR M solvent were mixed together and agitated thoroughly/vigorously for 5 minutes till they achieved equilibrium. The phases were then allowed to settle and get separated in a Separatory funnel. Once both the phases were separated, they were isolated and weighed, and a GC analysis was ran on both phases and the results were recorded.

Chapter 5: Results and Discussion

5.1 Identification of the impurities

As discussed in Chapter 4, compounds were first calibrated in GC-FID for the analysis and quantification of reaction components. Chromatogram for a typical calibration sample is presented in Figure 5-1. Calibration samples were prepared using components with technical grade purity and hence it still had some impurities present, but their content was very low as compared to reaction components.

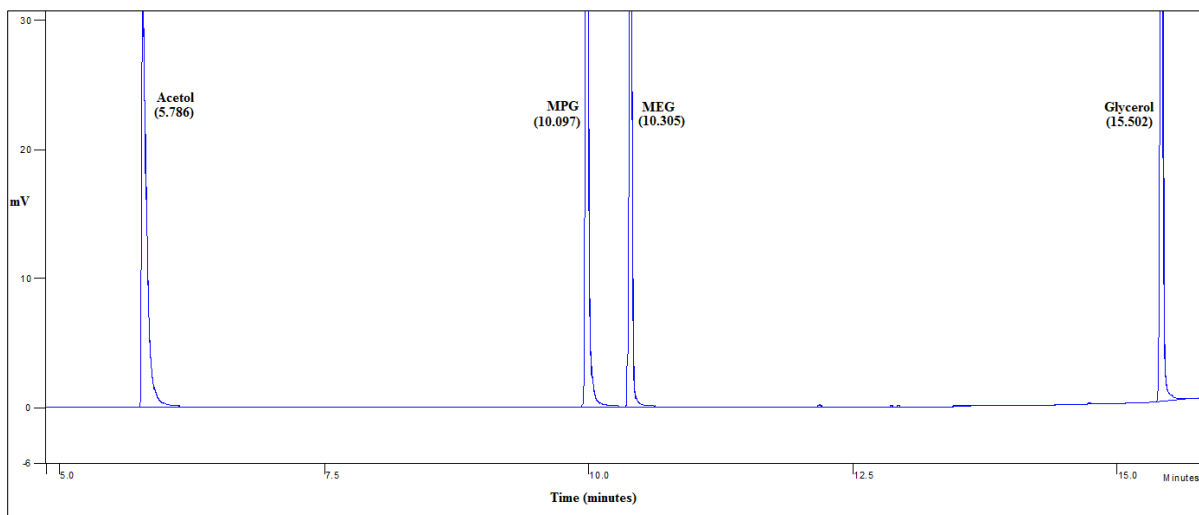


Figure 5-1: Chromatogram of calibration sample

Relative area of impurities constituted only (~ 100 ppm) of the combined area of all calibration components measured by the GC. Hence, chromatogram for calibration sample appeared relatively clean. However, chromatogram for a reaction sample looked more cluttered and clusters of small byproducts were seen around these primary products. Chromatogram for a reaction sample is presented in Figure 5-2. Relative area for these byproducts was found to be around 5 % of the combined area of all reaction components.

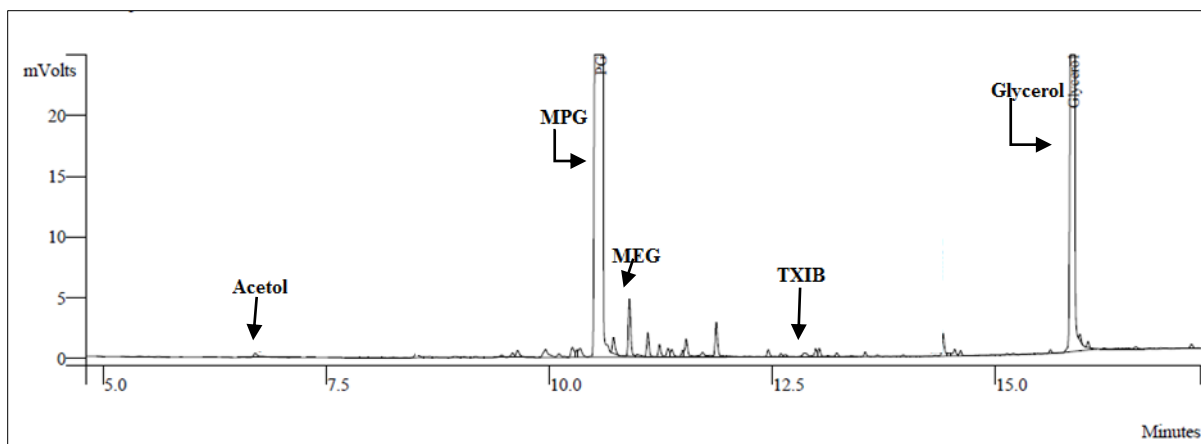


Figure 5-2: Chromatogram for a reaction sample

It is clear by comparing Figure 5-1 and Figure 5-2 and also from the relative area results that these impurities or byproducts are generated in the reaction itself.

Hydrogenolysis of glycerol is a two-step reaction as described earlier, with acetol as the main intermediate. Acetol is a highly reactive and unstable compound at high temperatures. This instability causes it to quickly dimerize or polymerize into other unstable components, which also react and change continuously into other compounds. Even compounds such as MPG and glycerol can undergo di or tri-merization that has been reported by Wolosiak Hnat et al.³⁹ MPG can also undergo degradation reactions that produce compounds like 1-propanol (1-PO) and 2-propanol (2-PO) as reported by various researchers^{22,39}. All these degradation and polymerization products constitute clusters, observed on the chromatogram in Figure 5-2. It becomes important to identify these groups before developing a kinetic model. Identification is also important for proposing ways to eliminate these impurities.

Various types of GC columns like packed bed column, polar column, etc. are used in industries, which have different principles of separation like molecular weight, polarity, etc. In the present case, column used for GC-FID had primary principle of separation based on

the boiling point difference between compounds and secondary separation based on the polarity difference between compounds due to slightly polar (~1%) GC column. It means that main separation of compounds will occur based on the boiling point differences, but compounds with the same boiling points will get separated based on the polarity differences between them.

5.1.1 Types of impurities

All these byproducts or impurities were difficult to identify due to relatively small differences between their boiling points and polarities. Further, their presence in small amounts posed problems in identifying them using the GC-MS technique. Hence, it was not possible to identify individual compounds. However, categorization of these byproducts/impurities based on boiling points may help in quantifying their formation rate. With this thinking, they were categorized into four categories as shown in Figure 5-3. Characteristics of each category have been discussed in sections 5.3.1.1 to 5.3.1.4.

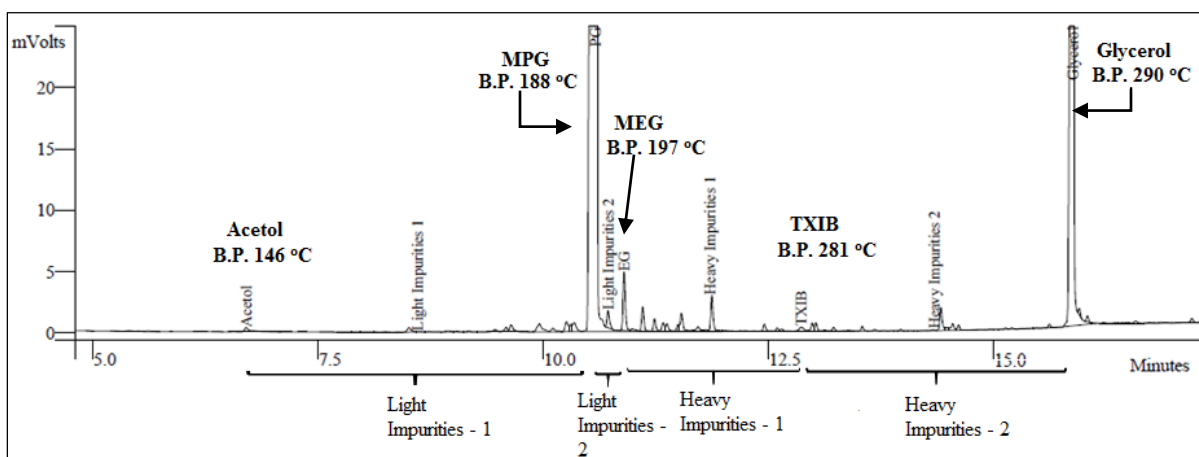


Figure 5-3: Classification of impurities on chromatogram of reaction sample

5.1.1.1 Light Impurities – I

Light impurities-I were basically classified as impurities that had lower boiling points as compared to MPG and Glycerol. These impurities will always come out after acetol and before MPG from the GC column, thus having higher boiling point than acetol and lower boiling point than MPG. Byproducts or impurities in this category will have boiling points in between 146 and 188 °C. It was determined from the liquid-liquid extraction results and results from reaction based on acetol that this category of impurities is the one that might be imparting yellow color to the final products and hence, they play an important role in processing of reactor effluent.

5.1.1.2 Light Impurities – II

Light impurities-II were classified as the impurities with the retention time in between MPG and MEG that is the impurities that come out after MPG but before MEG, from the GC column. So these impurities will be the compounds having boiling points in between 188.2 °C and 197.3 °C. Compounds in this category were difficult to distinguish due to low concentration and peak area mixing with MPG and MEG on the chromatogram. MPG and MEG are very close peaks on the chromatogram due to only 9 °C of boiling point difference.

5.1.1.3 Heavy Impurities – I

Heavy impurities-I were classified as the impurities with retention time in between MEG and TXIB (solvent for liquid liquid extraction). Hence these impurities were the compounds having boiling points in between 197.3 °C and 281 °C. These compounds might have formed

out of dimerizations or polymerizations of the acetol molecules and hence would have relatively high molecular weights.

5.1.1.4 Heavy Impurities – II

Heavy impurities-II were classified as the impurities with retention time in between TXIB and Glycerol, and which have relatively high boiling points close to glycerol's boiling point. So these impurities were the compounds having boiling points in between 281 °C and 290 °C. As with Heavy Impurities II, these compounds might have been formed out of polymerizations of intermediate and reactive compounds.

5.1.2 Removal of impurities using liquid-liquid extraction

The most widely used unit operation for the production of high-purity compounds in most of the commercial systems is distillation. Distillation mainly relies on the boiling point difference between compounds.

As seen previously, hydrogenolysis of glycerol produces MPG (primary product), MEG (main byproduct) and several other byproducts in small concentrations. When it comes to the separation of these compounds from each other, it becomes difficult to distill MPG from the rest in a single step due to marginal differences in the boiling points of those compounds, as already seen from the chromatogram in Figure 5-3. In order to achieve a minimum of technical grade MPG purity (99.5 wt%), multiple distillation columns would be required. This in turn means higher cost and lower economy than expected. Hence, an alternative to distillation in the form of liquid-liquid extraction was studied using a recoverable solvent TXIB. It was selected in collaboration with Terra BioChem. First, it was verified that the

TXIB was able to be recovered substantially after each use, using the procedure as described in Section 4.5.1.

TXIB can be recycled extensively with the use of a distilled water wash and hence fresh solvent was not needed during each run or wash. The used solvent only was purified by washing it with distilled water. It was then used multiple times to study the number of washes to remove the color and odor imparting light impurities.

An analysis of the data obtained from ten washes plotted as shown in Figure 5-4 gives a percentage distribution of the product that is MPG and other impurities. This includes MEG and two categories of light and heavy each.

Impurities were removed with each wash with TXIB; in particular light impurities-1 were removed to less than 0.07 % by ninth wash and by this wash a clear, colorless, and odorless MPG solution with other minor impurities including heavy impurities was obtained. The next wash showed a further drop in the light impurities content causing it to drop to ~0.05 %. This result in conjunction with the results from the acetol reaction affirmed that the light impurities, especially Light Category-I, were the compounds that imparted yellow color and foul odor to the reaction products. With each wash, light impurities' percentage fraction of the total of all the components went down which could be seen from the Figure 5-4.

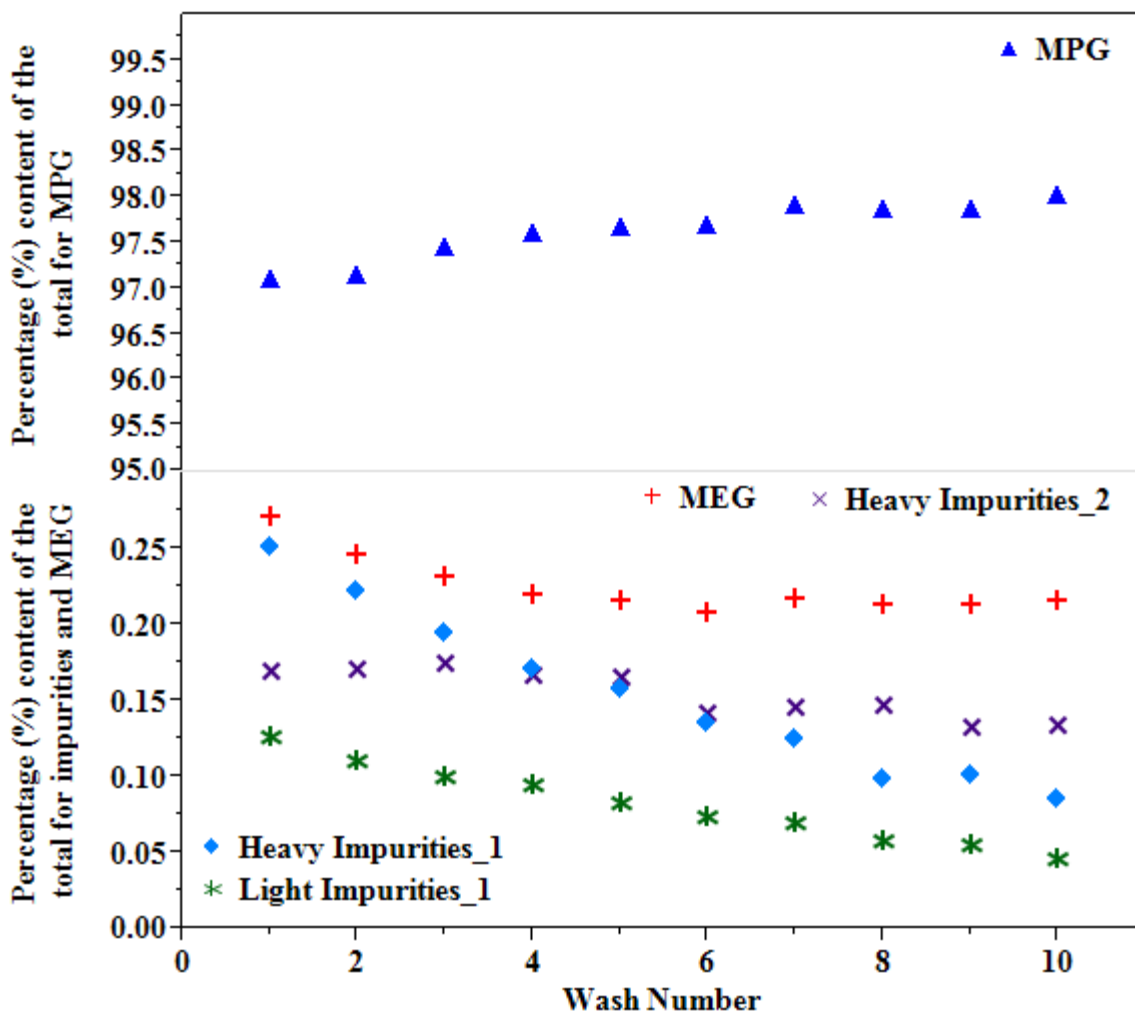


Figure 5-4: Percentage distribution of product and impurities

In general, Light impurities-II were lower in concentration compared to other components.

This was often less than 0.25 % of the total content in most of the cases.

Heavier impurities, that is heavy-I and heavy-II, were difficult to remove as could be seen from the Figure 5-4. Their content from the total mass (all compounds including glycerol, MPG, acetol, TXIB, MEG etc.) was significantly reduced by the number of washes and by the tenth wash their content was reduced to around 0.25% of the total.

All these results indicated that by ninth wash, a technical-grade MPG was obtained that could be sold at market price.

5.1.3 Partition coefficient

A partition coefficient for this system was defined as the distribution ratio of a solute in two different immiscible solvents (TXIB and PG). This is a measure of how much a solute distributes itself in one solvent than the other at equilibrium. If this coefficient is known for the impurities between a recoverable solvent phase (like TXIB) and PG (product phase), it can give a lot of information about how easy or difficult it is to remove impurities from the PG phase using the liquid-liquid extraction. An attempt to measure it was therefore made using the data obtained from GC analysis of the liquid-liquid extraction.

Light impurities-1 and heavy impurities-1, they showed almost a linear relationship between number of washes and percentage content. From these relationships it was concluded that light impurities-1 content was dropping almost at 0.0085 % per number of wash whereas, heavy impurities-1 content was dropping 0.0181 % per number of wash. This data and those linear relationships were then used to calculate the distribution coefficient.

Data for other impurities like heavy impurities-2 did not show linear relationship as significant as the other two and so, its data was not used.

As mentioned earlier, this data was obtained from GC analysis with FID, with all percentages obtained from an area and concentration relationship. Hence, after performing calculations, the distribution coefficient for light impurities-1 was found to be 0.12 on a mass basis. For example, this would mean that at equilibrium 0.12 g of impurities were present in the

dissolved form in TXIB as compared to 1 g in MPG. Similarly, the distribution coefficient for heavy impurities-1 was found to be 0.14.

The distribution coefficient values of 0.12 and 0.14 are relatively small compared to 1, which suggested that they were significantly difficult to remove or extract from the MPG phase. That was the reason why number of washes required to remove those impurities were so high.

Slopes of the lines obtained from a linear fit of the curves also justify this conclusion. Simply comparing the values of the slope and the distribution coefficient one can fairly say that heavy impurities-1 were marginally easier to remove compared to light impurities-1. Content-wise however, heavy impurities-1 were more concentrated than light impurities-1 and hence, could not be removed completely in ten washes even though it had a marginally high distribution coefficient.

5.2 Surface Area Analysis of Catalyst

A surface area analysis was run on the used catalyst samples as well as the fresh catalyst to determine whether the batch mode had any effect on the catalyst deactivation. All these sample surface areas were measured using the Micromeritics FlowSorb III Surface Area Analyzer as described in Section 4.4.3. Surface area analysis results of the fresh catalyst sample, used catalyst sample-1, and used catalyst sample-2 are recorded in the Table 5.1. Fresh catalyst was found to have a mean specific surface area of 35.87 m²/g with a single standard deviation of 0.18 m²/g. Used catalyst-I showed a surface area of 30.44 m²/g with a single standard deviation of 0.20 m²/g that is around 15 % less than the fresh catalyst.

Further, used catalyst-II showed a surface area of only 17.41 m²/g with a single standard deviation of 0.45 m²/g that was almost 50 % less than the fresh catalyst.

Table 5.1: Summary of results from surface area analysis

Catalyst type (Copper Chromite: G99B-0) from Süd Chemie	Avg. surface area (m ²)		Weight of the sample (g)	Specific surface area (m ² /g) – BET method	
	Adsorption	Desorption		Adsorption	Desorption
Fresh Catalyst	2.07	1.98	0.0552	37.56 ± 0.10	35.87 ± 0.18
Used Catalyst – 1	2.44	2.35	0.0773	31.52 ± 0.26	30.44 ± 0.20
Used Catalyst – 2	0.41	0.39	0.0224	18.45 ± 0.68	17.41 ± 0.45

Fresh catalyst had a surface area of 35.87 m²/g that was around 7.4 % less than what was reported in the previous report¹⁴. Fresh catalyst was unused for almost a year, which might be the cause of the drop. It is usually believed that catalyst slightly loses its activity if not used for longer times that might be due to the absorption of moisture over a period of time resulting in crystal growth.¹⁴

Used catalyst sample-I was taken after three reaction runs at the various conditions of temperature, pressure, and initial glycerol content. However, Used catalyst sample-II was retrieved after eight consecutive reaction runs at various reaction conditions of temperature, pressure, and initial glycerol content. Both the catalyst samples showed a significant drop in the catalyst activity that posed a question about the catalyst stability in the batch mode, and its ability to withstand continuous cycles of activation and reaction.

It was not expected for the catalyst to die out so soon because, previous report¹⁴ in continuous mode indicated only 7 % deactivation of the catalyst due to crystal growth after prolonged use. But the temperature difference might also be a contributing factor since,

previous report¹⁴ suggests that reaction was ran at 200 °C, 400 psig in continuous mode whereas in the present case, frequently temperatures of about 230 °C and pressures of about 500 psig were used which also could have caused catalyst to deactivate more rapidly.

Wolosiak-Hnat et al.³⁹ had observed a similar drop in the surface area when hydrogenolysis reaction with copper chromite catalyst was ran at 230 °C. They concluded that it might be happening due to the deactivation of the catalyst at higher temperatures as reported by Bienholz et al.^{39,59} Wolosiak-Hnat et al.³⁹ had further proposed that catalyst deactivation might also have happened due to heavy byproducts like di- and tri-glycerols, or poly-glycols being present in the system. Further, recent study done by Liu et al.⁶⁰ showed that metallic copper (Cu⁰) active sites were getting covered by Cr out of decomposition at temperatures beyond 200 °C.

Another reason might be the continuous operation of catalyst in a cycle of catalyst activation and actual reaction because, in the batch mode, it was difficult to keep the catalyst continuously in an activated mode, whereas in the case of continuous operation, it was easy to keep the reactor system anoxic and hence it was easy to keep the catalyst sample in the reduced/activated form for the prolonged durations. Further, it might be possible that even after washing with methanol post reaction, would not have removed the reaction components from the reaction surface completely, whose presence would reduce the surface area. In the continuous mode, due to continuous flow of methanol stream and effect of gravity, absorbed components from the surface would have got removed more efficiently.

Overall, it could be concluded from these results that for better catalyst lifetime, reaction runs at lower temperatures and pressures while maintaining sufficient MPG yield are useful. This

also helps to maintain anoxic conditions in the reactor continuously without the need of repetitive reduction process. Furthermore, a trade-off between catalyst stability and MPG yield is needed to achieve cost efficiency. Because, at higher catalyst weights, better MPG yields can be obtained at 200 °C. But at lower catalyst weights, better yields can be obtained at 230 °C. In addition to this, Catalyst stability is good at 200 °C than at 230 °C.

Xiao et al.²² observed only 5 % drop in glycerol conversion after using the catalyst fourth time for the hydrogenolysis reaction at 210 °C, 600 psig for 10 hr while MPG selectivity stayed unchanged at 98 %. Hence, it was concluded from the results of Xiao et al.²² and of the current study that catalyst could be used three times without significantly affecting the glycerol conversion and MPG selectivity. Therefore catalyst was used only thrice in the reactions for the kinetic study to ensure maximum level of accuracy with the data.

5.3 Kinetic Study

5.3.1 Mass Transfer Effects

Before any kinetic study is done, it is important to understand the conditions in which, mass transfer effects and heat gradient effects can be neglected. Absence of the limitations from both of these effects is essential in developing the accurate kinetic model. In the case of non-porous catalysts, only external diffusion from bulk to the solid-liquid interface or vice versa can play a role in limiting the mass transfer in the overall reaction. Absence of external diffusion effects is usually verified by studying the effect of rotational speed or the revolutions per minute (RPM) on the rate of the reaction. If the rate of the reaction is relatively same at and above a certain value of RPM, we can fairly say that the mass transfer effects out of external diffusion are negligible at or beyond that RPM speed. Further, it

means that concentration of components is relatively similar at the bulk and at the solid-liquid interface.

Literature reports different RPM speeds at which these effects were observed to be negligible. Kim et al.³⁸ reported a stirring speed of 350 RPM being used for their kinetic study over Pd promoted copper chromite catalyst. Lahr and Shanks¹⁷ reported negligible effects at and above speeds of 500 RPM. Vasiliadou et al.⁴⁴ used 1000 RPM as a stirring speed in their kinetic study over Cu-SiO₂ catalyst.

Even though Cu-based catalyst systems have similarities, one cannot just rely on the literature. In order to analyze the effect of RPM on the glycerol hydrogenolysis reaction, it was run at three different RPMs of 500, 1000, and 1200. Results from these three reaction runs are shown in the figures below. Primary components observed in all the reaction runs were mainly; glycerol (the reactant), acetol (the intermediate) in this reaction, and MPG (the main product of this reaction).

Variation of glycerol consumption with time at three different RPM speeds is presented in the Figure 5-5 shown below. Glycerol consumption was found to be fairly similar at all three RPM speeds.

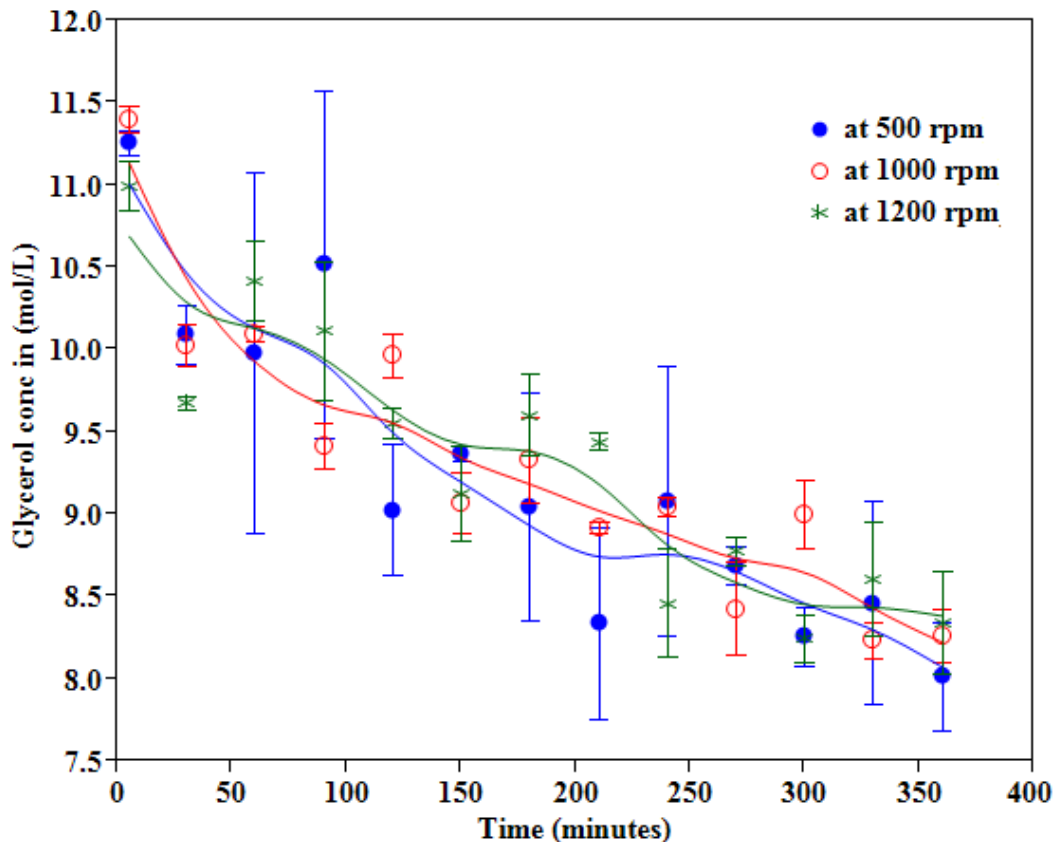


Figure 5-5: Variation of glycerol concentration with time at different RPM (T = 230 °C, P = 400 psig, Glycerol content = 90 wt% and Catalyst Weight = 3 g)

Glycerol consumption profile wasn't significantly different at three RPM runs. It might have been due to low conversion of glycerol as less amount of catalyst (1 wt% on glycerol basis) was used. Further, variation in the glycerol values was large, and single standard deviation overlapped at different points.

Variation in the concentration of acetol with time was also found to be fairly similar with minor differences of ± 0.02 mol/L at three RPM speeds as shown in Figure 5-6. A similar observation was made by Wolosiak-Hnat et al.³⁹, who observed only 0.8 % variation in the selectivity of transformation to acetol at different agitation speeds.

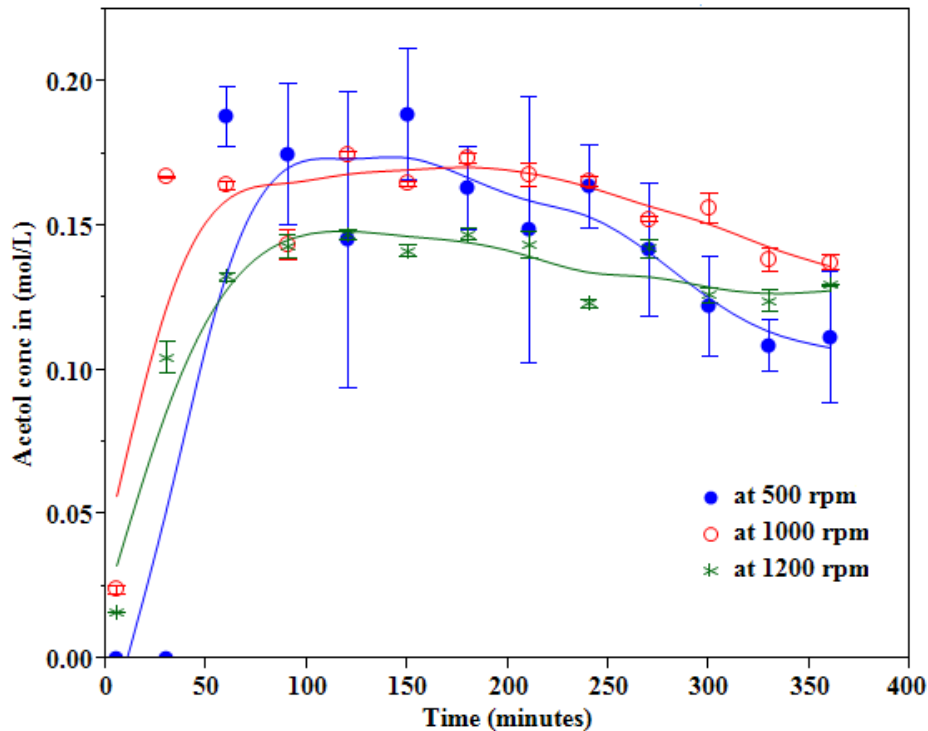


Figure 5-6: Variation of acetol concentration with time at different RPM (T = 230 °C, P = 400 psig, Glycerol content = 90 wt%, Catalyst weight = 3 g)

Minor variation in the acetol concentration could be due to a negligible effect of RPM on the glycerol dehydration step. Reaction liquid phase is saturated with glycerol and hence, glycerol might be externally diffusing fast from the bulk liquid to the solid-liquid interphase. Due to this fast external diffusion of glycerol, change in RPM won't make much of a difference. Concentration of glycerol at the interphase would be similar to the concentration in the bulk, and glycerol would readily get adsorbed on the catalyst surface and undergo dehydration. This logic was verified by running a reaction without agitation and the results of it are discussed in the Section 5.3.4.

Wolosiak-Hnat et al.³⁹ had concluded that low selectivity towards acetol could have been due to insignificant effect of agitation on hydrogenation step. However, this wasn't true in our case. It was observed that a higher hydrogenation rate and higher production of MPG

followed at higher RPM. This might be due to a difference in catalyst weights that was 1 wt% (glycerol basis) in our case, while Wolosiak-Hnat et al.³⁹ reported use of 8 wt%. Further, it could also be possible that at higher catalyst weight, acetol slowly diffused to the interphase, would have better chance of occupying active site due to availability of large number of active sites. At lower catalyst weight, it would have less number of active sites to occupy. So overall it could be said that at lower catalyst weight, RPM may have significant influence effect on hydrogenation rate than at higher catalyst weight.

Variation in the concentration of MPG versus time at three different RPM speeds is shown in Figure 5-7 below. MPG concentration values at 500 RPM were substantially lower than at 1000 RPM and 1200 RPM. However, they were fairly similar within error limits at RPM speeds of 1000 and 1200.

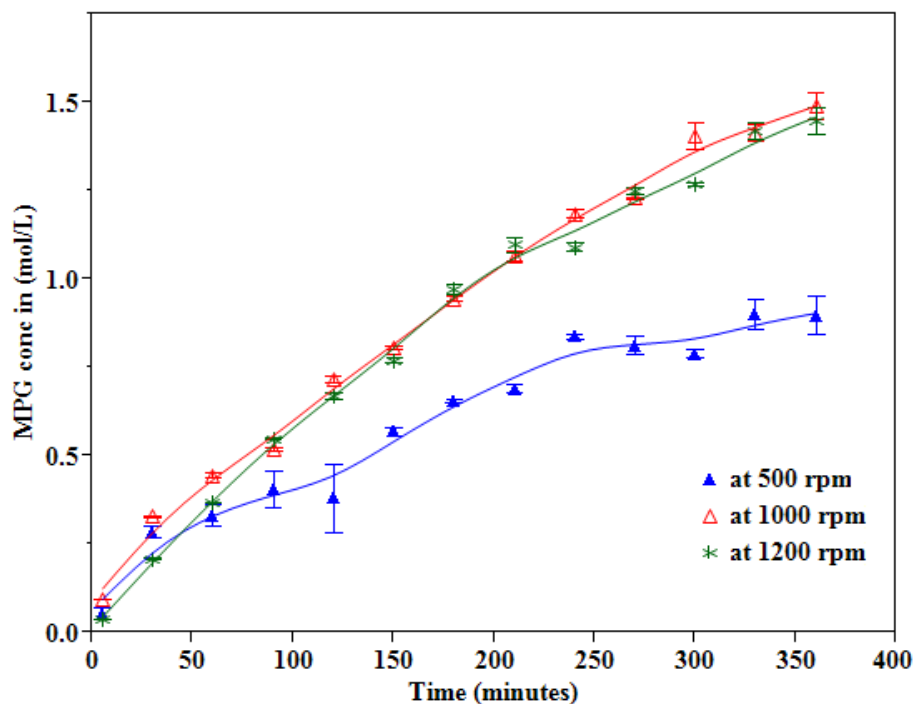


Figure 5-7: Variation of MPG concentration with time at different RPM (T = 230 °C, P = 400 psig, Glycerol content = 90 wt%, Catalyst weight = 3 g)

Based on these results it was decided that at and beyond 1000 RPM speed, there was sufficient stirring for the proper transport of glycerol and acetol to the catalyst active sites, and external diffusion effects were fairly negligible. Hence, all the planned reactions for the kinetic study were run at 1000 RPM.

Copper chromite being non-porous, posed fairly negligible internal diffusion effects. Equilibrium adsorption constant data was not adequately available in the literature and it is difficult to calculate precise adsorption data at high temperature of 200 °C and at high hydrogen pressure of 400 psig.³⁸ Hence, it was assumed that system was ‘surface reaction limited’ and power-law model was used to fit reaction data. Details about possible reaction steps involved in this heterogeneous reaction system are already discussed in Chapter 3.

5.3.2 Absence of Stirring

As an extension of the investigation into external mass transfer effects, a reaction was run without any stirring or mechanical mixing for the initial three hours of the reaction. After three hours of reaction, stirring was started at 500 RPM. This run gave interesting results, with the intermediate acetol concentration higher than the product MPG concentration, in the absence of stirring. Once the stirrer was started, acetol concentration immediately dropped to normal levels. This can be seen in Figure 5-8.

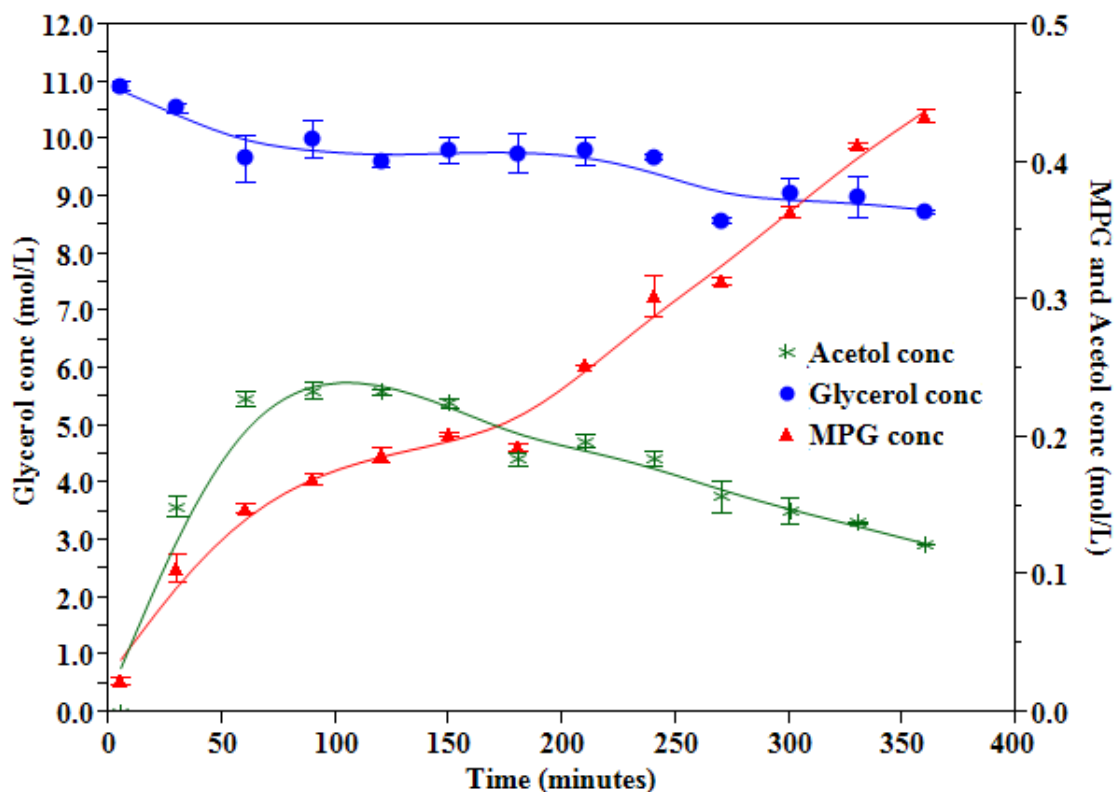


Figure 5-8: Concentration profiles under without stirring (first 3 hours) [T = 230 °C, P = 400 psig, Agitation = 500 RPM, Glycerol content = 90 wt%, Catalyst wt. = 3 g]

This data suggests that the second step of the hydrogenolysis reaction that is the acetol hydrogenation into MPG, requires good mixing and consistent agitation. This may also suggest that acetol hydrogenation is strongly external diffusion limited and because of this resistance, acetol concentration in the bulk and at the solid-liquid interphase may not be same and thus, less acetol will be available to occupy the active sites on the catalyst in order to get hydrogenated. Also, as seen earlier, acetol production from glycerol dehydration might be a fast reaction due to rapid diffusion and glycerol would be readily available for adsorption on the catalyst surface. A similar result on mass transfer limitations and diffusion retardation was suggested by the Xiao et al.²²

All the liquid samples were taken out using a sampling tube from the reaction. This sampling tube was at a certain distance from the catalyst basket, which suggests that when the stirring was absent during the reaction, all the concentrations for the components obtained from GC analysis may not be the same as the one in or near the catalyst basket. Under absence of stirring, the only mode of material transport was through diffusion. As said earlier, glycerol being in excess in concentration, it would have had the better chance of diffusing quickly to the surface of the catalyst and hence, it would probably try to occupy more active sites on the catalyst through adsorption. Having said this, there are other factors to consider also, like the size and the polarity of the glycerol molecule that would involve more detailed study at the molecular level. So on the same note, this result suggested competition for adsorption on the catalyst surface between glycerol, acetol, and MPG for desorption might be taking place. MPG formation rate is higher than the acetol production rate as already seen in section 2.3.1, because of this, whatever acetol would have been produced, would have got converted to MPG. This MPG, produced on the catalyst surface may not be diffusing back to the bulk easily in the absence of stirring and thus, acetol would have had to compete with desorbing MPG and adsorbed glycerol for occupying the catalyst sites. When the stirring was turned ON to 500 RPM, it ensured enough mixing and agitation so that acetol could occupy active sites and could get converted to MPG quickly, although the condition was still mass transfer limited.

5.3.3 Heat Transfer Effects

Even though this reaction is highly exothermic, no drastic change in the reaction temperature occurred apart from minute fluctuations ($\pm 5\%$) arising from the PID controller both during the activation process and the reaction process that might be due to the low conversions of

the reactant and hence, it was assumed that the heat gradients were absent. Also, as suggested by Vasilliadou et al.⁴⁴, liquids have higher thermal conductivity values than gases. With this reaction occurring in the liquid phase, we can safely say that heat transfer effects were negligible and reaction occurred in a kinetic regime.

5.3.4 Concentration of hydrogen in the liquid phase

Hydrogen was supplied in the gas form into the reactor, which would get dissolved in the mixture of aqueous glycerol solution and that dissolved hydrogen will be the one available for the reaction to occur in the liquid phase. So basically, hydrogen will diffuse from the gas phase to the bulk liquid. Then, from the bulk liquid to the solid-liquid interphase and finally it will get adsorbed onto the surface of the catalyst. Typically, adsorption of hydrogen on the catalyst active type is assumed to be dissociative type.²⁹ Due to low vapor pressure of other components, gas phase was assumed to be saturated with hydrogen only as suggested by Vasiliadou et al.⁴⁴ and further it was assumed that the gas-liquid mass transfer resistance for hydrogen, was negligible.

Only recorded data present for hydrogen in all of the experiments was hydrogen pressure. In order to incorporate this into the rate equation, concentration of hydrogen in the aqueous glycerol mixture in equilibrium with the vapor was needed. In order to get equilibrium data of hydrogen at the given reaction conditions, a Flash 2 model with the Wilson thermodynamic property method was used in Aspen Plus. Results from the Wilson property method, were re-verified using the NRTL property method in the same simulation that gave similar results. All these results are summarized in the Table 5.2 shown below.

Table 5.2: Results from the Aspen Simulation for the solubility of hydrogen

Hydrogen pressure (psig)	Hydrogen concentration in liquid (mol/L)	
	Wilson property method	NRTL property method
400	0.0141727	0.014051
500	0.018222	0.018048

5.3.5 Effect of various reaction parameters

Generally a kinetic model is developed based on studying the effects of various parameters on the rate of the reaction. Parameters that were primarily studied were temperature, pressure and the glycerol concentration. Range of variation for each parameter is already tabulated in Chapter 4.

5.3.5.1 Effect of temperature on the concentration profiles of reaction components

Temperature is the most important parameter that strongly affects any reaction. A small change in temperature produces significant difference in rate constants and hence, these differences are used to calculate the activation energy for the reaction using the Arrhenius Equation.

Changes in concentrations of reaction components versus time at different temperatures are presented in Figure 5-9 and Figure 5-10. Figure 5-9 depicts the results from the reaction ran at 500 psig of hydrogen pressure. Change in temperature from 200 °C to 230 °C induced drastic change in the concentration profiles of the reaction components, particularly MPG and acetol. Drop in glycerol concentration was rapid, which indirectly means that the rate of glycerol consumption was higher at higher temperature which was expected. In the case of

MPG, almost 5 to 6 times increase in the concentration of MPG was observed at the end of 6 hrs of reaction run. Further, at higher temperature of 230 °C, acetol showed initial buildup in the concentration, but quickly dropped after some time and then became steady or nearly constant with very small change in concentration. At lower temperature of 200 °C, even though acetol must have been getting produced, GC could not detect quantifiable amount.

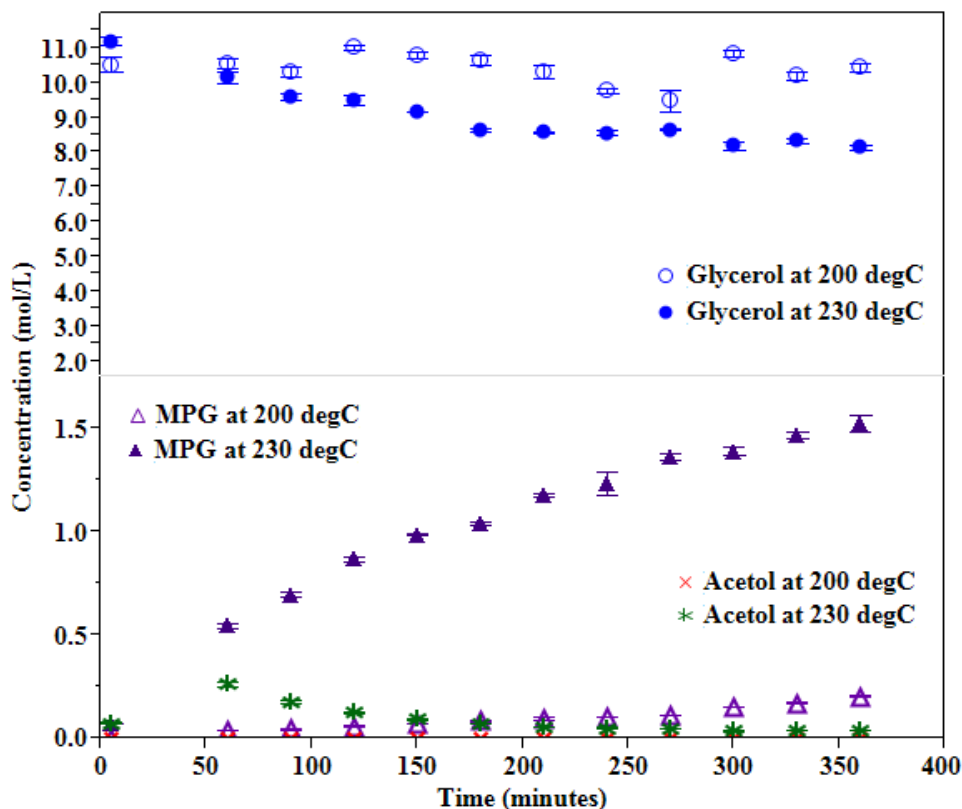


Figure 5-9: Concentration profiles at different temperatures [P = 500 psig, Agitation = 1000 RPM, Glycerol content = 90 wt%, Catalyst weight = 3 g]

Similar drastic effects were observed by Rode et al.⁵³ in both the batch and the continuous mode.

As described in Section 2.3.2, acetol hydrogenation to MPG is faster than the glycerol dehydration and hence, whatever acetol was being produced must have been quickly disappearing to form MPG. Also, as discussed in Section 2.3.1, acetol hydrogenation is

avored by lower temperatures which might also be the reason for no acetol detection at 200 °C.

Change in temperature from 200 °C to 230 °C for the reaction ran at 400 psig of hydrogen pressure, produced results similar to the reaction ran at 500 psig. Results are presented in Figure 5-10. Only observable difference from the earlier results was glycerol concentration at different times that did not show significant variation from lower temperature. Acetol also did not show an initial lump as observed in the case of higher pressure. Acetol concentration was rather consistent in this case at different times for 230 °C. Concentration of MPG at the end of 6 hrs showed similar 5-6 times increase from concentration at 200 °C.

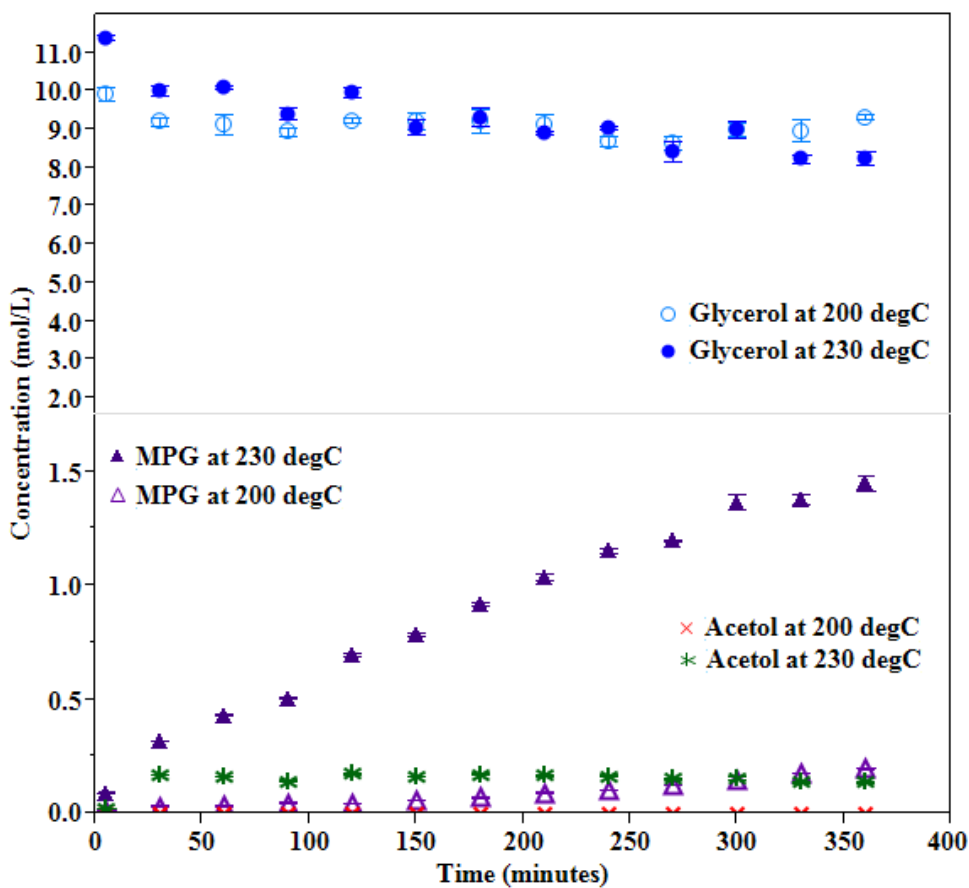


Figure 5-10: Concentration profiles at different temperatures [P = 400 psig, Agitation = 1000 RPM, Glycerol content = 90 wt%, Catalyst weight = 3 g]

Marginal difference in the acetol concentration from higher pressure case could be due to marginally higher hydrogenation rate at 500 psig. Effect of pressure is discussed in detail in the next section.

The difference in the glycerol composition at the starting time as seen in Figure 5-9 and Figure 5-10, appears from the fact that feed was an aqueous glycerol mixture. It was preheated to the reaction temperatures that would normally be around 200 – 230 °C at around 30 psig pressure in the overhead tank. Under this condition, water might have boiled off partly, if not completely, causing the concentration of glycerol in the feed mixture to vary slightly. Although, not all the cases studied showed such fluctuations, in some cases it was apparent. Another reason could have been that the glycerol was not dropping all at once.

MEG, which is basically formed out of C-C bond breakage, was rarely detected in our case and only in the case of higher temperatures, which is expected since, at higher temperatures cracking of glycerol and even of MPG takes place. Many researchers have made similar observations as discussed in Section 2.4.4. Also, MEG was detected in the case of reactions at higher RPM like 1000 RPM and 1200 RPM whereas, it wasn't detected at the same temperature and pressure when the reaction was ran at 500 RPM. C-C bond breaking might be taking place at higher RPM causing the glycerol to disintegrate into some impurities as suggested by Wolosiak-Hnat et al.³⁹

5.3.5.2 Effect of pressure on the concentration profiles of reaction components

Effect of pressure on the concentration profiles of the reaction components was studied separately at two different reaction temperatures. Variation of concentration of reaction components at 200 °C with pressure, is presented in Figure 5-11 as shown below. A change

in the hydrogen pressure from 400 psig to 500 psig, did not show as drastic an effect as the one observed in the case of change in temperature. When pressure was changed from 400 psig to 500 psig, keeping temperature at 200 °C, glycerol concentration showed considerable change. As observed earlier, Acetol did not show up at 200 °C. Usually, it is expected that at higher hydrogen pressures, hydrogenation rates are faster resulting in higher production of MPG.

Interestingly, MPG did not show any considerable effect on its concentration upon change in the pressure from 400 psig to 500 psig.

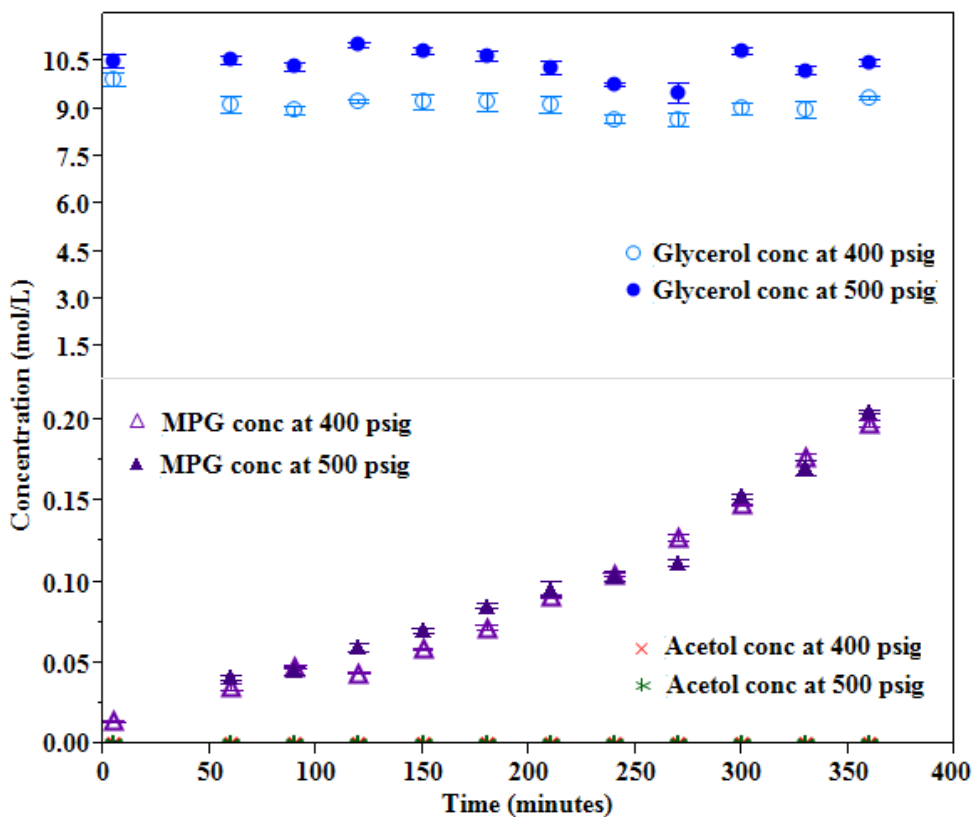


Figure 5-11: Concentration profiles at different pressures [T = 200 °C, Agitation = 1000 RPM, Glycerol content = 90 wt%, Catalyst weight = 3 g]

Variation in the glycerol concentration might not have been originated from the change in pressure. It could be an error from the GC results, due to high degree of variance in sample

replicates, especially at lower temperatures of 200 °C. Further, insignificant effect on MPG concentration by the change in pressure could be due to low conversion of glycerol as sufficient acetol might not have been produced that would cause significant change to the MPG concentration.

Slightly different results were obtained when change in pressure was induced in a reaction ran at 230 °C. Although, glycerol did not show considerable variation in the concentration profile upon change in pressure, MPG and acetol did show marginal differences. Acetol and MPG concentrations were found to be slightly higher at higher pressure of 500 psig as compared to 400 psig. Results for concentration variation for the change in pressure for reaction ran at 230 °C are presented in Figure 5-12.

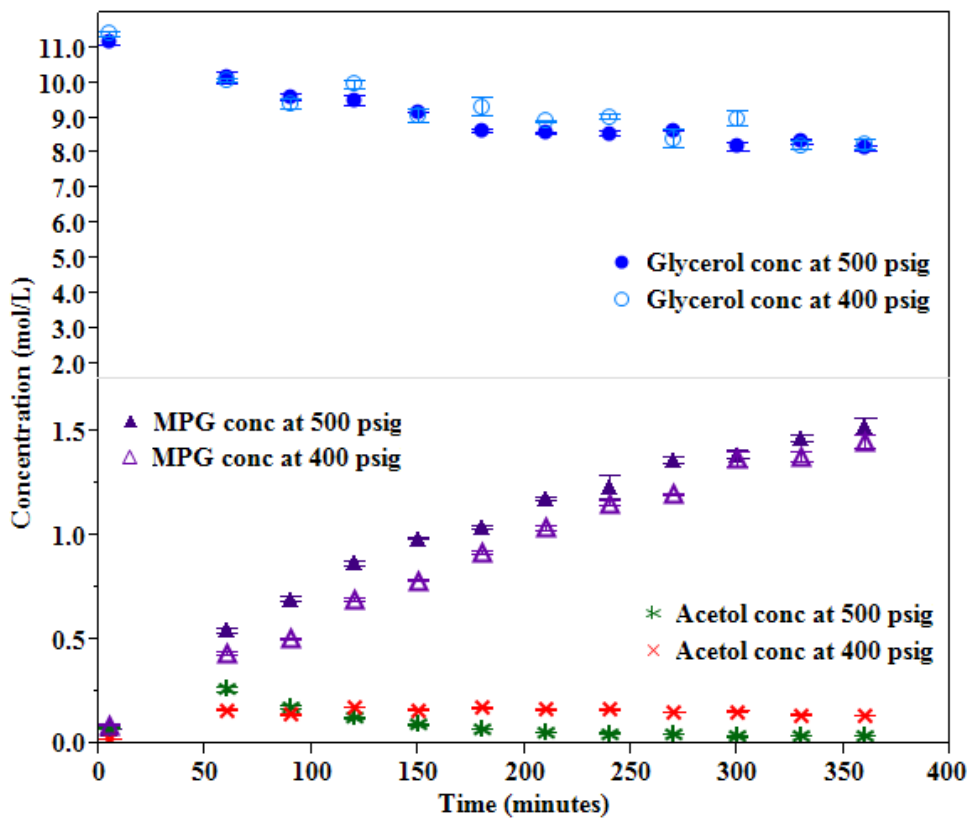


Figure 5-12: Concentration profiles at different pressures [T = 230 °C, Agitation = 1000 RPM, Glycerol content = 90 wt%, Catalyst weight = 3 g]

Researchers have observed a similar increase in the MPG production as discussed in Section 2.4.5. When hydrogen pressure is increased, it increases the solubility of hydrogen in the aqueous glycerol solution as seen from results in Section 5.3.3. This in turn means, more hydrogen becomes available for the hydrogenation step to proceed. This further explains why acetol concentration dropped when the pressure was increased from 400 psig to 500 psig as seen in Figure 5-12. One explanation could be that more acetol reacted to form MPG instead of going toward polymerization.

In the case of impurities, they were quantitatively detected only at higher temperatures such as 230 °C. No quantifiable amounts of impurities were detected at 200 °C or lower. Change in pressure showed considerable effect on the concentration profiles of impurities as discussed below. Concentration profile for light impurities at different pressures is presented in Figure 5-13.

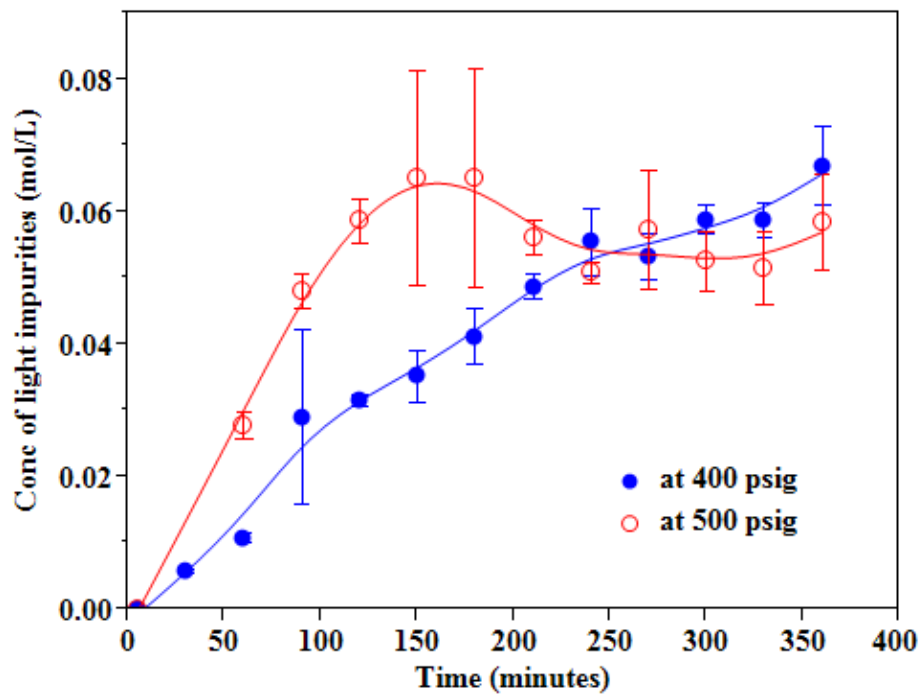


Figure 5-13: Effect of pressure on light impurities [T = 230 °C, Agitation = 1000 RPM, Glycerol content = 90 wt%, Catalyst weight = 3 g]

Pressure did not show a drastic effect on light impurities. When the pressure was at 500 psig, light impurities initially increased sharply, but became steady or slightly dropped after 3 - 3.5 hours whereas in the case of lower pressure of 400 psig, concentration of light impurities rose continuously at a steady rate over a period of time. In contrast, effect of pressure change on the concentration profile of heavy impurities showed reverse change in which concentration of heavy impurities was higher at 400 psig than at 500 psig that is presented in Figure 5-5.

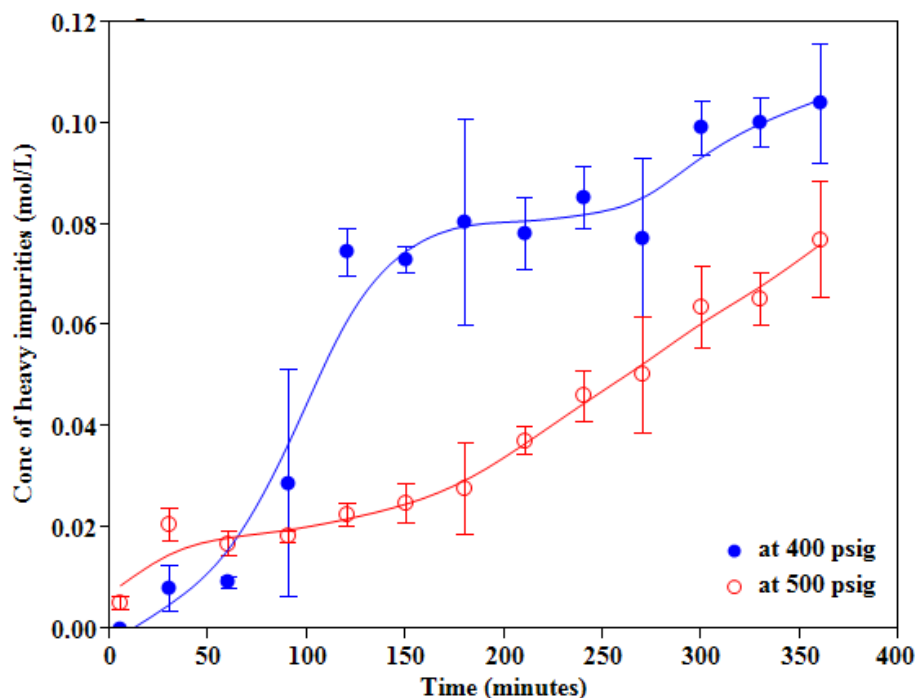


Figure 5-14: Effect of pressure on heavy impurities [T = 230 °C, Agitation = 1000 RPM, Glycerol content = 90 wt%, Catalyst weight = 3 g]

Heavy impurities also showed a significant difference in concentration when the pressure was changed from 400 psig to 500 psig. At lower pressure, the concentrations of heavy impurities were considerably higher for most of the reaction time, than at higher pressures as seen in Figure 5-14. This may be due to the higher rate of hydrogenation of acetol from larger concentrations of dissolved hydrogen at higher pressures as suggested by Wolosiak-Hnat et al.³⁹ Because of this, acetol's side reactions get hindered and most of the acetol goes to MPG production. This could explain the marginal increase in MPG observed earlier at higher pressures, as shown in Figure 5-11. Wolosiak-Hnat et al.³⁹ had also observed a drop in the concentration of impurities like C-C degradation products and others, when the pressure was increased.

Both of these results were interesting since it was believed that acetol, other reactive intermediates, or MPG gets hydrogenated via excess hydrogenolysis and form degradation products, this might be the reason for higher concentration of light impurities. Also, because all these reactive intermediates are quickly getting hydrogenated, they might not be present in enough amount so as to form polymerized products that mainly constitute heavy impurities, and this could lower the concentration of heavy impurities at higher hydrogen pressure.

5.3.5.3 Effect of initial glycerol content on the concentration profiles of the reaction components

Being a complex reaction, glycerol hydrogenolysis produces a complex set of products due to polymerization and other side reactions. Even the intermediate compounds such as acetol, are highly reactive and degrade easily. Water or solvents like methanol have been found useful in reducing these degradation products.¹⁸ Hence, Dasari et al.¹⁸ recommended at least 10-20 wt% of water content in the initial reactant mixture.

Change in the initial glycerol content showed a significant change in MPG production even when the reactions were ran at 500 RPM that were still mass-transfer limited. MPG production went up by almost 30 %, when the initial glycerol content was increased from 80 wt% to 90 wt% in a reaction ran at 230 °C as seen in Figure 5-15. Acetol however, did not show considerable difference in the concentration profile when initial glycerol content was changed. Effect of initial glycerol content on the glycerol concentration profile was inconclusive due to great degree of variance out of GC results.

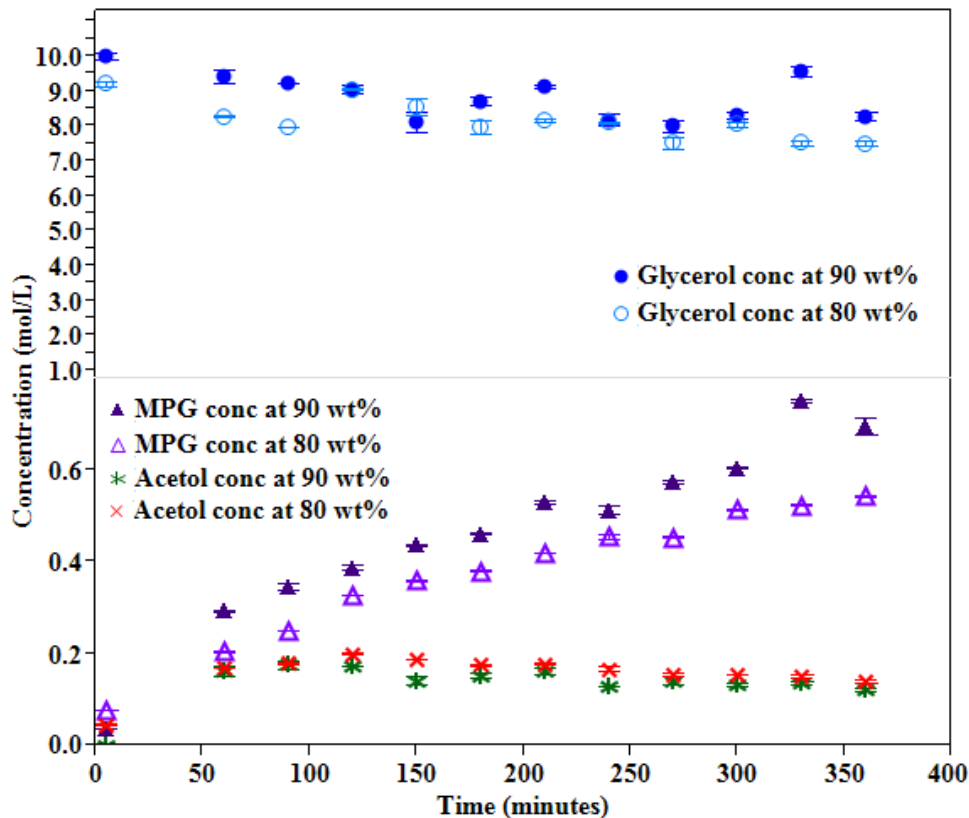


Figure 5-15: Concentration profiles at different initial glycerol content [T = 230 °C, P = 500 psig, Agitation = 500 RPM, Weight of catalyst = 3 g]

One obvious reason for this result includes, higher glycerol concentrations lead to more catalyst sites getting occupied. This in turn will lead to more conversion towards MPG, giving better yield. But it may not be true in all the cases because, in the batch mode, Rode et al.⁵³ observed a drop in the conversion of glycerol upon increase in the glycerol content, which they attributed to the overloading of glycerol as compared to the available catalyst sites. But at higher glycerol concentrations, amount of catalyst present in the reaction system also becomes important. Xiao et al.²² observed increase in the MPG production with increase in glycerol content because the catalyst weight was proportional to glycerol and which also increased with glycerol content. Xiao et al.²² further had pointed out that in the case of Rode et al.⁵³ catalyst weight was same irrespective of glycerol concentration, which caused MPG

production to go down in their case. Contrastingly, in our case, change in the glycerol content showed increase in MPG production irrespective of catalyst weight, which was constant. Reason for this difference could be solvent and hydrogen pressure. Rode et al.⁵³ used 2-propanol as solvent and a pressure of 52 bar whereas in our case, we had used water as a solvent and hydrogen pressure of 35 bar. It might have been possible that higher pressure of hydrogen could have caused more hydrogen atoms to occupy active sites on the catalyst surface, reducing availability for glycerol.

At 200 °C, effect of change in the glycerol content on the hydrogenolysis of glycerol is presented in Figure 5-16 shown below.

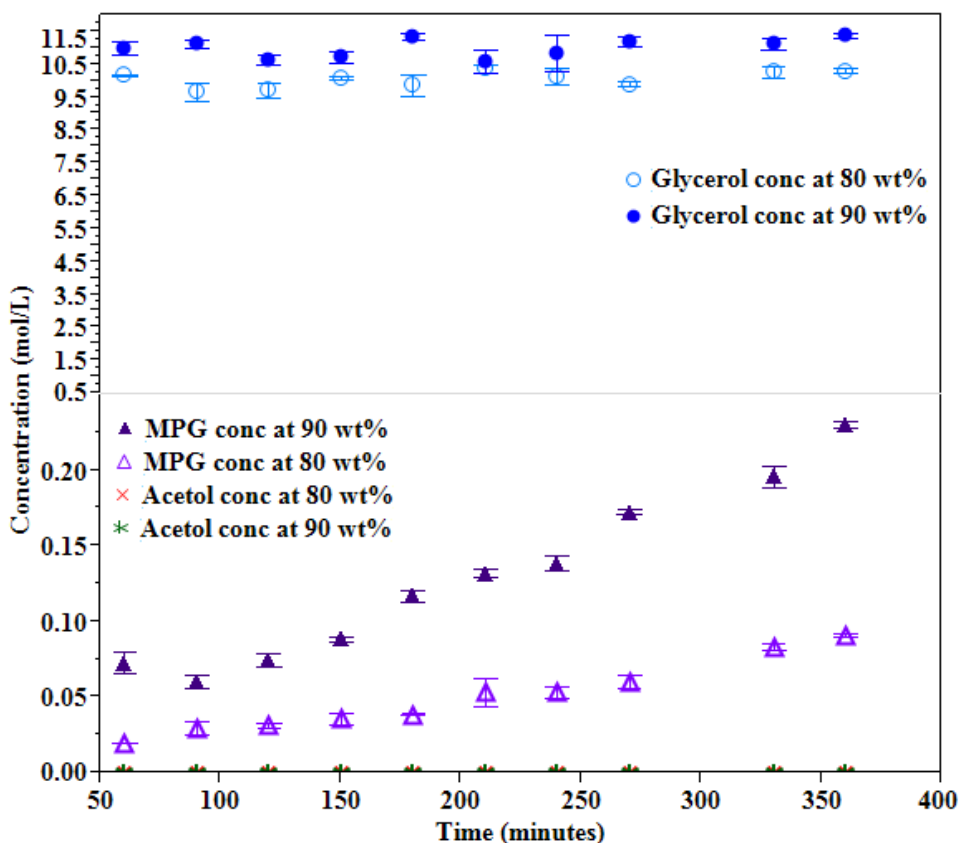


Figure 5-16: Concentration profiles at different initial glycerol contents [T = 200 °C, P = 500 psig, Agitation = 1000 RPM, Catalyst weight = 3 g]

At 200 °C, a change in the initial glycerol content from 80 wt% to 90 wt% induced more than 100 % change in the MPG production at six hours of reaction time as could be seen in Figure 5-16. As found earlier, acetol was not detected at 200 °C and glycerol concentration profile showed inconclusive result upon change in the initial glycerol content. This drastic rise of more than double in the production of MPG upon 10 wt% change in the starting glycerol concentration, could have been due to low conversion levels of glycerol at 200 °C.

Both of these results suggested strong influence of the initial glycerol content on the production of MPG. Previous researchers have reported similar influence on the MPG yield.¹⁸

5.3.6 Mass Balance

A mass balance was performed on all the three reaction runs whose results were used for modeling purposes. It was done to verify that no extra moles of carbon were getting produced in the reaction apart from what was being fed. A typical mass balance for a reaction ran at 230 °C, 400 psig is presented in Table 5.3 below.

Table 5.3: Mass balance for hydrogenolysis of glycerol at 230 °C and 400 psig

Name of the component	Initial value (mol/L)	Final value (after 6 hours of reaction time) (mol/L)	Moles of carbon in each component (mol)	
			Initial	Final
Glycerol	11.4	8.26	9.405	6.8145
Acetol	0	0.137	0	0.113025
MPG	0	1.45	0	1.19625
Light Impurities	0	0.067	0	0.055275
Heavy Impurities	0	0.104	0	0.0858
Total	11.4	10.018	9.405	8.26485
% Deficit	12.10 %		12.12 %	

This difference in initial and final mole balance for the reaction might be due to inability to detect all impurities and to calculate accurate molecular weight of those impurities. Further, some of the material might have been washed away with methanol when the filled catalyst basket was washed post reaction. These two factors are the most probable reasons for mole deficit. Other losses might have been through production of CO₂ that constituted (~ 2-3 %) of reactor gas effluent stream with rest being hydrogen.

All the three reactions used for kinetic modeling gave similar results in material balance. Also, other reactions carried out during parameter study gave better material balance with only 2-3 % difference between initial and final number of carbon moles. It must have been due to low conversion of glycerol and absence of quantifiable impurities. Absence of quantifiable impurities leaves ‘catalyst wash’ and CO₂ formation as the most probable reasons for the deficit in number of moles.

5.4 Kinetic Model

5.4.1 Preliminary order determination by Integral Method

For developing the kinetic model, data was used based on the MPG production and how significant the drop in the glycerol concentration was. Hence, data from three reaction sets was selected and analyzed for this study.

Before any model was obtained from nonlinear regression, it is important to calculate initial guesses for the reaction orders and the reaction rate constant ‘k’ values, for the regression to converge in minimum number of iterations. Hence, the integral method was used to calculate the preliminary order of the reaction before the full regression analysis was run on the

reaction data. As seen previously from Section 5.3.5.3, initial glycerol concentration did show significant influence on the reaction rate and hence, zero reaction order with respect to glycerol was out of question. Using the integral method, $\ln\left(\frac{C_A}{C_{A_0}}\right)$ vs. *time* and $1/C_{A_0}$ vs. *time* did give a straight line and hence it was verified in all the three reaction runs, that the integral method was giving good fit for 1st and 2nd order analysis.

In the case of hydrogen concentration, it was maintained constant for the entire reaction run since the total hydrogen pressure was maintained constant. As we have seen previously from Section 5.2.5.2, reactions were ran only at two different hydrogen pressures of 400 psi and 500 psi. This two point pressure data, although sufficient enough to determine the order against hydrogen, was not enough for the most accurate prediction of the value and hence, based on the values reported in literature^{38,44}, which were close to 1, it was decided to use reaction order with respect to hydrogen as 1 throughout all the calculations. Since the hydrogen concentration was constant throughout a reaction, it didn't affect evaluations of reaction orders or of other parameters.

5.4.1.1 Analysis of the reaction ran at (230 °C an 400 psig, 1000 RPM)

Order analysis for the reaction ran at 230 °C, 400 psig, and 1000 RPM, is presented as shown below in Figure 5-17. Orders of 1 and 2 were tested for a fit using the integral method. It gave very good fit with high regression coefficient values as shown.

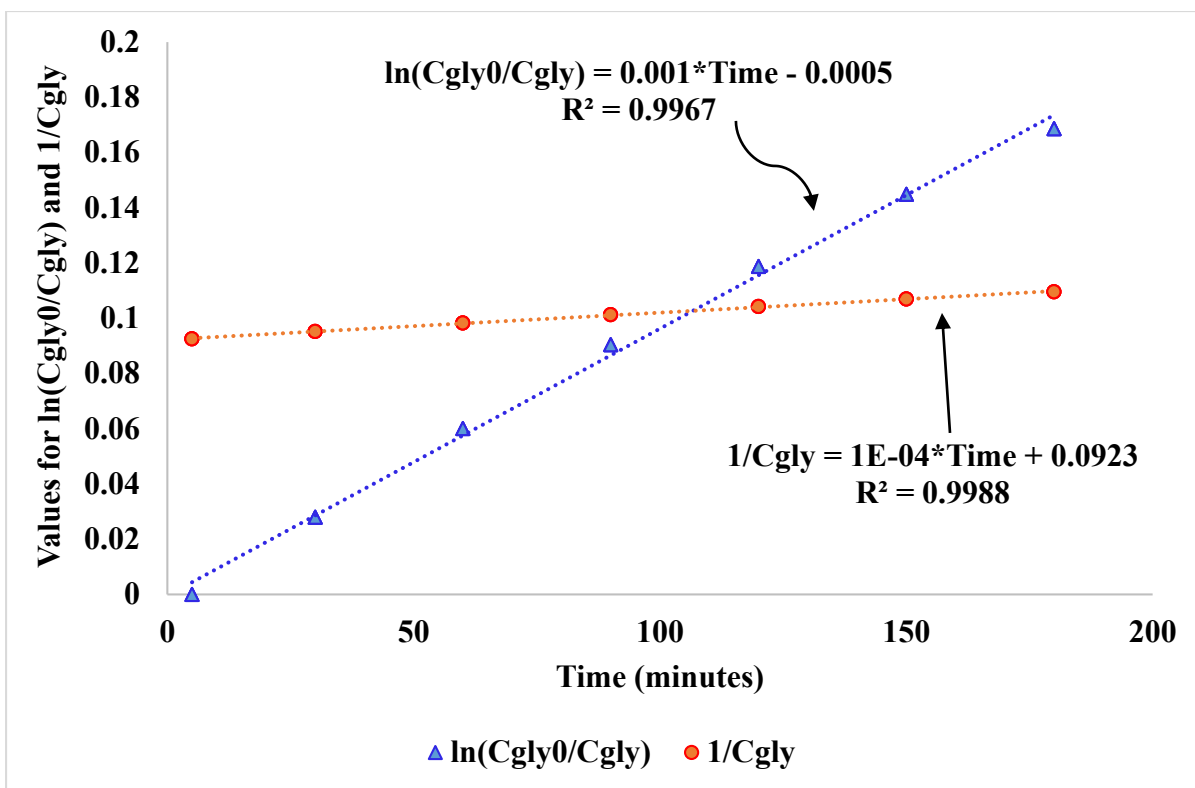


Figure 5-17: Order analysis for the reaction data at [T = 230 °C, P = 400 psig, Agitation = 1000 RPM, Glycerol content = 90 wt%, Catalyst weight = 3 g]

R^2 value for 2nd order analysis is slightly higher than the analysis for first order. It can be said that order could be either 1, or 2. Since these results gave very good fit for 2nd order against glycerol, the slope of 1/Cgly vs. time curve gave a value that could be used as a rate constant and which was of the order 10^{-4} on a ‘minutes’ basis. Based on these values of order and the slope of these lines, a full nonlinear regression analysis was then run to calculate the exact order for glycerol consumption and against MPG and impurities production.

5.4.1.2 Analysis of the reaction ran at (230 °C, 500 psig)

Order analysis for the reaction ran at higher pressure of 500 psig than previous, showed similar results as presented in Figure 5-18. Results for 1st and 2nd order indicated good fit with very good R^2 values.

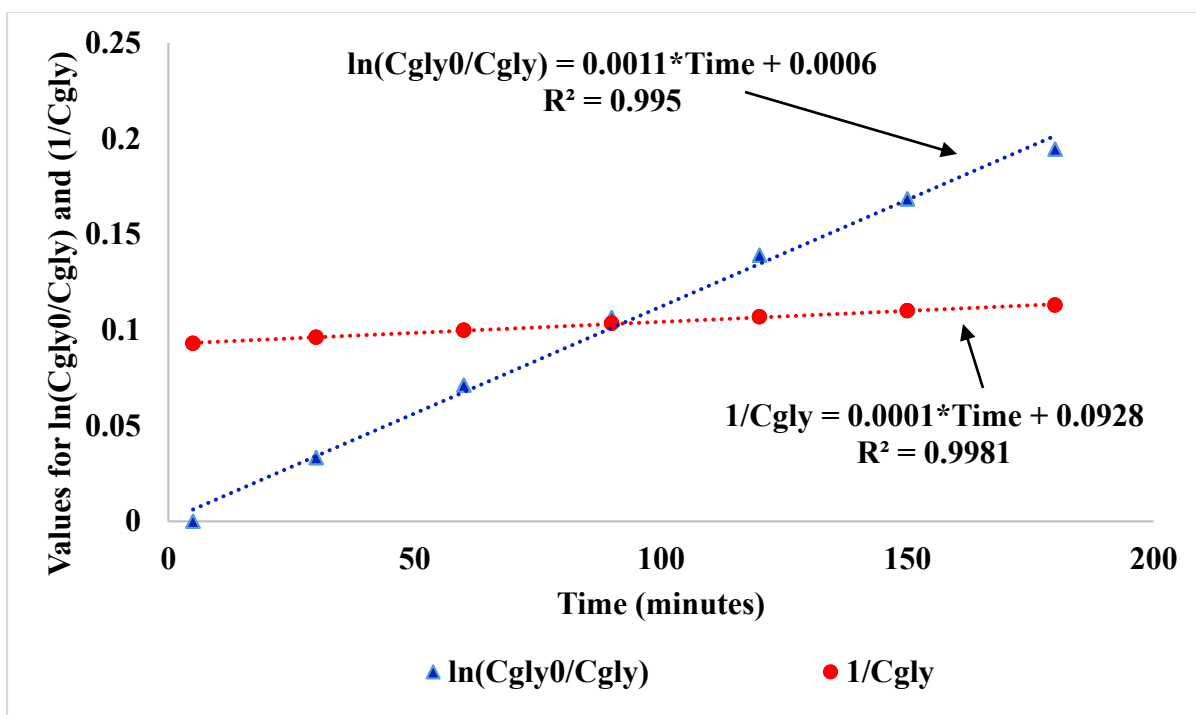


Figure 5-18: Order analysis for the reaction data at [T = 230 °C, P = 500 psig, Agitation = 1000 RPM, Glycerol content = 90 wt%, Catalyst weight = 3 g]

Results out of these analyses were used as a starting point for a full nonlinear regression analysis and even, the slope of these lines plotted gave an initial guess value for the rate constant that was of the order of 10^{-4} (minutes basis). It was also used in the regression analysis too.

5.4.1.3 Reaction order analysis for reaction ran at (230 °C, 400 psig, 1200 RPM)

When the reaction was ran at higher RPM speed of 1200, as already verified, it was free from external mass transfer effects, hence its data was used for the kinetic study. 1st and 2nd order analysis for the reaction data gave very close results as shown in Figure 5-19. In this case, both 1st and 2nd order analyses gave nearly perfect fits and it was a bit difficult to decide whether order of 1 was correct or 2.

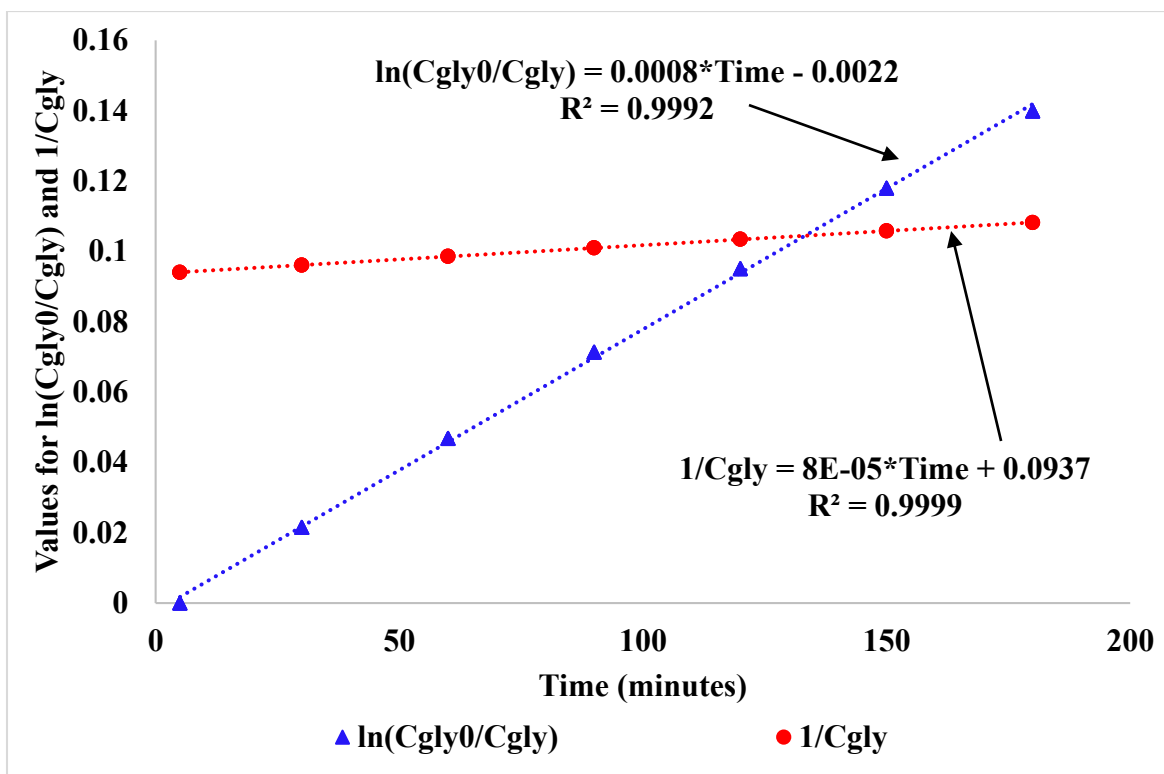


Figure 5-19: Order analysis for the reaction data at [T = 230 °C, P = 400 psig, Agitation = 1200 RPM, Glycerol content = 90 wt%, Catalyst weight = 3 g]

Slope of the lines were slightly less than seen in previous two cases and was found to be 8×10^{-5} for 2nd order and 8×10^{-4} for 1st order and both on ‘minutes’ basis. These values were used to regress the data using polymath.

5.4.2 Rate Equations

This reaction network is a complex set of series and parallel reactions as described by many researchers that is already discussed in Section 2.3. However, a relatively simple two step model that is commonly accepted and first proposed by Dasari et al.¹⁸ was modified with the addition of a new category of ‘impurities’ and used to model the kinetic data as shown in Figure 5-20.

As said before, compounds detected in the GC analysis were glycerol, acetol, MPG, MEG, and byproducts. At lower temperatures, because of the very poor conversion of glycerol, acetol was hardly detected. At higher temperatures, acetol was detected and its concentration would rise initially and would drop down a bit and become almost close to steady. Hence, two approaches were considered; one in which, for modeling the kinetic data it was assumed that for most part of the reaction once the initial hour was passed, rate of acetol production equaled the rate of acetol consumption. While developing the model, the rate of MPG production and the rate of both impurities production was modeled against glycerol consumption instead of acetol. In the second and more proper approach, MPG and the impurities concentration were modeled against the acetol concentration and the order with respect to it was found. Results from both of the approaches are summarized in the next Section 5.3.3.

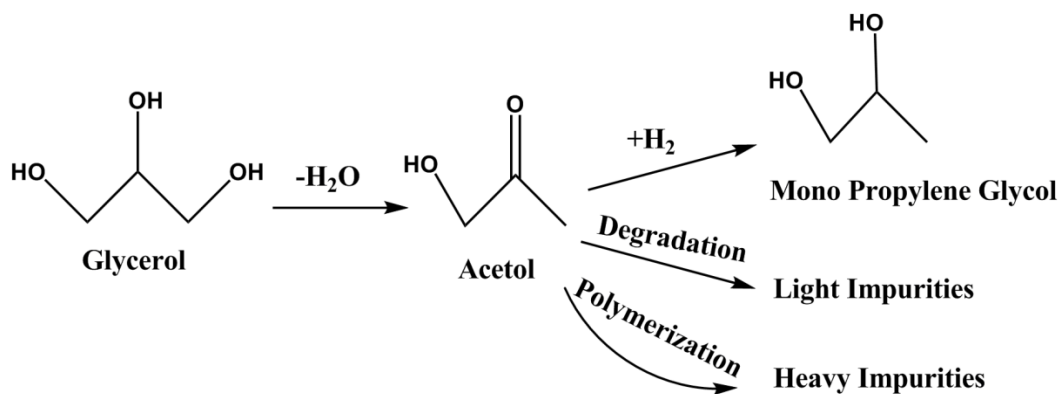


Figure 5-20: Proposed hydrogenolysis reaction model

Using the first approach, equations for the concentration of various compounds were written as below. Rate of glycerol consumption could be written as shown below with the initial guess values obtained from the integral method as described in the previous Section 5.4.1.

$$-r_{glycerol} = \frac{-dF_{gly}}{dW} = k_1 \times C_{gly}^a \quad (1)$$

where, $-r_{glycerol}$ = rate of consumption of glycerol; k_1 = rate constant;

a = reaction order with respect to glycerol; F_{gly} = glycerol flow rate (mol/s)

W = catalyst weight (g)

A similar model was developed for the rate of MPG production, r_{mpg} as described below.

$$r_{mpg} = k_2 \times C_{gly}^b \times C_{H_2} \quad (2)$$

where, r_{mpg} = rate of production of MPG; k_2 = rate constant;

b = reaction order with respect to glycerol; C_{H_2} = concentration of hydrogen (constant)

Similarly, light impurities that were calculated from the impurity analysis, were incorporated into the kinetic model as shown below.

$$r_{li} = k_3 \times C_{gly}^c \times C_{H_2} \quad (3)$$

where, r_{li} = rate of production of light impurities; k_3 = rate constant;

c = reaction order with respect to glycerol; C_{H_2} = concentration of hydrogen (constant)

Heavy impurities production was also modeled on a similar note as shown below.

$$r_{hi} = k_4 \times C_{gly}^d \times C_{H_2} \quad (4)$$

where, r_{hi} = rate of production of heavy impurities; k_4 = rate constant;

d = reaction order with respect to glycerol; C_{H_2} = concentration of hydrogen (constant)

In the second approach, the previously discussed Equation 1 was the same for the glycerol consumption. However, two new equations were added for modeling the rate of MPG

production and the impurity production with respect to acetol, as shown below in Equation 5 and Equation 6. Contrasting to the first approach, here it was assumed that whatever MPG and impurities getting produced, were coming from the acetol. Also, glycerol to acetol was assumed to be the slowest step as discussed earlier in Section 2.3.1.

$$r''_{mpg} = k_{mpg} \times C_{acetol}^{\alpha} \times C_{H_2} \quad (5)$$

Where, k_{mpg} = rate constant for MPG production reaction, C_{acetol} = concentration of acetol;

C_{H_2} = concentration of hydrogen (constant) and r''_{mpg} = rate of formation of MPG

$$r''_{impurities} = k_{impur} \times C_{acetol}^{\beta} \times C_{H_2} \quad (6)$$

Where, $r''_{impurities}$ = rate of impurities production; k_{impur} = rate constant

C_{acetol} = concentration of acetol; C_{H_2} = concentration of hydrogen (constant)

All these Equations 1, 5, and 6 were equated to each other by comparing the rate of acetol production as shown below:

$$\begin{aligned} & \textbf{Net rate of acetol production} \\ & = \textbf{Rate of acetol production from glycerol} \\ & - \textbf{Rate of consumption of acetol} \end{aligned}$$

Now, the rate of acetol production equals the rate of glycerol consumption, as it was assumed that only acetol was getting produced from the glycerol and no other intermediate, and the rate of consumption of acetol equals the sum of the rate of production of MPG and the rate of production of impurities. Hence, we can write,

$$r_{acetol} = -r_{glycerol} - (r_{mpg} + r_{impurities}) \quad (7)$$

Results for both the approaches are summarized in the sections that follow.

5.4.3 Nonlinear Regression Analysis for the First Approach

Preliminary reaction order and the rate constant data obtained using integral method as described in Section 5.3.1 and the values obtained, were supplied as an initial guess values for a full nonlinear regression analysis that was ran on the data sets using POLYMATH® by using the rate equations described in the Section 5.3.2.

Results for the first approach method obtained from the nonlinear regression are summarized in the Table 5.4. All the three cases of high temperature of 230 °C gave extremely close results for the reaction order against glycerol for the rate of glycerol consumption as described in Table 5.4. Results were 3.26, 3.36 and 3.09 that gave an average of 3.24 without significant drop in the R^2 values when back regressed. For the case of MPG production, regression analysis gave order approximately around 2.7 in all the three cases with nice R^2 value. However in the case of impurities, it was extremely difficult to regress the data and all the three runs gave results with great degree of variation and poor R^2 values. This might be due to inconsistent data for the impurities and due to difficulty in accurately quantifying the data from the GC analysis.

Table 5.4: Results from the nonlinear regression analysis (1st Approach)

Parameter	Values at 230 °C, 400 psig, 1000 RPM	Values at 230 °C, 500 psig, 1000 RPM	Values at 230 °C, 400 psig, 1200 RPM	Average	Regression coefficients (R ²)		
					at 230 °C, 400 psig, 1000 RPM	at 230 °C, 500 psig, 1000 RPM	at 230 °C, 400 psig, 1200 RPM
k ₁ (from Eqn 1)	7.78*10 ⁻⁹ (L ³ /mol ² .s. g cat)	8.11*10 ⁻⁹ (L ³ /mol ² .s. .g cat)	9.95*10 ⁻⁹ (L ³ /mol ² .s. g cat)	8.61*10⁻⁹ (L ³ /mol ² .s. g cat)	0.982	0.951	0.967
k ₂ (from Eqn 2)	1.204*10 ⁻⁷ (L ³ /mol ² .s. g cat)	1.22*10 ⁻⁷ (L ³ /mol ² .s. .g cat)	1.223*10 ⁻⁷ (L ³ /mol ² .s. g cat)	1.215*10⁻⁷ (L ³ /mol ² .s. g cat)	0.986	0.996	0.997
k ₃ (from Eqn 3)	10 ⁻¹⁰ – 10 ⁻¹³ (L ⁷ /mol ⁶ .s.g cat)			10⁻¹¹			
k ₄ (from Eqn 4)	10 ⁻⁸ - 10 ⁻¹² (L ³ /mol ² .s.g cat)			10⁻¹⁰			
order – a (from Eqn 1)	3.26	3.36	3.09	3.24	0.982	0.951	0.967
order – b (from Eqn 2)	2.677	2.677	2.677	2.677	0.986	0.996	0.997
order – c (from Eqn 3)	3 – 8			6			
order - d (from Eqn 4)	1-3			1.5			

Although nonlinear regression gave best results with orders of around 3 for glycerol consumption and MPG production, physically it makes no sense because, according to the collision theory in thermodynamics, it is highly unlikely that 3 molecules of reactant will

collide to form a new product. Usually, only upto 2 molecules can collide and form a new component. Hence, a nonlinear regression with reaction orders of 2 was forced in polymath for the already discussed rate expressions and it gave decent results, if not great. Values of regression coefficient dropped from 0.98 to 0.84. Values of rate constants for glycerol consumption obtained were around $5.5 \times 10^{-7} \text{ L}/(\text{mol} \cdot \text{s} \cdot \text{gcat})$ and for MPG production, around $2.036 \times 10^{-5} \text{ L}^2/(\text{mol}^2 \cdot \text{s} \cdot \text{gcat})$. Further, forcing equation (3) discussed above for light impurities to second order, gave rate constant approximately as $9.4 \times 10^{-7} \text{ L}^2/(\text{mol}^2 \cdot \text{s} \cdot \text{gcat})$ with a regression coefficient of 0.92. These results realistically make more sense. For the production of heavy impurities, reaction order with respect to glycerol was already about 1.5. Hence, concentration values for heavy impurities were not forced for a 2nd order regression.

5.4.4 Nonlinear regression analysis for the second approach

Values obtained for k_1 and order 'a' were still valid for modeling using the second approach. Only equations 5, 6, and 7 were needed to be regressed. It was difficult to regress the kinetic data for the MPG and the impurities with respect to acetol and did not give degrees of correlation. A summary of results obtained from the second approach could be found in the Table 5.5 shown below.

Table 5.5: Nonlinear regression results for the second approach

Parameter	Values at 230 °C, 400 psig, 1000 RPM	Values at 230 °C, 500 psig, 1000 RPM	Values at 230 °C, 400 psig, 1200 RPM
k_{mpg}	approx. $10^{-1} - 10^{-3}$		
$k_{\text{impurities}}$	approx. $10^{-1} - 10^{-3}$		
reaction order - α	approx. 0.25-0.5		
reaction order - β	approx. 0.25 - 3		

Second approach did not give good results as it was extremely difficult to model the acetol formation, as acetol was simultaneously getting produced and getting consumed, at different rates. Hence, a reaction with pure acetol as the main reactant was ran on the same catalyst at the conditions of 230 °C, 400 psig, 1000 RPM, and with 20 wt% initial acetol content. This reaction gave a better picture of how acetol reacts as well as several interesting results. Results from this reaction were then used to regress the data to calculate the actual order against acetol.

GC analysis for the reaction with acetol did not show any MEG formed irrespective of the reaction time, which reaffirmed that MEG was formed as a part of C-C bond breaking and would have only come from glycerol and not the acetol. Further, GC analysis showed formation of light impurities-I at a consistent rate over the course of the reaction suggesting that the majority of light impurities would have come from acetol. It was also interesting to see not many heavy impurities were detected during the same analysis. All these results indicate that the source of the light impurities that impart color and odor to the product, might be the acetol degradation as earlier thought.

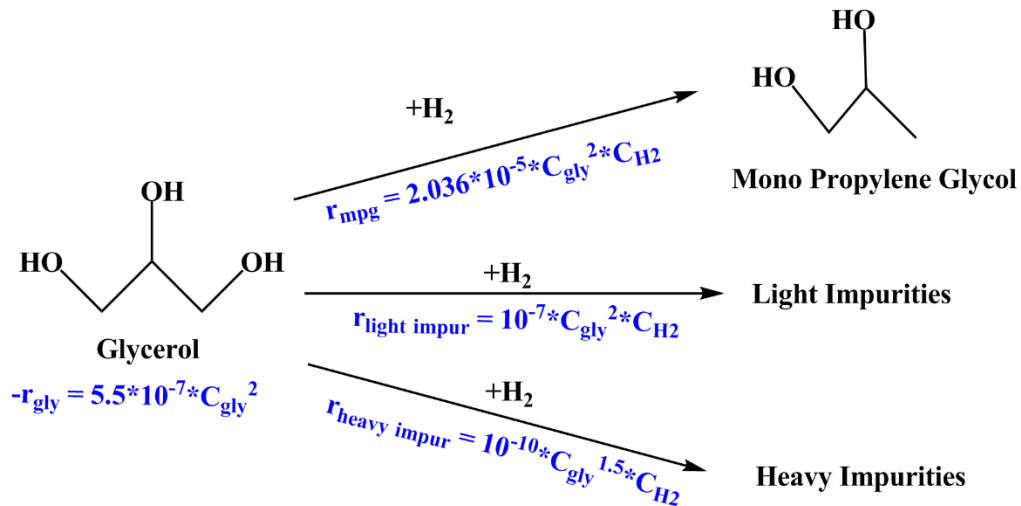
Data obtained from the reaction with acetol was regressed to get orders of the reaction of acetol consumption, MPG production, and light impurities production with respect to acetol. The results are summarized as shown in Table 5.6:

Table 5.6: Kinetic parameter values from acetol reaction

Parameter	Value of k at 230 °C, 400 psig and 20 wt% acetol	Reaction order (w.r.t acetol)	Regression coefficients (R ²)
k _{acetol}	1.091E-3	1.311	0.9839
k _{mpg}	0.100	3.155	0.9657
k _{li}	0.586	3.336	0.9826

Although results from this reaction gave decent values for the orders and rate constants, more rigorous study would be required before they can be incorporated into the comprehensive reaction model.

Due to poor results at 200 °C, activation energy could not be determined. But, based on all the other results obtained from the previous three sections, a kinetic model as shown in the Figure 5-21 below based on glycerol was accepted for further analysis, although it goes to the products and impurities via fast reaction intermediate like acetol.



This model underlies the assumption of acetol as a very fast intermediate

Figure 5-21: Final kinetic model for calculations

Chapter 6: Engineering Significance

As discussed earlier, hydrogenolysis of glycerol over copper chromite is already a commercialized process due to strong economic aspects of this reaction. A highlight of this process is that the main product MPG sells at more than twice the cost of glycerol. Table 6.1 shows bulk costs for glycerol and MPG.

Table 6.1: Bulk costs of MPG and Glycerol

Name of the material	Bulk Cost (\$/100 lb)
Glycerol (99.5%) ¹⁵	42
MPG (99.5+ %) ¹⁴	89

Lot of other factors are involved on the industrial scale. Typically on the industrial scale, the process will involve glycerol and water fed from a feed tank then mixed with hydrogen. This mix stream of aqueous glycerol and hydrogen will be preheated to almost reaction temperature via a preheater. This preheated stream will then be sent to the reactor, where hydrogenolysis of glycerol will be carried out. Products from the reactor will mainly consist of gas phase components and liquid phase components. Components from the gas phase that will be rich in hydrogen, can undergo purification via an absorption column and purified hydrogen can be recycled back to the feed stream of hydrogen. Liquid phase components involve mainly glycerol, MPG, acetol, MEG, and other byproducts that can be separated by various techniques of distillation, extraction, etc. Also unreacted glycerol recovered, can be recycled back to the feed stream with or without purification depending on the quality.

Further, this entire operation could be even more profitable when glycerol produced from biodiesel can be directly used for hydrogenolysis of glycerol. Future research may ultimately

lead to the commercialization of that process too. If that process gets commercialized that could be a big boost to the biodiesel industry.

Currently companies like Terra BioChem LLC, TX; Archer Daniels Midland Company (ADM), Decatur, IL, etc. produce propylene glycol from technical grade glycerol using hydrogenolysis process over a catalyst. Terra BioChem uses copper chromite as a catalyst for MPG production whereas, the catalyst used by ADM is undisclosed⁶¹. Most of these industries use distillation for separation of MPG from other coproducts and impurities.

Results from the current study indicated that MPG purification to technical grade was achievable with liquid-liquid extraction. Further, simulation of a packed bed reactor in polymath using the results obtained from the kinetic study, showed that residence time did not make any significant changes ($\sim 0.01\%$) in the selectivity of components as residence time was increased. The selectivity towards MPG was consistent around $99.4 - 99.5\%$, selectivity towards light impurities was around 0.48% and the selectivity towards heavy impurities was steady around 0.02% , when the residence time was increased. However, glycerol conversion increased rapidly with increase in residence time till 20 minutes. After 20 minutes, glycerol conversion rose steadily till 60 minutes of residence time. After 60 minutes of residence time, any further increase did not produce significant change to the conversion ($\sim 0.5\%$). At 60 minutes of residence time, conversion of glycerol obtained was 96.77% with selectivity towards MPG at 99.5% . Results from the effect of residence time on the conversion of glycerol and on selectivity towards products are presented in Figure 6-1.

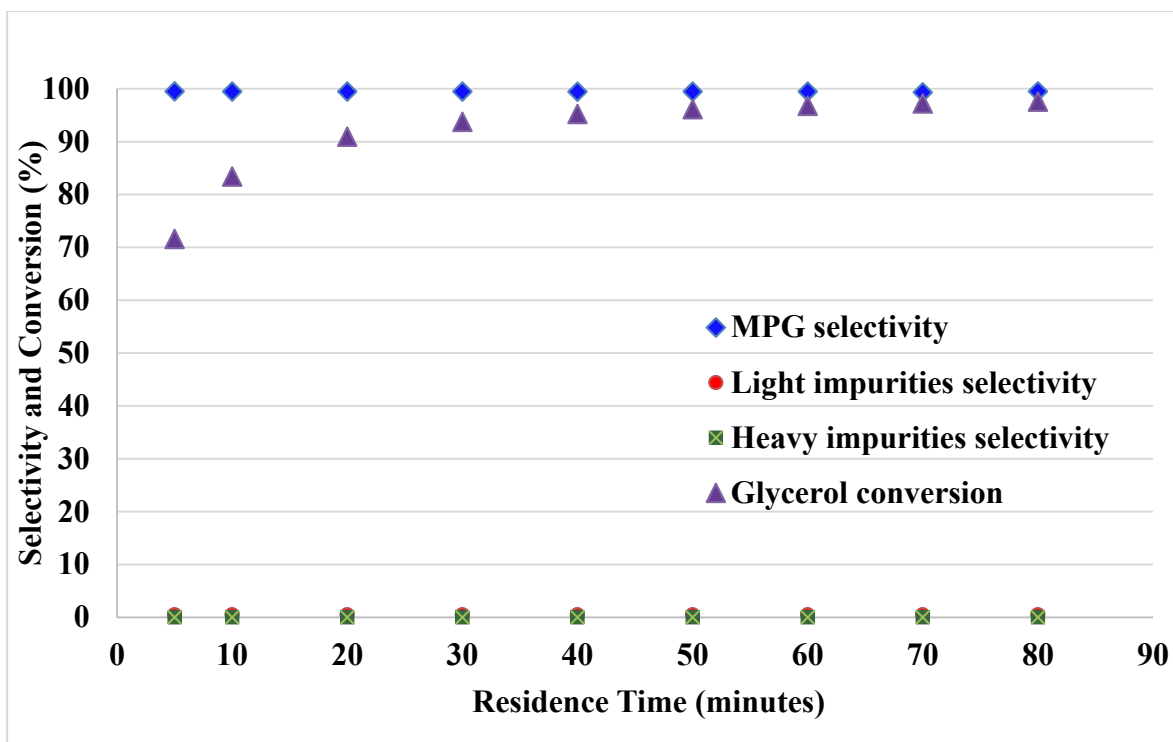


Figure 6-1: Effect of residence time on conversion of glycerol and on selectivity towards products

Use of liquid-liquid extraction instead of distillation or in conjunction with distillation can be an alternative for consideration while developing industrial hydrogenolysis process in future.

Also, industrial operations with residence time of 60 minutes is an option worth looking towards minimization of byproducts and better MPG yields.

Chapter 7: Conclusions

Most of the defined objectives from Chapter 1 were studied and completed. In the case of identification of the impurities that was objective 1 of this study, this work gave interesting results. Although this work was not able to identify each and every impurity formed in this reaction using the GC analysis, it was still able to categorize various types of impurities found and hence four categories of impurities were classified and studied. This work was also able to identify impurities that imparted yellow color and foul odor to the final product of the reaction. Light impurities-I was the class of impurities that imparted yellow color and foul odor. Results indicated that they might have formed from the degradation of acetol.

Liquid-liquid extraction results showed that it can be a cheap and economical alternative for removing these impurities in multiple washes. TXIB solvent, which was used in this process, was easily recoverable thereby lowering the total solvent requirement and in turn raw material cost. Analysis from the liquid-liquid extraction gave important result about the partition coefficient of the light impurities and the heavy impurities. Partition coefficient for the light impurities for TXIB/MPG phase was found to be 0.12 (w/w) at equilibrium and for the heavy impurities it was calculated as 0.14 (w/w) at equilibrium. Both these results signified the difficulty in the removal of these compounds.

Based on the kinetic data obtained, the reaction was successfully modeled. The reaction order with respect to glycerol for the consumption of glycerol was found to be around 2 with a rate constant of 5.5×10^{-7} (L/mol.sec.g catalyst). For the production of MPG, order with respect to glycerol was found to be 2 with a rate constant of 2.036×10^{-5} (L²/mol².sec.g catalyst) that hinted at a faster rate of hydrogenation. Impurities were successfully modeled by assuming the molecular weights of them similar to that of MPG. Thus, light impurities showed an order

of around 2 with a rate constant in the range of $10^{-6} - 10^{-7}$ ($L^2/mol^2 \cdot sec \cdot g$ catalyst). Heavy impurities whereas, showed an order of around 1.5 with a rate constant in the range of $10^{-9} - 10^{-10}$ ($L^2/mol^2 \cdot sec \cdot g$ catalyst).

Surface area analysis showed that the surface area of the catalyst used in the batch mode and at higher temperatures and pressures showed substantial degradation which suggested that in order to improve the catalyst lifetime, optimal conditions of temperature and pressure need to be used that may involve lowering the temperature and pressure while maintaining the MPG yield.

Industrial significance of the hydrogenolysis of glycerol over copper chromite and future direction of research in this area was also presented.

Chapter 8: Future Work

- Analysis of the products formed on the copper chromite catalyst using acetol and MPG as the main reactant for the hydrogenolysis reaction that will provide more insight into degradation of these compounds.
- Analysis of parameter effects on the acetol reaction
- Effect of the addition of the buffers on the kinetics of this reaction system.
- Calculating adsorption kinetics data and measurement of the adsorption rate constants for the hydrogenolysis reaction for the production of propylene glycol over copper chromite that will provide more insights into the reaction network.
- Simulating liquid-liquid extraction in the Aspen Plus for purification of the products and recoverable reactants

Bibliography

- (1) Leaky, R. *The Origin of Humankind*; Science Masters Series, Basic Books: New York, 1994; pp xiv-xv.
- (2) *The Coal Resource: A Comprehensive Overview of Coal*; World Coal Institute: London, May 2005.
- (3) Willke, T.; Vorlop, K. D. Industrial bioconversion of renewable resources as an alternative to conventional chemistry. *Appl. Microbiol. Biotechnol.* **2004**, *66* (2), 131-142.
- (4) *Annual Energy Outlook 2013*; U.S. Energy Information Administration, U.S. Department of Energy, United States Government Printing Office: Washington, DC, 2013.
- (5) Demirbas, A. Political, economic and environmental impacts of biofuels: A review. *Appl. Energy* **2009**, *86*, S108-S117.
- (6) RFA World Fuel Ethanol Production <http://ethanolrfa.org/pages/World-Fuel-Ethanol-Production> (accessed August, 2013).
- (7) Ma, F. R.; Hanna, M. A. Biodiesel production: A review. *Bioresour. Technol.* **1999**, *70* (1), 1-15.
- (8) *Monthly Biodiesel Production Report*; U.S. Energy Information Administration, U.S. Department of Energy, U.S. Government Printing Office: Washington, DC, 2014.
- (9) Pachauri, N.; He, B. Value Added Utilization of Crude Glycerol from Biodiesel Production: A survey of Current Research Activities. Annual ASABE Meeting Presentation, Portland, Oregon, July 9-12, 2006.

- (10) Behr, A.; Eilting, J.; Irawadi, K.; Leschinski, J.; Lindner, F. Improved utilisation of renewable resources: New important derivatives of glycerol. *Green Chem.* **2008**, *10* (1), 13-30.
- (11) Green, D.; Perry, R. *Perry's Chemical Engineers Handbook*; 8 ed.; McGraw Hill, New York: 2008.
- (12) Werpy, T.; Petersen, G. *Top Value Added Chemicals from Biomass, Volume 1: Results of Screening for Potential Candidates from Sugars and Synthesis Gas*; 2004. SciTech Connect. <http://www.osti.gov/scitech/servlets/purl/15008859> (accessed Sep 15, 2013)
- (13) Othmer, K. *Kirk-Othmer Encyclopedia for Chemical Technology*; Wiley, New York: 2008.
- (14) Sovine, S. D. Heterogenous Catalysis of Glycerol to Propylene Glycol over Copper Chromite. M.S. Thesis, University of Louisiana at Lafayette, August 2012.
- (15) Landress, L. ICIS Pricing Sample Glycerine Report. <http://www.icis.com/chemicals/glycerine/us/> (accessed July, 2014).
- (16) Chiu, C.-W.; Dasari, M. A.; Suppes, G. J.; Sutterlin, W. R. Dehydration of glycerol to acetol via catalytic reactive distillation. *AIChE J.* **2006**, *52* (10), 3543-3548.
- (17) Lahr, D. G.; Shanks, B. H. Kinetic analysis of the hydrogenolysis of lower polyhydric alcohols: Glycerol to glycols. *Ind. Eng. Chem. Res.* **2003**, *42* (22), 5467-5472.
- (18) Dasari, M. A.; Kiatsimkul, P. P.; Sutterlin, W. R.; Suppes, G. J. Low-pressure hydrogenolysis of glycerol to propylene glycol. *Appl. Catal., A* **2005**, *281* (1-2), 225-231.

- (19) Schmidt, S. R.; Tanielyan, S. K.; Marin, N.; Alvez, G.; Augustine, R. L. Selective Conversion of Glycerol to Propylene Glycol Over Fixed Bed Raney® Cu Catalysts. *Top. Catal.* **2010**, *53* (15-18), 1214-1216.
- (20) Ma, L.; He, D. H. Hydrogenolysis of Glycerol to Propanediols Over Highly Active Ru-Re Bimetallic Catalysts. *Top. Catal.* **2009**, *52* (6-7), 834-844.
- (21) Torres, A.; Roy, D.; Subramaniam, B.; Chaudhari, R. V. Kinetic Modeling of Aqueous-Phase Glycerol Hydrogenolysis in a Batch Slurry Reactor. *Ind. Eng. Chem. Res.* **2010**, *49* (21), 10826-10835.
- (22) Xiao, Z. H.; Li, C.; Xiu, J. H.; Wang, X. K.; Williams, C. T.; Liang, C. H. Insights into the reaction pathways of glycerol hydrogenolysis over Cu-Cr catalysts. *J. Mol. Catal., A* **2012**, *365*, 24-31.
- (23) Braca, G.; Raspolli Galletti, A. M.; Sbrana, G. Anionic ruthenium iodorcarbonyl complexes as selective dehydroxylation catalysts in aqueous solution. *J. Organomet. Chem.* **1991**, *417* (1-2), 41-49.
- (24) Drent, E.; Jager, W. W. Hydrogenolysis of glycerol. U.S. Patent 6,080,898 A, Jun 27, 2000.
- (25) Chheda, J. N.; Huber, G. W.; Dumesic, J. A. Liquid-Phase Catalytic Processing of Biomass-Derived Oxygenated Hydrocarbons to Fuels and Chemicals. *Angew. Chem., Int. Ed.* **2007**, *46* (38), 7164-7183.
- (26) Maris, E. P.; Ketchie, W. C.; Murayama, M.; Davis, R. J. Glycerol hydrogenolysis on carbon-supported PtRu and AuRu bimetallic catalysts. *J. Catal.* **2007**, *251* (2), 281-294.

- (27) Jiang, T.; Zhou, Y. X.; Liang, S. G.; Liu, H. Z.; Han, B. X. Hydrogenolysis of glycerol catalyzed by Ru-Cu bimetallic catalysts supported on clay with the aid of ionic liquids. *Green Chem.* **2009**, *11* (7), 1000-1006.
- (28) Wang, S. A.; Zhang, Y. C.; Liu, H. C. Selective Hydrogenolysis of Glycerol to Propylene Glycol on Cu-ZnO Composite Catalysts: Structural Requirements and Reaction Mechanism. *Chem.-An Asian J.* **2010**, *5* (5), 1100-1111.
- (29) Zhou, Z. M.; Li, X.; Zeng, T. Y.; Hong, W. B.; Cheng, Z. M.; Yuan, W. K. Kinetics of Hydrogenolysis of Glycerol to Propylene Glycol over Cu-ZnO-Al₂O₃ Catalysts. *Chin. J. Chem. Eng.* **2010**, *18* (3), 384-390.
- (30) Balaraju, M.; Rekha, V.; Prasad, P. S. S.; Prasad, R. B. N.; Lingaiah, N. Selective Hydrogenolysis of Glycerol to 1, 2 Propanediol Over Cu-ZnO Catalysts. *Catal. Lett.* **2008**, *126* (1-2), 119-124.
- (31) Wolosiak-Hnat, A.; Milchert, E.; Lewandowski, G.; Grzmil, B. Influence of reduction time of copper based catalysts: Cu/Al₂O₃ and CuCr₂O₄ on hydrogenolysis of glycerol. *Pol. J. Chem. Technol.* **2011**, *13* (4), 71-76.
- (32) Guo, X. H.; Li, Y.; Song, W.; Shen, W. J. Glycerol Hydrogenolysis over Co Catalysts Derived from a Layered Double Hydroxide Precursor. *Catal. Lett.* **2011**, *141* (10), 1458-1463.
- (33) Mane, R. B.; Ghalwadkar, A. A.; Hengne, A. M.; Suryawanshi, Y. R.; Rode, C. V. Role of promoters in copper chromite catalysts for hydrogenolysis of glycerol. *Catal. Today* **2011**, *164* (1), 447-450.

- (34) Brandner, A.; Lehnert, K.; Bienholz, A.; Lucas, M.; Claus, P. Production of Biomass-Derived Chemicals and Energy: Chemocatalytic Conversions of Glycerol. *Top. Catal.* **2009**, *52* (3), 278-287.
- (35) Hosgun, H. L.; Yildiz, M.; Gercel, H. F. Hydrogenolysis of Aqueous Glycerol over Raney Nickel Catalyst: Comparison of Pure and Biodiesel By-Product. *Ind. Eng. Chem. Res.* **2012**, *51* (10), 3863-3869.
- (36) Maris, E. P.; Davis, R. J. Hydrogenolysis of glycerol over carbon-supported Ru and Pt catalysts. *J. Catal.* **2007**, *249* (2), 328-337.
- (37) Kim, N. D.; Oh, S.; Joo, J. B.; Jung, K. S.; Yi, J. The Promotion Effect of Cr on Copper Catalyst in Hydrogenolysis of Glycerol to Propylene Glycol. *Top. Catal.* **2010**, *53* (7-10), 517-522.
- (38) Kim, N. D.; Park, J. R.; Park, D. S.; Kwak, B. K.; Yi, J. Promoter effect of Pd in CuCr₂O₄ catalysts on the hydrogenolysis of glycerol to 1,2-propanediol. *Green Chem.* **2012**, *14* (9), 2638-2646.
- (39) Wolosiak-Hnat, A.; Milchert, E.; Lewandowski, G. The Influence of Technological Parameters on Hydrogenolysis of Glycerol in the Presence of CuCr₂O₄ Catalyst. *J. Adv. Oxid. Technol.* **2012**, *15* (2), 405-417.
- (40) ten Dam, J.; Hanefeld, U. Renewable Chemicals: Dehydroxylation of Glycerol and Polyols. *ChemSusChem* **2011**, *4* (8), 1017-1034.
- (41) Auneau, F.; Michel, C.; Delbecq, F.; Pinel, C.; Sautet, P. Unravelling the Mechanism of Glycerol Hydrogenolysis over Rhodium Catalyst through Combined Experimental-Theoretical Investigations. *Chem. Eur. J.* **2011**, *17* (50), 14288-14299.

- (42) ten Dam, J.; Kapteijn, F.; Djanashvili, K.; Hanefeld, U. Tuning selectivity of Pt/CaCO₃ in glycerol hydrogenolysis - A Design of Experiments approach. *Catal. Comm.* **2011**, *13* (1), 1-5.
- (43) Montassier, C.; Giraud, D.; Barbier, J. Polyol Conversion by Liquid Phase Heterogeneous Catalysis over Metals. In *Studies in Surface Science and Catalysis, Heterogeneous Catalysis and Fine Chemicals*, Proceedings of an International Symposium, Volume 41 ed.; Guisnet, M., Barrault, J., Bouchoule, C., Duprez, D., Montassier, C., and Pérot, G.; Eds.; Elsevier: 1988; pp 165-170.
- (44) Vasiliadou, E.; Lemonidou, A. Kinetic study of liquid-phase glycerol hydrogenolysis over Cu/SiO₂ catalyst. *Chem. Eng. J.* **2013**, *231*, 103-112.
- (45) Wu, Z. J.; Mao, Y. Z.; Song, M.; Yin, X. Q.; Zhang, M. H. Cu/boehmite: A highly active catalyst for hydrogenolysis of glycerol to 1,2-propanediol. *Catal. Comm.* **2013**, *32*, 52-57.
- (46) Mohamad, M. H.; Awang, R.; Yunus, W. M. A review of acetol: Application and Production. *Am. J. Appl. Sci.* **2011**, *8*, 1135-1139.
- (47) Nakagawa, Y.; Tomishige, K. Heterogeneous catalysis of the glycerol hydrogenolysis. *Catal. Sci. Technol.* **2011**, *1* (2), 179-190.
- (48) Yuan, Z. L.; Wang, L. N.; Wang, J. H.; Xia, S. X.; Chen, P.; Hou, Z. Y.; Zheng, X. M. Hydrogenolysis of glycerol over homogenously dispersed copper on solid base catalysts. *Appl. Catal., B* **2011**, *101* (3-4), 431-440.
- (49) Chemical Processing.com Special Report
http://www.chemicalprocessing.com/assets/wp_downloads/pdf/CP0802_Biofuel.pdf
(accessed August, 2013).

- (50) Huang, L.; Zhu, Y. L.; Zheng, H. Y.; Li, Y. W.; Zeng, Z. Y. Continuous production of 1,2-propanediol by the selective hydrogenolysis of solvent-free glycerol under mild conditions. *J. Chem. Technol. Biotechnol.* **2008**, *83* (12), 1670-1675.
- (51) Prince, E. Crystal and Magnetic Structure of Copper Chromite. *Acta Crystallogr.* **1957**, *10*, 554.
- (52) Khasin, A. A.; Yur'eva, T. M.; Plyasova, L. M.; Kustova, G. N.; Jobic, H.; vanov, A.; Chesalov, Y. A.; Zaikovskii, V. I.; Khasin, A. V.; Davydova, L. P.; Parmon, V. N. Mechanistic features of reduction of copper chromite and state of absorbed hydrogen in the structure of reduced copper chromite. *Russ. J. Gen. Chem.* **2008**, *78* (11), 2203-2213.
- (53) Rode, C. V.; Ghalwadkar, A. A.; Mane, R. B.; Hengne, A. M.; Jadkar, S. T.; Biradar, N. S. Selective Hydrogenolysis of Glycerol to 1,2-Propanediol: Comparison of Batch and Continuous Process Operations. *Org. Proc. Res. Dev.* **2010**, *14* (6), 1393-1400.
- (54) Makarova, O. V.; Yureva, T. M.; Kustova, G. N.; Ziborov, A. V.; Plyasova, L. M.; Minyukova, T. P.; Davydova, L. P.; Zaikovskii, V. I. The Nature of Hydrogen Interaction with Oxide Copper-Containing Catalysts .1. the State of Copper Chromite and Its Catalytic Activity in the Conversion of Acetone to Isopropanol. *Kinet. Catal.* **1993**, *34* (4), 608-612.
- (55) Prasad, R.; Singh, P. Applications and Preparation Methods of Copper Chromite Catalysts: A Review. *Bull. Chem. React. Eng. Catal.* **2011**, *6* (2), 63-113.
- (56) Kim, N.; Oh, S.; Joo, J.; Jung, K.; Yi, J. Effect of preparation method on structure and catalytic activity of Cr-promoted Cu catalyst in glycerol hydrogenolysis. *Korean J. Chem. Eng.* **2010**, *27* (2), 431-434.

- (57) Fogler, H. S. *Essentials Of Chemical Reaction Engineering*; 1st ed.; Pearson Education Inc.: Boston, 2010.
- (58) Carnahan, B.; Luther, H. A.; Wilkes, J. O. *Applied Numerical Methods*; 1 ed.; John Wiley & Sons Inc: New York, 1969.
- (59) Bienholz, A.; Schwab, F.; Claus, P. Hydrogenolysis of glycerol over a highly active CuO/ZnO catalyst prepared by an oxalate gel method: influence of solvent and reaction temperature on catalyst deactivation. *Green Chem.* **2010**, *12* (2), 290-295.
- (60) Liu, D.; Zemlyanov, D.; Wu, T.; Lobo-Lapidus, R. J.; Dumesic, J. A.; Miller, J. T.; Marshall, C. L. Deactivation mechanistic studies of copper chromite catalyst for selective hydrogenation of 2-furfuraldehyde. *J. Catal.* **2013**, *299*, 336-345.
- (61) ADM Propylene Glycol <http://www.adm.com/en-US/products/evolution/Propylene-Glycol/Pages/default.aspx> (accessed July, 2014).

Kanitkar, Swarom R. Bachelor of Technology, September 2010, Visvesvaraya National Institute of Technology; Master of Science, University of Louisiana at Lafayette
Major: Engineering, Chemical Engineering option
Title of Thesis: Modeling and Analysis of the production of Propylene Glycol over Copper Chromite
Thesis Director: Dr. Stephen Dufreche
Pages in Thesis: 144; Words in Abstract: 147

ABSTRACT

Production of 1,2-propanediol through hydrogenolysis of glycerol over Copper-Chromite is a promising reaction pathway that has large potential markets. However, production is complicated by low catalyst stability and significant difficulty in preventing or removing unwanted reaction byproducts. These unwanted byproducts impart yellow color and foul odor, making the product sell at a much cheaper cost. In collaboration with a commercial partner, the authors investigated an economical way of liquid-liquid extraction for removing these unwanted byproducts. The authors also tried to model the production of MPG over copper chromite catalyst, that involved analysis of the kinetics of the reaction and of the parameter effects on the reaction. Analysis of the impurities and kinetic data gave excellent insights on ways to classify the impurities and ways to remove them. Industrial importance of this hydrogenolysis process and the direction for future research has also been discussed in the current work.

Biographical Sketch

Swarom Ravindra Kanitkar was born on April 6, 1988 in Aurangabad, Maharashtra, India. He took his education from primary to higher secondary in SBES High School and SBES Science College, Aurangabad, Maharashtra, India. He then went on to earn a Bachelor of Technology in Chemical Engineering at Visvesvaraya National Institute of Technology in Nagpur, Maharashtra, India, where he captained and represented the institute's chess team. He then attended University of Louisiana at Lafayette to earn a Master's degree in Engineering with a Chemical Engineering option.